EXPLORING SUBMARINE GROUNDWATER DISCHARGE INTO THE DELAWARE INLAND BAYS OVER DIVERSE SCALES WITH DIRECT MEASUREMENTS AND MODELING

by

Christopher John Russoniello

A thesis submitted to the Faculty of the University of Delaware in partial fulfillment of the requirements for the degree of Master of Science in Geology

Summer 2012

EXPLORING SUBMARINE GROUNDWATER DISCHARGE

INTO THE DELAWARE INLAND BAYS OVER DIVERSE SCALES

WITH DIRECT MEASUREMENTS AND

MODELING

by

Christopher John Russoniello

Approved: ____
Holly Anne Michael, Ph.D.
Professor in charge of thesis on behalf of the Advisory Committee

Approved: ____
Susan McGeary, Ph.D.
Chair of the Department of Geological Sciences

Approved: ____
Nancy Targett, Ph.D.
Dean of the College of Earth, Ocean, and the Environment

Approved: ____
Charles G. Riordan, Ph.D.
Vice Provost for Graduate and Professional Education

ACKNOWLEDGMENTS

I would like to thank Dr. Lenny Konikow for invaluable modeling instruction and insight; Dr. Ward Sanford for providing data and a conceptual framework for my modeling exercises; Dr. Richard Winston for helping to troubleshoot modeling problems, whether they were real or imagined;

Cristina Fernandez for creativity and organization in our collaboration along with her amazing ability to learn and teach; James Heiss, Lindsay Byron, Audrey Sawyer, Sean Krepski, and all of the other folks from the Geology department who helped in our field efforts; Andrew Musetto, Kevin Meyers, Deon Knights and the other undergraduates that made data collection possible;

Dr. John Bratton, Joel Banaszak, and Dr. David Krantz for providing the geophysical data on which our direct hydrogeological measurements were planned.

Finally, I am indebted to my thesis committee members, Scott Andres and Dr. John Madsen, for thoughtful insight and my adviser,Dr. Holly Michael, for instruction, assistance and support throughout my research.

This manuscript is dedicated to my parents who have continually nurtured my interest in our blue planet and instilled a sense of wonderment in its inner workings.

It is also dedicated to Margaret for endless motivation and support shown in countless ways over the past few years.

TABLE OF CONTENTS

LIST OF TABLES

LIST OF FIGURES

ABSTRACT

Fresh submarine groundwater discharge (SGD) has been identified as an important source of nutrient fluxes to bays. One of the primary difficulties for quantifying fluxes of SGD-borne nutrients is that estimates of SGD vary widely and depend both on location and method of measurement. This study uses watershed-scale models and site-scale measurements to estimate net fresh SGD and characterize temporal and spatial controls on variability of SGD.

MODFLOW models of the Delaware Inland Bays, a Mid-Atlantic coastal watershed, show that fresh SGD is 40% greater than stream baseflow on average—5% greater in March and 73% greater in August. Bays account for 12% of watershed area and bay arms reach nearly two-thirds the distance to the landward watershed edge. Flux to these arms accounts for the majority of SGD. Sensitivity analyses indicate that horizontal hydraulic conductivity in the aquifers is the dominant variable controlling the magnitude of fresh SGD, and that SGD is generally greater than baseflow across the range of reasonable parameter values. Hydraulic properties in shallow aquifers have greater potential impact on SGD rates than deeper aquifer properties. Particle tracking indicates that 40% of SGD is greater than one year and ranges upwards of 100,000 years old.

A multi-disciplinary field investigation conducted at Holts Landing, Indian River Bay, DE, including 552 seepage meter and 92 porewater salinity measurements along with marine seismic and resistivity surveys, characterized shallow sediments, porewaters salinity and SGD. These data show a link between geologic heterogeneity

and the spatial distribution of SGD on a range of spatial and temporal scales. This work finds that low-permeability paleovalley sediments at the bayfloor overlie underlying fresh groundwater plumes. SGD up to 100% fresh was measured along the interfluve coast; farther offshore fresh SGD was absent. Above the paleovalley, fresh SGD was absent but fresh groundwater flowed into the bay along the edge of the low-permeability sediment at the paleovalley/interfluve boundary, where SGD up to 36% fresh was measured. High saline SGD rates were also measured along the paleovalley/interfluve border. This suggests the presence of a shore-parallel density-driven circulation cell similar to that expected perpendicular to the interfluve coastline. In-situ porewater salinity was consistent with SGD salinity patterns. Clusters of seepage meter measurements (1m spacing) indicate that SGD varies more on spatial scales of 1 to 5 m than temporally on tidal timescales, which may explain the absence of tidal and seasonal temporal trends in the complete dataset.

This study shows that groundwater flowpaths, mixing of fresh and saline groundwater, and the spatial distribution of SGD are controlled by local geology and are sensitive to temporal variations in the terrestrial hydraulic gradient. Modeling indicates that it will take years before efforts to reduce nutrient loading to land surface will be seen in reduced nutrient loading through SGD. It is important for managers to consider implications of these complications in estimates of SGD-born nutrient loads.

Chapter 1

INTRODUCTION

Submarine Groundwater Discharge (SGD) has been increasingly identified as an important source of nutrients to coastal watersheds. SGD includes both a fresh component, which is driven by the terrestrial hydraulic gradient, and a saline portion, which is driven by density gradients and transient forces such as tides, waves, and currents. Understanding of SGD rates, along with nutrient concentrations in discharging water, is required to estimate nutrient loading by groundwater.

Many factors complicate this estimation, including geologic heterogeneity, variations in water density, chemical reactions, and temporally varying forces. Geologic and chemical heterogeneity broaden the range of measurable hydraulic properties and chemical end-members. The angled fresh/saline density interface as well as tides, waves, and currents drive saline surface water/groundwater exchange. Seasonal variations in the terrestrial gradient are driven by varying recharge and groundwater pumping. In order to provide a more comprehensive understanding of nutrient loading by SGD, the effects of these complexities must be better constrained.

The fresh component of SGD carries new nutrients to estuaries, and saline SGD contributes recycled components. Fresh flux is controlled by temporally variable stresses, topography and heterogeneous hydraulic properties in the aquifer, all of which are difficult to characterize. Aquifer recharge rates are primarily determined by precipitation and evapo-transpiration rates, which vary seasonally. After recharging the aquifer, any water that is not extracted will exit as either stream baseflow ot discharge to coastal surface water. The balance between discharge to streams and discharge to estuaries and oceans is controlled largely by the balance between topographic elevation, and water table elevation, which depends on hydraulic properties of aquifer sediments and recharge rates. Numerical models allow the testing of hypotheses and comparison to real world data so that we can understand how each control affects fresh SGD and quantify how much uncertainty exists within the system.

Geology affects the distribution between stream baseflow and SGD, and it also controls the distribution of SGD along coastlines. In a homogeneous aquifer, the angled density gradient combined with freshwater flow driven by the terrestrial head gradient generally forces a narrow fresh outflow gap. Geologic heterogeneity and transient forcing create more complex discharge patterns and enhanced subsurface mixing than predicted by simple models. Mixing of fresh groundwater with oxygenated saline baywaters and chemically reactive sediments can induce transformations of the freshwater-borne nutrients and other chemicals; this will affect loading to coastal surface waters. Understanding how geology on a variety of scales controls fresh SGD along coastlines is a large step toward understanding the associated chemical cycles.

The work presented herein examines how the interplay between heterogeneous coastal geology, bay hydrodynamics, temporally variable forcing factors and a driving terrestrial hydraulic gradient affect the spatial distribution of fresh SGD. The results provide a physical framework for understanding chemical evolution along flowpaths and ultimately, the loading of nutrients and other chemicals to coastal waters.

Chapter 2

QUANTIFYING SUBMARINE GROUNDWATER DISCHARGE INTO THE DELAWARE INLAND BAYS WITH A NUMERICAL MODEL

2.1 Introduction

Eutrophication has been increasingly recognized as a problem in coastal waters and accompanying this is an increased need to understand nutrient pathways to estuaries [e.g. Selman and Greenhalgh, 2007]. Submarine groundwater discharge (SGD), which is “any flow of water out across the seafloor” [Burnett et al., 2006], is recognized as an important vector for nutrient loading of estuaries [e.g. Johannes, 1980; Slomp and Capellen, 2004; Spiteri et al., 2008]. While recirculating saline water may account for as much as 96% of total SGD [Li et al., 1999; Santos et al., 2009] the fresh component of SGD is responsible for new inputs of nutrients and chemicals to estuaries [e.g. Charette and Buesseler, 2004; Knee and Payton, 2011]. This fresh SGD is driven by the terrestrial hydraulic gradient. Because terrestrial groundwater often contains elevated concentrations of nutrients with respect to baseflow [Kroeger et al., 2007], understanding what controls the flow of groundwater from coastal aquifers into estuaries is crucial for understanding nutrient loading to these water bodies.

Computer models are among the most useful tools for answering questions about rates and controls on fresh watershed-scale SGD to estuaries because of problems encountered with field techniques used to measure SGD. For example, error inherent in these measurements propagates through to prevent separation of the fresh from the saline components [e.g. Ganju and Schoellhamer, 2006; Michael et al., 2011] or do not spatially average measurements on a scale allowing prediction of watershed-scale discharges [e.g. Michael, 2003; Chapter 3 this document]. Radiochemical tracers have been used to estimate total (fresh and saline) and saline components of flux, respectively, with end member mixing models [e.g., Mulligan and Charette, 2006]. Uncertainty and heterogeneity in end member concentrations propagate to fresh SGD estimates. Salinity can be used as a tracer for fresh SGD, but methods depend on knowledge of surface water inputs and a rigorous understanding of surface water hydrodynamics [Ganju and Schoellhamer, 2006; Lee and Kim, 2007; Ganju, 2011]. Seepage meters can easily separate the fresh and saline components of discharge, but because of geological heterogeneity on a variety of scales, many meters are required to obtain a spatially averaged discharge rate for entire estuaries [e.g. Michael et al., 2003; Chapter 3 this document].

Coastal hydrogeology is especially difficult to study because of the heterogeneous geologic setting [e.g. Lee 1977; Bratton et al., 2004], temporally variable forcing [e.g. Michael et al., 2003; King et al., 2009], and mixing of water with different densities [e.g. Cooper, 1964; Fetter, 2001]; to avoid these complexities, modelers may employ simplifying assumptions to provide meaningful results [e.g. Custodio, 1987; Motz and Sedighi, 2009]. Although a number of shorter time scale processes control saline recirculation (e.g. waves, currents, and tides) they do not directly control the terrestrial SGD component. Net fresh SGD is primarily controlled by forces varying on longer timescales, such as seasonal recharge and pumping patterns.

Variable-density numerical modeling codes have been widely used for decades to study coastal groundwater systems [e.g. Oki, 1999; Kaleris et al., 2002; Langevin, 2003] and to address questions about heterogeneity and rates of SGD [e.g. Langevin 2003]. However, these variable density codes require extra computational power and boundary value information to provide solutions and they may not significantly increase accuracy for predictions regarding net fresh flux over single density code [e.g. Motz and Sedighi, 2009]. Thus, single density simulations are effective tools for the study of fresh SGD.

Though geologic heterogeneity is an important control on the spatial distribution of SGD into coastal embayments, the scale that must be modeled explicitlyis dependent on the scale of the questions being asked. In this study, spatially averaged properties were chosen for model layers because the freshwater budget, not small scale distribution of fresh groundwater discharge, was of primary interest. Large-scale models of coastal watersheds simplify temporal and geologic complexities associated with coastal watersheds but may still provide reasonable estimates of groundwater discharge rates and flowpaths [e.g. Hill, 2006].

The purpose of the work presented in this chapter is to estimate the balance between fresh SGD and baseflow into an estuary on the Atlantic Coastal Plain and to understand how aquifer hydraulic properties and temporal forcing factors affect that balance.

2.2 Description of the Inland Bays Watershed

The Inland Bays Watershed, located on the Atlantic Coast of Delaware (Figure 2.1), is 670 km^2 in area and lies on a wedge of coastal plain sediments that thickens shoreward and southward. Land surface in the watershed gently slopes from 15 m (NAVD88) to sea level at the Atlantic Coast. Terrestrial water discharges into Indian River and Rehoboth Bays (collectively known as the Delaware Inland Bays) and directly into the Atlantic Ocean. Both shallow estuaries are prone to wind effects that can overshadow the 0.3 to 1.0 m tidal ranges [NOAA/NOS, 2010]. The bays themselves originated when rising sea levels drowned incised river valleys of the paleo-Indian River system. Today the bottoms of these shallow estuaries consist of sediment ranging from low-permeability clay and peat deposited in quiet water lagoonal, channel, and marsh environments, to sands and gravels deposited in overwash environments and the flood tide delta of the Indian River Inlet[Ramsey, 2011]. Together, the bays account for 12% of the surficial watershed area with neighboring wetlands accounting for an additional 3%. Fresh water inputs to the bays include direct precipitation, surface-water runoff and SGD [Wang et al., 2008]. Approximately 113 cm of precipitation is evenly distributed throughout the year [NOAA/NCDC 2010] and average monthly temperatures range between 2°C and 25°C [NOAA/NCDC, 2010]. Accounting for evapo-transpiration and land use/land cover, recharge estimates range between 30 and 50 cm in the watershed [Sanford, 2010]. Additional important anthropogenic controls on the system include pumping of groundwater for water supply and ditching for drainage. Ditching affects not only runoff patterns but can also affect connectivity with the uppermost confined aquifer at locations where ditches completely penetrate a thin surficial confining layer [Andres and Howard, 2002].

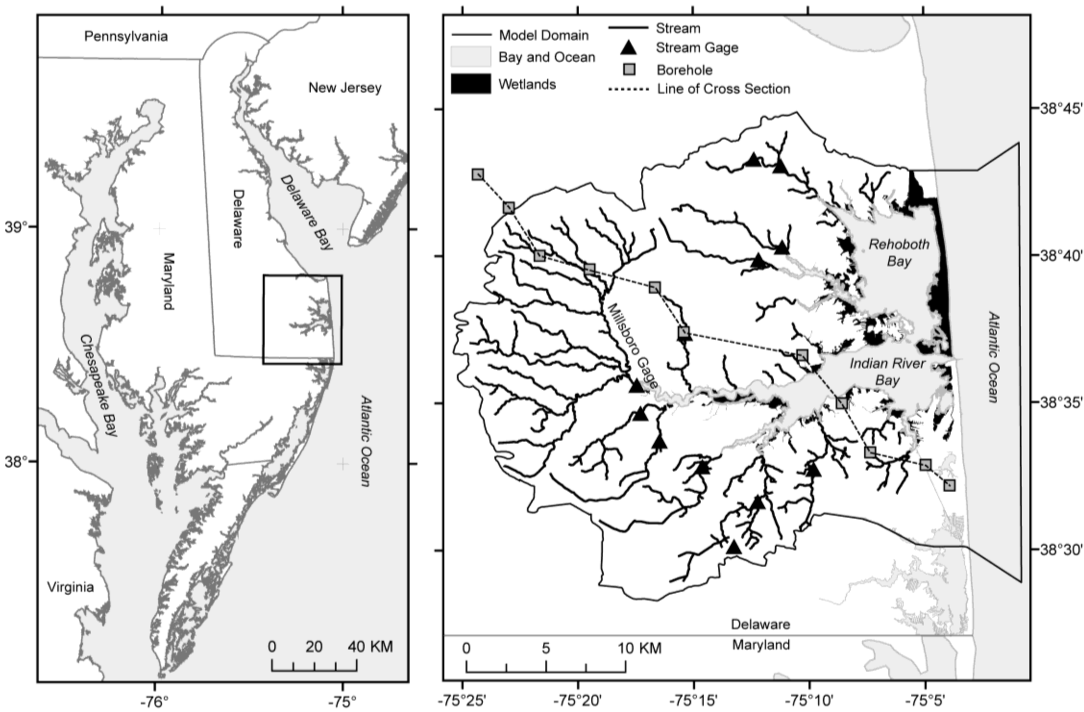

Figure 2.1: Site map of the modeled area. Left panel shows the Delmarva Peninsula and immediate surroundings with a box around the geographic limits of the right panel, which is a map of the modeled domain. Right panel also shows all model boundaries.

Historically, forest and agriculture have been the dominant land uses in Sussex County, though the last few decades have seen rapid urbanization of the Inland Bays Watershed and planners have estimated a 61% population growth between 2000 and 2030 [Delaware Population Consortium, 2006]. Eutrophication from increased septic and continuing agricultural loading of N and P is a recognized problem in the watershed [US EPA, 2002; DNREC, 2007] and resulting frequent algal blooms have plagued the estuary [Andres, 1991; Wang and McKenna, 2008]. Groundwater nutrient concentrations elevated by anthropogenic loading and long groundwater residence times suggest a slow response to any management efforts to decrease nutrient loading to the bays [Andres, 1991; Wang and McKenna, 2008].

In coastal Sussex County, the primary units used for water supply are those of the Miocene-aged upper Chesapeake Group (Consisting of the Cat Hill Formation (Fm.), and Bethany Fm.), and the overlying Pleistocene-aged Beaverdam Fm. [Andres, 1986; Andres and Klingbeil, 2006] (Table 2.1). Underlying these units, the St. Marys Fm., a thick, low permeability, silty clay that lies at 60 to 130 m depth in Eastern Sussex County functions an aquitard. [Andres, 1987; Andres and Klingbeil, 2006]

Table 2.1: Relation Between Geologic Formation and Hydrologic Units

Geological Unit (Formation)	Hydrological Unit (Aquifer)
Beaverdam Fm.	Surficial Aquifer
Bethany Fm.	Pocomoke/Ocean City Aquifer
Cat Hill Fm.	Manokin Aquifer
St. Marys Fm.	Confining Unit

The aquifer system above the St. Marys Fm. is comprised of three aquifer units (Manokin below, Pocomoke between, and Beaverdam above). These three aquifers are each contained by the Cat Hill Fm. below, Bethany Fm. between, and Beaverdam Fm. Above, respectively (Figure 2.2). The post St Marys units are heterogeneous but generally coarsen upwards with sediments ranging from clay to gravel [Andres, 2004; Mclaughlin et al., 2008]. The aquifers are hydraulically separated by variably-continuous, lower-permeability lenses. Thin Pleistocene and Quaternary-aged surficial units deposited in offshore to muddy estuarine environments vary in character with fine-sediment units acting as locally continuous low permeability confining caps [Ramsey, 2010; Ramsey, 2011].

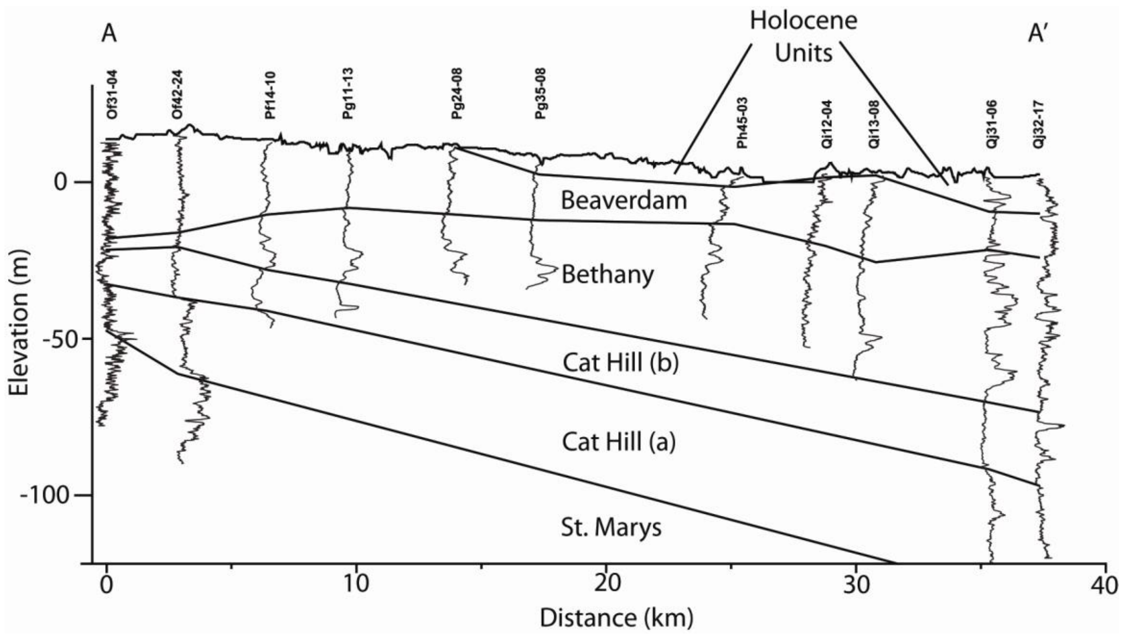

Figure 2.2: Cross section A-A’ illustrates the layered geological formations of Eastern Sussex County. Gamma logs are of wells in the Delaware Geological Survey database (DGS identifier numbers are above wells). [Modified from Andres and Klingbeil, 2006].

2.3 Model Development

2.3.1 Geometry and Discretization

A MODFLOW 2000 [Harbaugh et al., 2000] model was developed using the ArgusOne graphical user interface [Winston, 2000]. The grid has 7 layers, 233 columns and 201 rows, with 240,695 active cells. All cells are 152.4 m on a side and range in thickness from 3 m to 70 m depending on aquifer geometry. Model layer 1 represents surficial deposits, layers 2-4 the Beaverdam, layer 5 the Bethany, and layers 6 and 7 the Cat Hill Fm. Delaware Geological Survey (DGS) raster products depicting depth to geological units for the Bethany, Cat Hill and St Mary's Fms. [Andres and Klingbeil, 2006] were used as the primary source for determining the geological framework of this model. These raster products only include onshore geometry as there is a lack of reliable offshore data. To extend stratigraphy offshore, depth to the St. Marys Fm. was picked from a shore-parallel seismic record [Benson et al., 1986]. General onshore stratigraphic trends for the overlying contacts were extended offshore to the eastern model edge based on these depth picks.

A LiDAR-derived Digital Elevation Model (DEM) [upublished DGS Data accessed 01-15-2011] (2-meter grid, aggregate average RMSE of 10.2 cm, maximum of 14.8cm) was the principle data source for determining land surface elevations. Features such as unsurveyed observation wells, stream and drain elevations, and model boundaries were assigned elevations extracted from the nearest grid cell. Model geometry offshore and in the bays was constrained by subaqueous bathymetric data retrieved from the NOAA National Geophysical Data Center [NOAA/NGDC, 2010].

2.3.2 Watershed Delineation

The ground-watershed was independently determined via two approaches and compared to the surficial watershed to define the model boundary locations. Groundwater-level records from the Manokin and Pocomoke aquifers were contoured to produce a head-map, which shows a groundwater divide in the deeper aquifers roughly coinciding with the surficial peninsular divide between the Atlantic Ocean and the Chesapeake Bay (Figure 2.3). Groundwater basins were also delineated from simulated hydraulic heads in the uppermost and lowest model layers of a USGS

MODFLOW model of the entire Delmarva Peninsula [Sanford, 2010]. The simulated basins for both the topmost and lowest model layers correspond well with each other indicating that groundwater sheds are similar throughout the aquifer thickness (Red and green dots in Figure 2.3). The boundaries chosen for this model are consistent with hydraulic head data. At the scale of analysis, these boundaries also correspond well with the topographically derived surficial watershed. Model boundaries were extended to include Little Assawoman Bay to the south as a constant head boundary so that the southern inland bays watershed groundwater divide would be determined with the current model rather than prescribed a priori by a no-flow boundary.

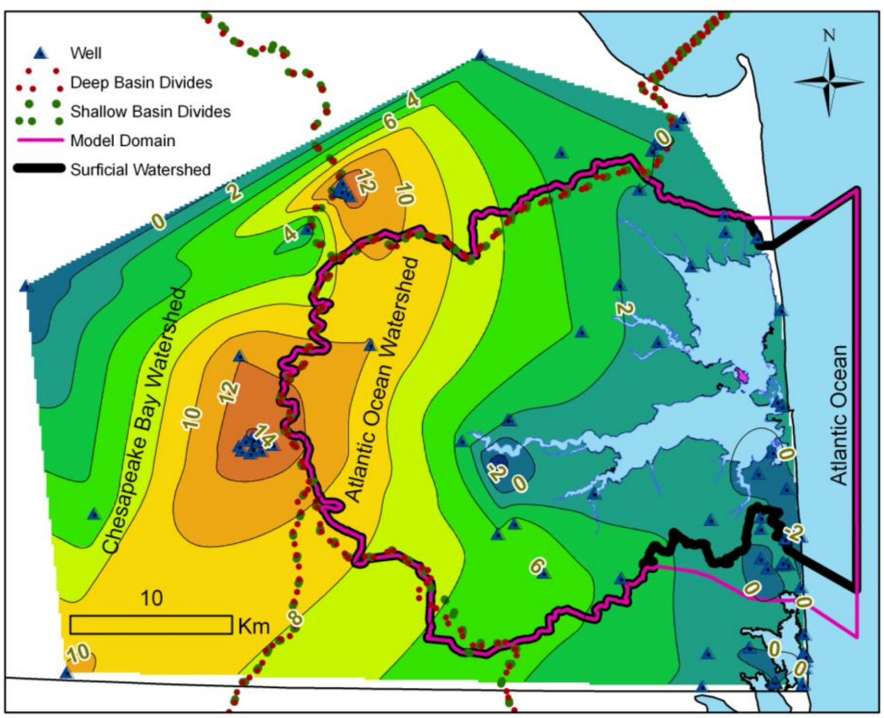

Figure 2.3: Different estimations of the Inland Bays watershed boundaries. Dotted lines are basins derived for both the shallowest and deepest layers of a model of the entire Delmarva Peninsula. Interpolated hydraulic heads from wells in the Manokin and Pocomoke Aquifers are shaded and contoured at a 2 m interval.

2.3.3 Constant Head and Stream Boundaries

Because this model assumes single-density flow, an equivalent freshwater constant head was applied to model cells representing the Inland Bays and Atlantic Ocean (Figure 2.1). A head value equal to mean sea level plus 0.025 times the depth of surface water was chosen to represent seawater of typical ocean salinity and density in each bay and ocean cell. Water entering or leaving the model across this boundary is representative of submarine groundwater recharge or discharge, respectively. Single density simulation was chosen for a number of reasons; foremost among them was a lack of subsurface salinity data and the increased computational requirements for variable density models. Though a simplification, this freshwater equivalent head boundary should provide reasonable estimates of groundwater flowpaths and fresh SGD as only the fresh portion of the system is considered [Motz and Sedighi, 2009]. A variable-density simulation would likely show different spatial patterns of SGD than those predicted by this single-density code (Figure 2.10); terrestrial-sourced SGD would likely be confined to a thinner, fresher, outflow face. This thinner fresh outflow face could result in more resistance to flow and decreased discharge, but should not result in a significant change in overall volume of fresh SGD. We neglect any physical factors driving SGD other than hydraulic gradient (e.g. tides, waves, currents, bioirrigation). Compared to the other sources of uncertainty in the model, this simplification should contribute minimally to the total propagated uncertainty.

Natural and manmade stream boundaries were represented using the stream flow routing package (SFR) [Niswonger and Prudic, 2006] (Figure 2.1). This boundary type combines a 1.) 2-way flux boundary controlled by difference in head between the aquifer and stream and a streambed conductance value with 2.) calculations of cell-to-cell advective streamflow to determine where water enters and leaves through streams. Streambed conductance is based on channel width, depth, bed thickness and vertical K of the bed materials . Little of these data were available, so constant values were assumed for all stream boundary parameters (Table 2.2) and vertical K was prescribed to equal that of layer 1. One-way head-dependent flux boundaries (represented with the DRN package and hereafter referred to as drains) were prescribed across estuary-fringing wetlands.

Table 2.2: Stream boundary parameter values

Parameter	Value
Width	1 m
Depth	0.1 m
Thickness	0.1 m

2.3.4 Recharge

Recharge values for the steady state model were obtained from model inputs originally developed for the Delmarva Peninsula [Sanford, 2010]. That dataset was created with a linear regression of baseflow values, land use/land cover data, precipitation and evapo-transpiration estimates [Sanford, 2010]. Recharge was applied to the top model layer as a, spatially-varying stress that averaged 44 cm/year in cells that are not surface water or wetlands. This is equal to 39% of precipitation as recorded at the nearest long-term NOAA rain gage [NOAA/NCDC, 2010]. Recharge values are similar to estimates elsewhere along the eastern seaboard: recharge on Cape Cod averages 45% of precipitation [Masterson and Barlow, 1994], and in coastal New Jersey recharge ranges from 30-46 cm/yr [NJGS, 2005].

Monthly potential evapotranspiration was calculated from average daily temperature and day length for that month with a USGS Thornthwaite GUI [McCabe and Markstrom, 2007]. Aquifer recharge was determined by subtracting potential evapo-transpiration (the evapo-transpiration that would occur if water were unlimited) from precipitation values. Average monthly values of precipitation and temperature for the years 1895 to 2010 were obtained from the NOAA weather station at Georgetown, DE, [NOAA/NCDC, 2010] which is approximately 10 km northwest of the study area. These values were used to determine evapo-transpiration and recharge rates for each month. The average recharge calculated with this method was 44 cm/year, which matches well with the average 44 cm/year of the recharge dataset [Sanford 2010]. The recharge entering the aquifer each month as a percentage of aquifer recharge during the entire year was calculated. For transient simulations, the twelve values were multiplied by the initial steady state recharge raster to determine recharge during each month of the year for each model cell. During summer months, recharge values were negative because potential ET was greater than precipitation.

2.3.5 Pumping Wells

Locations of groundwater pumping wells were obtained from an electronic database of well records for the state of Delaware [DGS, 2012] which is maintained by the Delaware Geological Survey (DGS) staff. This database is populated with all data regarding well construction, purpose, location, chemistry and hydraulic head data collected during DGS investigations. All wells within the model domain were extracted so that they could be incorporated into the model as pumping wells.

A second database, populated with historical water-use data [unpublished DGS records], provided estimates of pumping rates for commercial, municipal and agricultural wells. This water-use database was incomplete and lacked pumping data for the majority of wells in the model area but average pumping rates for each well type were calculated from the dataset. These average values were applied as pumping rates estimates for wells of that type within the model domain. After comparison with aerial imagery [Google, 2009], wells zoned for agriculture in residentially developed areas were removed from the water-use list and not considered in pumping estimates as they are likely unused presently. Irrigation well pumping values were determined by multiplying irrigated farmland area as determined from aerial imagery [Google, 2009] with average irrigation rates for Sussex County corn and soybean crops, which are the dominant irrigated crops in the study area [USDA, 2009]. These irrigation wells were joined with GIS software with depth data from their nearest neighbor in the water-use database to calculate a depth from which water is pumped. In all, 968 wells were included in the model, pumping at an average rate of 0.91 m^3/s. The water use database consists of a compilation of estimates and incomplete data that is representative of water usage-records and reporting in Sussex County and throughout the state of Delaware [Andres, 2010]. As such, these data are inexact, but match well with the only other estimate of pumping values in Sussex County discovered in a literature search, which was 1.1 m^3/s, [Wheeler, 1999]. All pumping wells were represented with the MNW2 package [Konikow et al., 2009] for ease of data entry and to allow screened intervals across more than one model unit. Particle Tracking

MODPATH (Pollock, 1994) particle tracking was used to model the age and flowpaths of fresh groundwater discharging into the bays. Particles were placed on the top edge of all 4190 bay cells and the pathlines were tracked backward to recharge locations. Porosity was prescribed as 0.2 for all units, a typical value for coastal sediments (e.g. Fetter 2001).

2.3.6 Hydraulic Properties

An average hydraulic conductivity (K) for each model layer was determined based on unpublished values from the watershed DGS, 2012]. These values were compared to literature values for this watershed[e.g. Johnston, 1973; Andres, 1987]. Grain size information was consistent with literature values [Fetter, 2001]. These estimates were used as starting points for calibration.

2.3.6.1 Steady State Calibration

Calibration of the steady state model was intended to find a best match for model parameters to historical field measurements. Historical groundwater levels and stream baseflow were used in calibration. Groundwater level data were obtained from the DGS well record database [DGS, 2012]. Wells in the watershed with more than 4 head observations were selected as calibration points for the steady state model. Historical values were averaged and individual wells were each assigned a weight based on the number of observations, number of years of record and proximity to other wells such that all wells were assigned a value between 0.35 and 0.99. Baseflow estimates for 11 streams based on low flow stream gaging (Figure 2.1) in the model area [Ullman et al., 2002] were compared against modeled baseflow values as an additional calibration dataset.

2.3.6.2 Transient Calibration

Transient simulations, using results of steady-state simulations as a starting condition, were run for 5 years, each with 12 1-month stress periods, to a dynamic steady state. Simulated baseflow values at gage locations (Figure 2.1) were compared to the sum of long-term monthly discharge averages from a stream gage at Millsboro Pond outlet [USGS 2011] (Figure 2.1) and a subset of historical water elevations from 150 wells. That subset included only wells with at least 2 years of recorded head data, an observation in every calendar month and 20 or more individual water level observations. All observed head values for a single calendar month were averaged, so that each of the 12 months was assigned a single average value. In the transient model, observations were compared to drawdown rather than absolute head values as in the steady state model. Calibration to changes in head relative to a well specific datum are more accurate than comparison to absolute head residuals because error from measured well elevations and an inexact initial hydraulic head field propagates to absolute residuals.

2.4 Calibration

2.4.1 Steady State Model Calibration

The model was manually calibrated to match historical values of average baseflow and groundwater levels by varying layer horizontal and vertical K values (Kx and Kz, respectively). The sum of squares for the weighted residual of groundwater levels in 326 observation wells was 100.34 m^2 (average raw residual of 0.01 m); for these conditions, the sum of stream baseflow values was 155% of the sum of measured baseflow values. Increasing Kx values allowed modeled baseflow to equal the sum of field-measured baseflow values, but resulted in the sum of squares for the weighted residual of ground water levels reaching a value of 203.03 m^2 (average raw residual of 0.84 m). Values for the best match to baseflow, well head observations and combined (the "Base" model) are reported in Table 2.3. The Kx values that produced the best match to groundwater levels were 73% of the chosen Base value and the best match for baseflow was with Kx values 127% of Base values. Simplifications (such as imperfect representation of geologic heterogeneity and system geometry) along with propagated uncertainties due to calibration data likely affect model calibration, but should not significantly affect flowpaths or conclusions drawn from sensitivity analyses.

Table 2.3: Best calibration K values.. Table lists Kx and Kz values that cause closest match to hydraulic head and baseflow calibration values as well as those chosen for the Base steady state model.

Unit	**Best Well Match**		**Base**		**Best Baseflow Match**	
	Kx	Kz	Kx	Kz	Kx	Kz
Surficial	7.060E-04	2.241E-05	1.112E-03	3.530E-05	1.412E-03	4.483E-05
Beaverdam	7.060E-04	2.241E-05	1.112E-03	3.530E-05	1.412E-03	4.483E-05
Bethany	4.800E-04	1.524E-05	7.560E-04	2.400E-05	9.600E-04	3.048E-05
Manokin A	5.440E-04	1.727E-05	8.568E-04	2.720E-05	1.088E-03	3.454E-05
Manokin B	2.720E-04	8.635E-06	4.284E-04	1.360E-05	5.440E-04	1.727E-05

2.4.2 Transient Model Calibration

The transient base model was calibrated by varying specific yield (Sy) through a range of reasonable values (0.05-0.3) to determine a best match to calibration points for the transient Base model. The residual sum of squares between simulated and expected drawdowns was lowest (0.28 m^2) if steady state Base K values were retained while Sy was set to 0.12. Correlation between simulated and expected baseflow magnitudes was highest with a Sy/Kx of either 0.3/Base or 0.1/10x Base (98.2% and 98.5%, respectively). Calibration is complicated by both 1.) a system indiscriminately sensitive to Kx and Sy and 2.) different best parameter values for matching well drawdown or baseflow correlation. This mismatch of best fits shows that a range of values for either K or Sy could reasonably be established as the best fit values. Thus, transient Base conductivity values were kept identical to those chosen in the steady state Base model and an arbitrary value of 0.1 was selected for the Base Sy value. The transient Base model, with a 0.1 Sy, had a 96.4% correlation and sum of residual squares for drawdowns of 0.31 m^2. Sensitivity to parameters is reported in section 2.6.

Matching between historical and measured values varied at different well locations in the Base transient model. At some well locations correlation between simulated and observed drawdowns was excellent while at others correlation was low or even negative. The same is true for the sum of squares of drawdown residual (Figures 2.4 & 2.5). In general an increase in the number of unique field measurements of well hydraulic head at a location led to higher correlation ($R^2 \rightarrow 1$) and lower sum of squares of residual (sum of squares→0) between observations and modeled drawdown values for a well, but this was not true in all cases (Figure 2.4). The same held true for the length of period of record, so wells with a longer time period of records generally correlated more strongly with the model ($R^2 \rightarrow 1$, sum of squares→0). All wells with long-term datasets and many individual observations had low residuals and high correlation, but so did many wells with shorter, smaller datasets. This suggests that this model matches the long-term average trends, but not single unique observations, which vary from the mean if the system was not near the average when the measurement was made. In general, wells closer to the bays matched simulated heads better than wells further from it and wells south of Indian River Bay matched more closely than those to the north (Figure 2.5). There are at least two explanations for this distribution. The more obvious is that the model better matches hydraulic properties and geologic geometry in the southern section of the model than areas north of Indian River Bay. The second possibility is that the field measurements of hydraulic head more closely matched the long term average south of the bay than records of wells to the north because there is a higher density of automated dataloggers deployed in the south. North of Indian River Bay water levels are more likely to be measured only during sporadic field visits by DGS staff rather than at rapid, regular intervals.

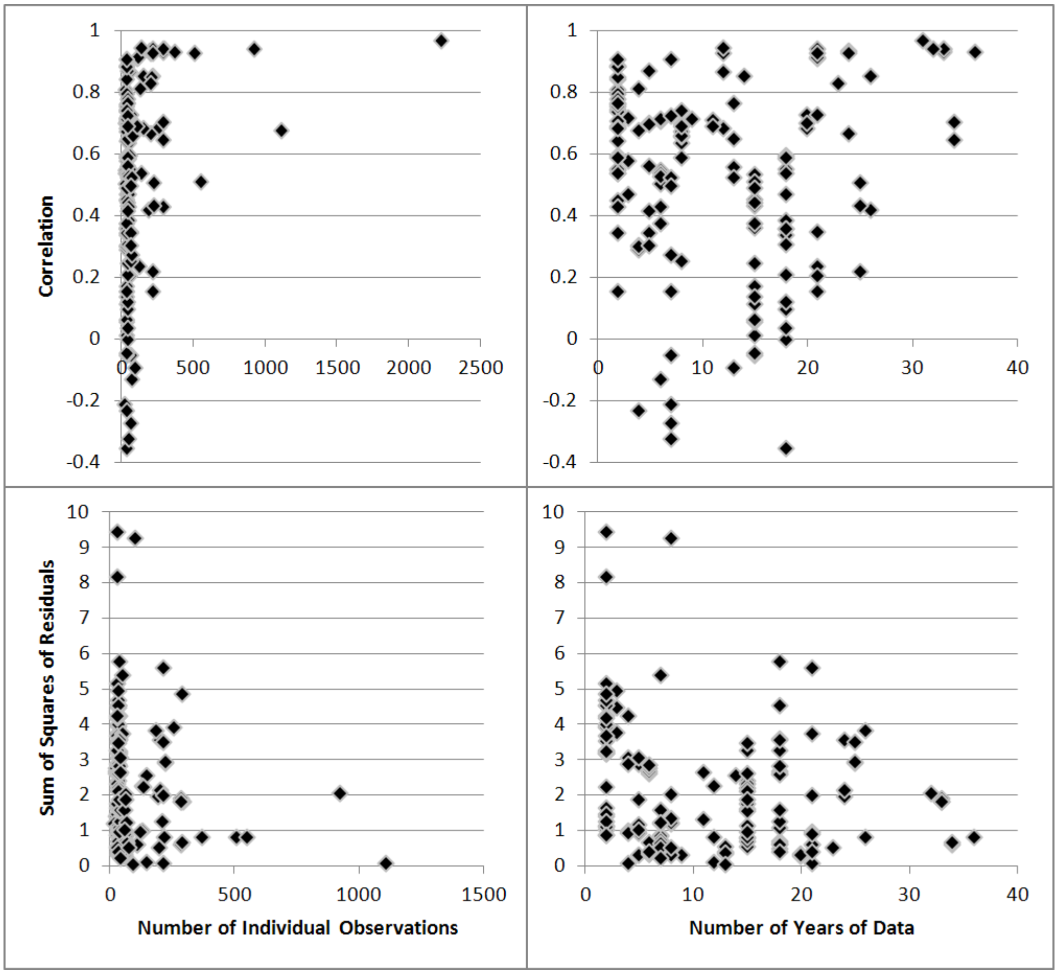

Figure 2.4: Plots of calibration results of the transient Base model. An increase in the number of unique measurements at a well or overall time range during which records were collected at an individual well generally increases the agreement between modeled and field-measured values. Both correlation between monthly trends and sum of squares of the residuals tend to yield better agreement with larger and longer datasets.

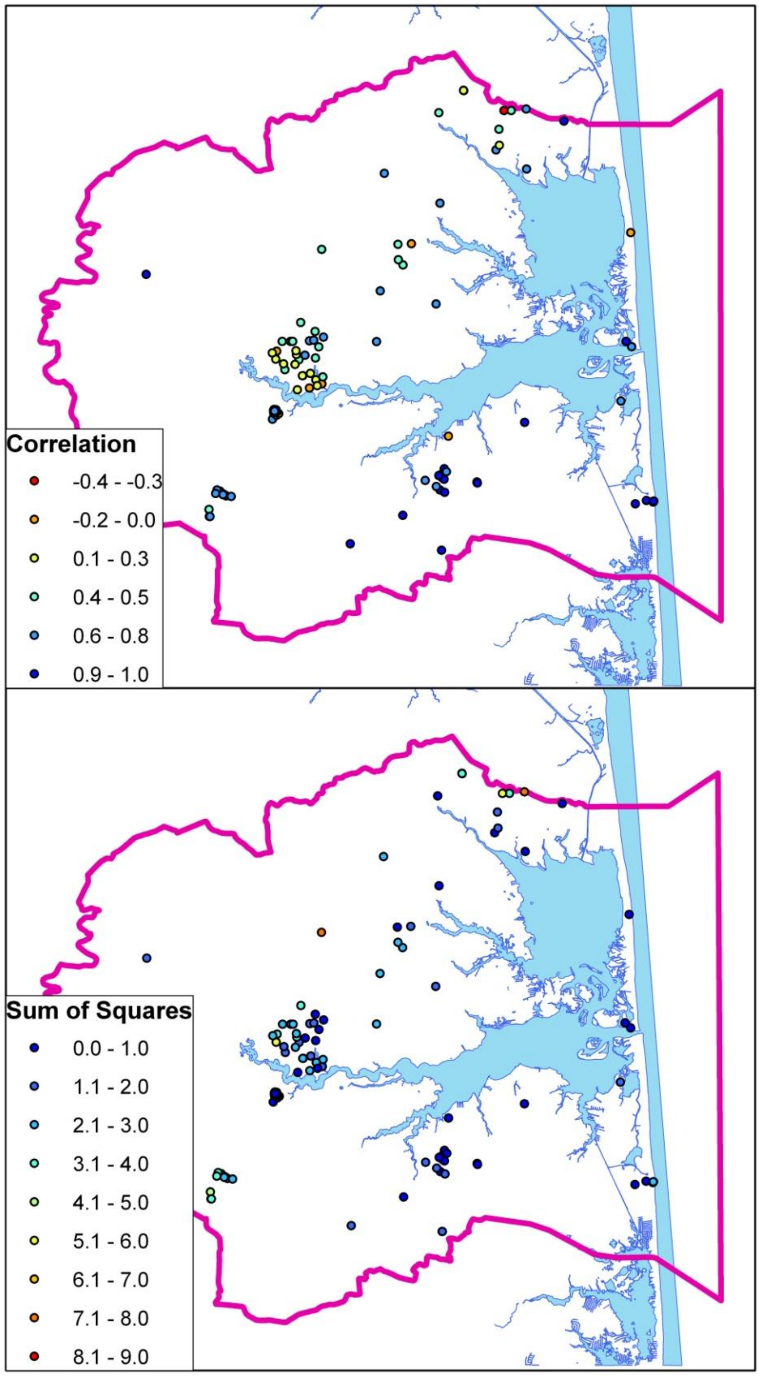

Figure 2.5: Calibration results for the Base transient model. A.) correlation coefficient of the relationship between observed and measured drawdown over the course of a year, and B.) sum of squares of drawdown residuals.

2.5 Results

2.5.1 Base Steady-State Model

The modeled water table is a muted expression of the surface topography that outcrops at streams and other surface water bodies. This matches expectations and water table maps [Andres and Martin, 2005]. Discharge to the ocean and bay constant head boundaries accounts for about 52% of all water discharging from the aquifer, baseflow accounts for another 37%, and pumping accounts for the final 10% (Figure 2.6). Additionally, streams and baywater recharge through the streambed and bayfloor boundaries. The net flux (flux out minus flux in) from the aquifer to the ocean and bay constant head boundaries is 40% greater than net flux lost through the stream boundary. Simulated groundwater velocities are greater in the western half of the model where higher topographic relief supports higher gradients toward the bays and streams. Along the coast, where land elevations are closer to sea level, hydraulic gradients and groundwater velocities are lower (Figure 2.7).

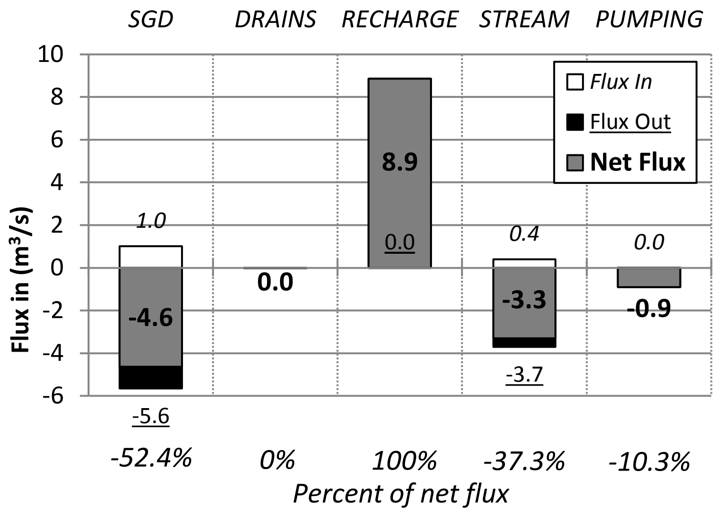

Figure 2.6: Net Flux through boundaries in the Base calibrated steady-state model. Refer to Figure 2.1 for model boundary delineation.

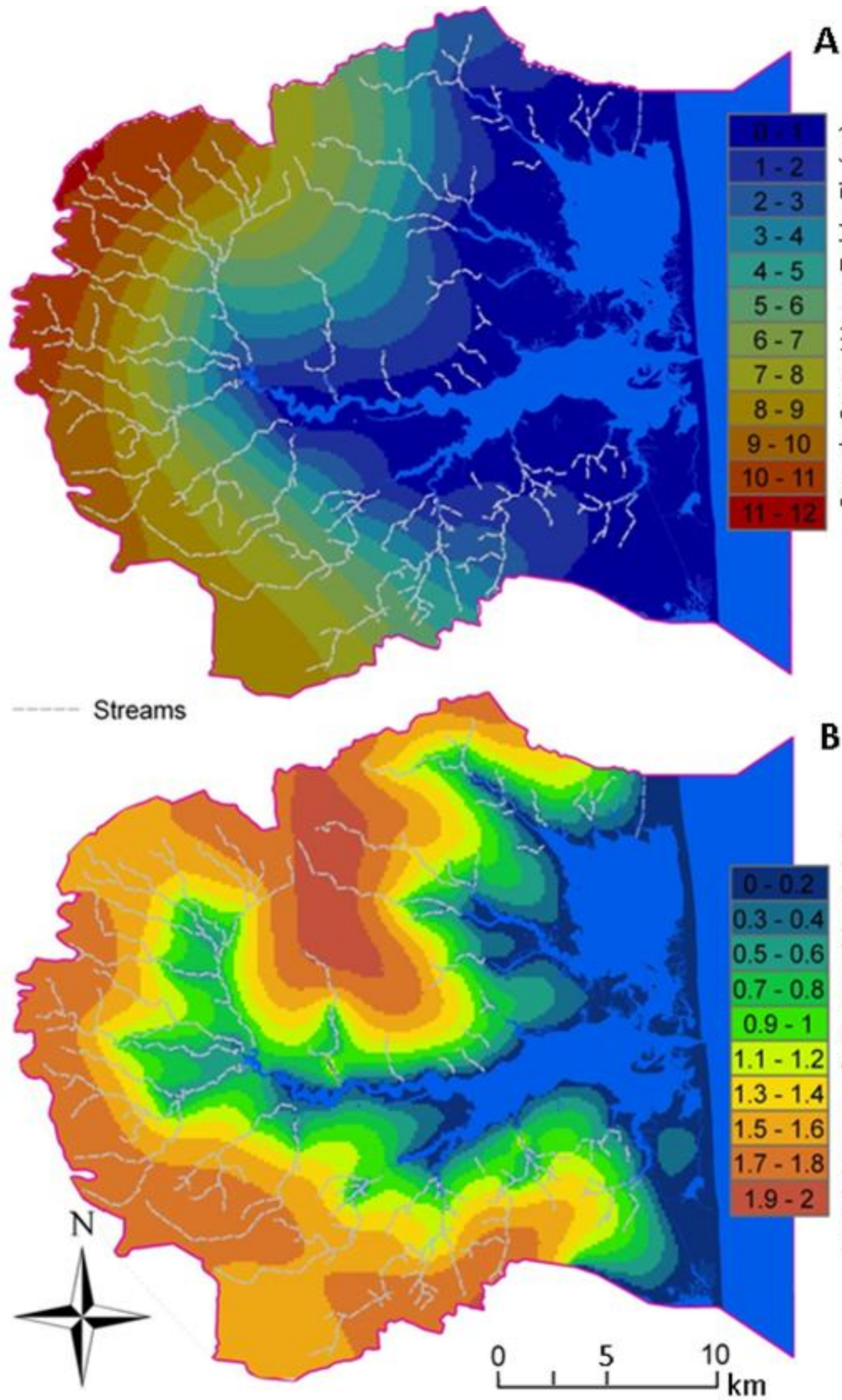

Figure 2.7: Water table elevation maps. A.) the steady state water table elevation of the Base model and B.) the annual range of water table elevations for the Base transient model.

2.5.2 Base Transient Model

Because the steady state and transient models used the same annual average recharge rates, average results of the Base transient model are within 2.5% of those of the steady state model (Figures 2.6, 2.8). SGD rates are slightly lower (98%) and baseflow is slightly elevated in the transient model with respect to the steady state model (105%). The net yearly storage change is zero, but fluxes in and out of storage are non-zero because transience allows storage to change during a stress period each month. There is an average hydraulic head difference of 1.12 m between winter and summer months (Figure 2.7).

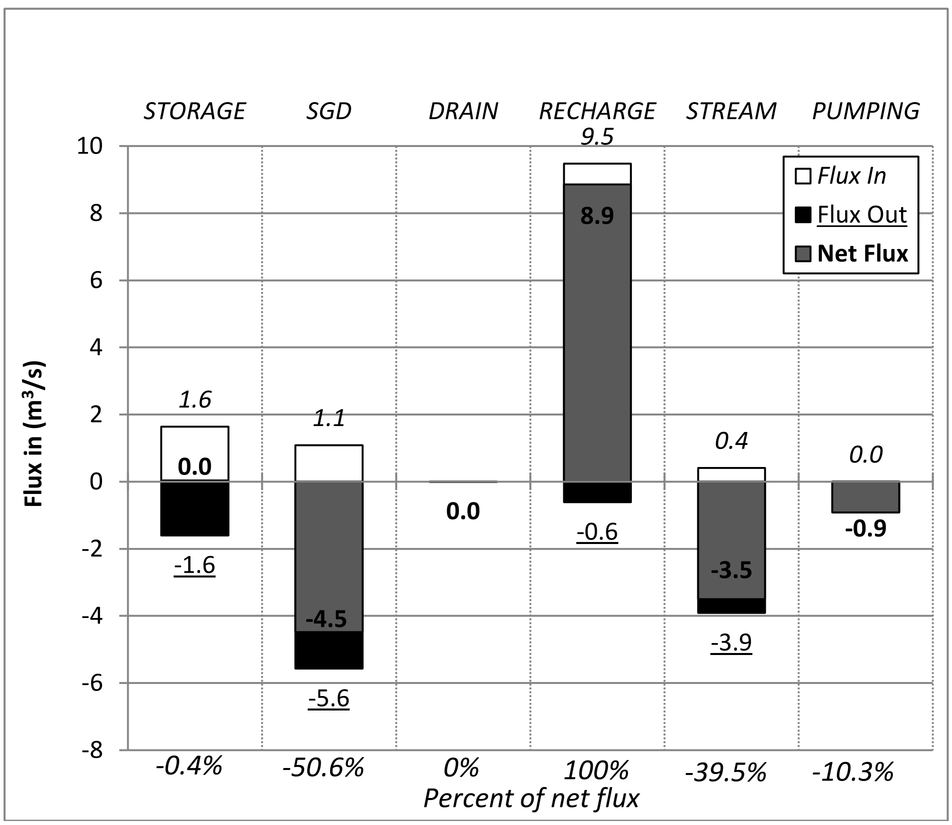

Figure 2.8: Average flux over 12 months through boundaries in the Base transient model

Both baseflow and SGD are negatively related to recharge (R^2 = -0.84, -0.98, respectively) (Figure 2.9). The shapes of the SGD and baseflow curves indicate that SGD responds more quickly to recharge changes, while baseflow lags behind recharge on the recession side of the curve. This trend is especially noticeable in the months of June and July, when baseflow exceeds SGD. Water is lost from storage during the 4 driest months and enters storage during the 6 wettest months; net storage change during September and August is near zero.

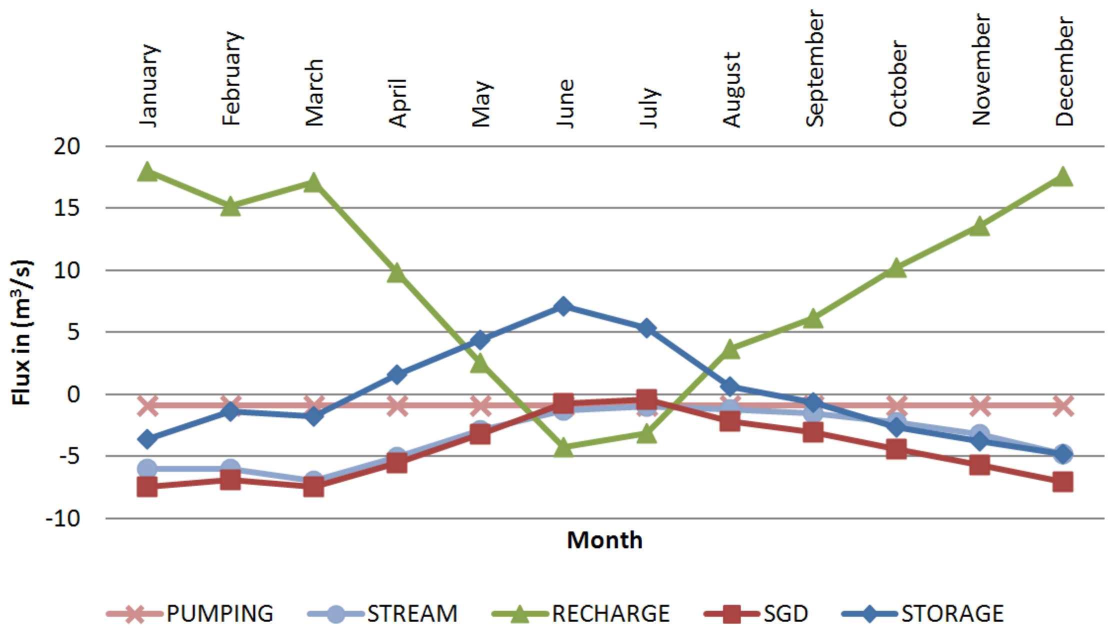

Figure 2.9: Monthly average boundary fluxes over 12 months in the Base transient model

2.6 Sensitivity Analyses

Analyses were conducted to determine the sensitivity of fluxes to uncertain parameters and boundary conditions. Each tested parameter was increased and decreased so that effects on SGD, baseflow and the relation between the two could be inferred (Tables 2.4a & 2.4b). Global changes in Kx have the largest impact on the balance of discharge between the bays and streams. An increase of all Kx values by a factor of 10 results in an increase of SGD from 52% to 86% of all flows from the system and reduces baseflow to only 3% of flows from the system. A global decrease in Kx values has the opposite effect, more than halving SGD and almost doubling baseflow. Changes to the Kx of an individual layer affect the system similarly as changing the Kx for the entire system but changes to SGD and baseflow are of lesser magnitude than if all layers were varied in bulk. Changes to Kz are similar in effect to changes to the Kx parameter: Kz increases result in increased SGD and decreased baseflow, but changes are about an order of magnitude less than those caused by Kx variation (Table 2.4a).

Simulation results show that the hydraulic heads and fluxes from the system are more sensitive to Kx changes in shallower and thicker layers (Table 2.4a) and least sensitive to Kx changes to in the Manokin aquifer, which is to be expected as it is deepest and represents a relatively small fraction of the total model domain thickness. The system is most sensitive to changes in Kx of the Bethany Fm., which is the thickest unit. The effect of globally changing Kx values is greater than the sum of changing each layer's Kx value individually. Heads and fluxes are most sensitive to changes in Kz in the surficial aquifer, which can be attributed to the direct relation it has to surface stream and bay boundaries, which are insensitive to Kz variation in the deeper layers.

Transient model Sensitivity of the transient model to parameters was similar to sensitivity of the steady state model, so fewer parameters are presented (Table 2.4b). The effect of changing whole-model K was found to be similar in magnitude as that resulting from K changes in the steady-state simulations. The analysis also shows fluxes are sensitive to the Sy of the aquifers. Sy was shown to affect the average yearly ratio of SGD to baseflow by 10% over a range of reasonable values (Table 2.4b).

Table 2.4a: Results of steady-state sensitivity analyses. Table shows response of modeled SGD and baseflow to stress and hydraulic parameter variations. The upper cell in each box shows whole model discharges across SGD/stream boundaries (m^3s^{-1}). The lower cell in each box shows the percent of SGD relative to baseflow. Blue color bars show relative flux variation in model runs where recharge or pumping were varied. Red and Green color bars show relative flux variation in model runs where Kx or Kz (respectively) were changed.

	Stress Multiplier					
Parameter	0.5	0.9	**Base**	1.1	1.5	2
Recharge	2.5 / 1.0	4.3 / 2.8	**4.6 / 3.3**	5.0 / 3.8	6.3 / 6.1	X
	259%	152%	**140%**	130%	104%	
Pumping	4.8 / 3.6	4.7 / 3.4	"	4.6 / 3.3	4.5 / 3.0	4.3 / 2.8
	134%	136%		141%	146%	154%

	Kx Multiplier			Kz Multiplier		
Parameter	0.1	**Base**	10	0.1	**Base**	10
All	2.2 / 5.8	**4.6 / 3.3**	7.7 / 0.3	4.3 / 3.7	**4.6 / 3.3**	4.9 / 3.1
	37%	**140%**	2662%	116%	**140%**	158%
Surficial	4.3 / 3.7	"	6.4 / 1.5	4.5 / 3.5	"	4.7 / 3.3
	116%		417%	128%		143%
Beaverdam	4.2 / 3.7	"	6.5 / 1.5	4.4 / 3.5	"	4.7 / 3.3
	114%		431%	127%		143%
Bethany	4.0 / 3.9	"	6.6 / 1.3	4.4 / 3.5	"	4.7 / 3.2
	102%		507%	127%		145%
Manokin A	4.4 / 3.6	"	5.9 / 2.0	4.6 / 3.3	"	4.6 / 3.3
	123%		294%	139%		140%
Manokin B	4.5 / 3.4	"	5.4 / 2.5	4.6 / 3.3	"	4.6 / 3.3
	132%		217%	140%		140%

Table 2.4b: Results of the transient model sensitivity analyses. Value display scheme as in Table 2.4a except that blue bars show relative flux variation in model runs where Sy was varied.

Parameter	Parameter Multiplier 0.1	Parameter Multiplier **Base**	Parameter Multiplier 10	
All Kx	-2.2 / -5.8 37%	-4.6 / -3.4 134%	-7.6 / -0.4 2104%	
All Kz	-4.2 / -3.8 111%	"	-4.8 / -3.2 151%	
	Parameter Multiplier 0.5	Parameter Multiplier **Base**	Parameter Multiplier 2	Parameter Multiplier 3
All SY	-4.5 / -3.5 128%	-4.6 / -3.4 134%	-4.6 / -3.4 137%	-4.6 / -3.3 138%

2.6.1 MODPATH Results

MODPATH-derived groundwater ages of SGD in the Inland Bays ranged from 2.1 days to 8.1 million years with a median age of 19.4 years (Figure 2.10). MODPATH points were distributed evenly throughout the bays thus so groundwater ages in each cell were weighted by flux (Figure 2.11). A plot of this data illustrates that a large portion of water discharging as SGD is young (45% is younger than 1 year; 88% is younger than 10 years). It is clear that ages are generally young (<10 years) in areas of high discharge; water with longer residence times (>10 years) contributes to only a small portion of flux into the Inland Bays.

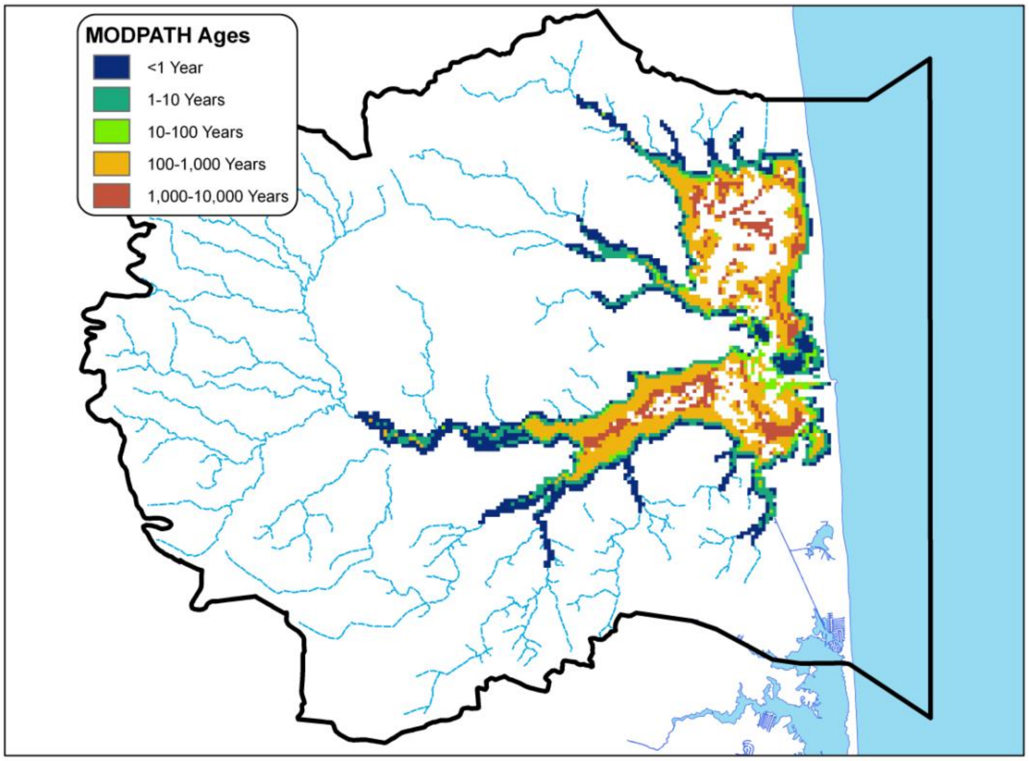

Figure 2.10: MODPATH-modeled residence times for water discharging as SGD through a particular cell.

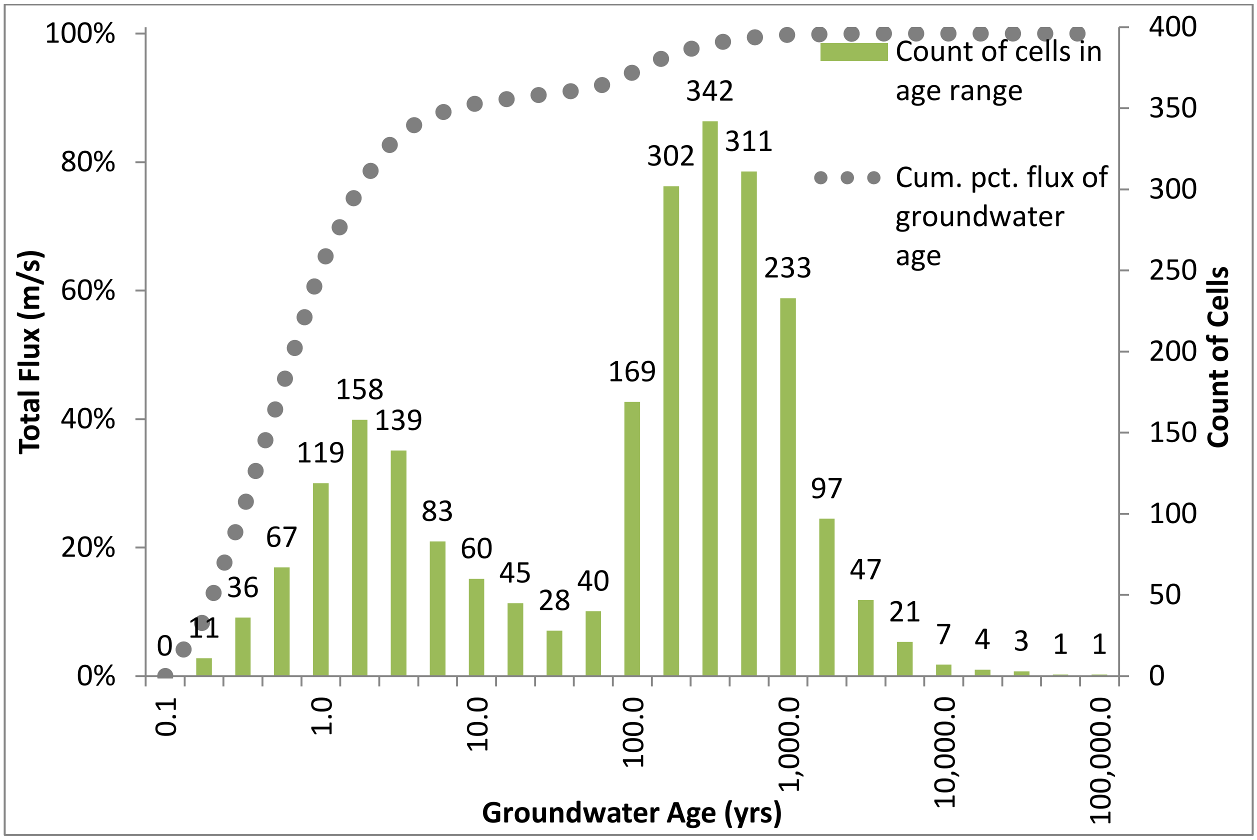

Figure 2.11: Plot of modeled residence time vs. SGD rate for each bay cell. SGD in the majority of cells is older than 10 years, but close to 90% (by volume) is less than 10 years old.

2.7 Discussion

2.7.1 Water Table Elevation Relative to Land Surface

The water table elevation is the primary control on the proportion of water between aquifer discharge as SGD or baseflow. Both the stream and constant head boundaries are head-dependent flux boundaries, so the elevation of the water table in a model cell relative to the boundaries directly controls flux of an individual cell through a stream or SGD boundary. In cells with these boundaries, an increase in water table elevation relative to the boundary causes additional water to flow through these boundaries. At constant head boundaries elevation of the water table is linked to the constant head elevation and the hydraulic gradient is limited by what are frequently low topographic gradient. So long as there is any hydraulic gradient toward the bay, SGD will be non-zero. At stream boundaries, head increase yields increased baseflow. Unlike the SGD boundary, baseflow will turn off if head drops below the stream elevation in a cell even though a hydraulic gradient may still drive flow to the bay. This illustrates the nonlinear response of baseflow to hydraulic head changes within a cell. Furthermore, this shows that SGD occurs over a wider range of water table elevations than baseflow.

Because all simulations are steady state (or transient steady state over an annual period), net change to aquifer storage is zero and increased recharge to the aquifer translates directly to increased discharge from the aquifer. Water primarily exits the aquifer as either SGD or baseflow (Table 2.4, Figures 2.6 and 2.8), so it is flux through these boundaries that is most affected by variations in model input.

The main controls on water table elevation are recharge, hydraulic conductivity, and topography as they determine relative hydraulic head gradients to streams and the coastline. These three controls are interrelated and intimately linked to the flux of water through boundaries and especially the distribution between baseflow and SGD.

2.7.1.1 Recharge and Pumping

Model results (Table 2.4a) show that higher recharge values favor an increase in the proportion of water discharging as baseflow; conversely, decreased recharge yields a lower proportion of flux to baseflow. This agrees with the conceptual model (discussed in section 2.7.1) as recharge increases directly result in increased water table elevation. This increased water table results in increased head gradients to stream boundaries that had already been flowing. If increased recharge in a cell raises the water table elevation from below a stream boundary to above it, baseflow will flow across the boundary where discharge had previously been zero. Simulations reveal that increased recharge preferentially favors an increase to discharge as baseflow over SGD, likely a product of the non-linear nature of the stream boundary.

Accurate representation of the recharge boundary is extremely important for groundwater models, but recharge boundaries are difficult to constrain because estimates have high uncertainty [Sophocleous, 2003; Chinkuyu et al., 2008]. Simulations results show variation of recharge over a reasonable range yields consistently higher SGD than baseflow (Table 2.4a). Though SGD is consistently greater, the SGD/baseflow proportion varies widely.

The amount of water extracted by pumping in the watershed affects both SGD and baseflow fluxes similarly to that expected by an equal and opposite change to recharge. Doubling the pumping in all wells decreases the amount of water leaving through both SGD and baseflow, but has a preferential impact on baseflow (SGD and baseflow decrease by 7% and 15%, respectively) (Table 2.4a). This uneven effect may be expected for the same reason as from recharge variation; distributed pumping lowers the water table throughout the entire watershed so fewer areas of the water table rise above the elevation of nearby stream boundaries. Changes to pumping have only modest effects on the system compared to recharge, because the estimated Base pumping rates are much smaller than recharge values.

2.7.1.2 Hydraulic Conductivity

Hydraulic conductivity is directly related to water table elevations through Darcys Law. Assuming other values are equal, decreased K yields a proportional increase to water table elevation and proportional increase to baseflow compared to SGD. The sandy sediments of this aquifer have high K values and thus low hydraulic gradients, which in part explains the relatively high proportion of groundwater that discharges as SGD. This conclusion holds true for both Kx and Kz, but the model is less sensitive to changes to Kz than Kx (Figure 2.4a). Because increased Kz values allow water to more easily move from deeper to shallower (and vise-versa) the correlation between increased Kz is linked to less resistance for water to migrate to a deeper layer and move through the system. This increases the effective transmissivity by increasing the aquifer thickness through which water may flow.

2.7.1.3 Topography

Flux through stream and SGD boundaries depends on the hydraulic gradient between the water table elevation and the modeled or prescribed head of the boundary. Recharge and conductivity have a large impact on the water table elevation, but the topography controls the elevation of the boundary. So it is the relation between land and topographic elevation that controls flux.

Topography is well defined compared to other parameters but it is clear that cells with deeper stream valleys have greater baseflow for a given water table elevation. In areas where stream are more deeply incised, baseflow should be elevated compared to if stream incision were less prominent.

Near the bays the maximum hydraulic gradient is topographically limited, which limits the maximum potential flux through nearby SGD boundaries. This is shown in model results where elevated SGD values are found in areas with greater topographic relief, but not in lower-relief areas closer to the Atlantic coast (Figure 2.12).

The Delaware Inland Bays system is unique because arms of the bays reach far inland to areas with greater relief. In comparison, coastal bays in the neighboring states of Maryland and New Jersey are generally more linearly-shaped back-barrier bays [e.g. Oertel and Kraft, 1994]. The Indian River and Rehoboth Bays reach far inland to areas of higher topographic gradient where higher hydraulic gradients can exist without topographic limitation. In these areas, water tables are correspondingly elevated (Figure 2.7a). Here, hydraulic gradients are not as limited by low-relief and can drive larger amounts of SGD than in the lower-elevation nearshore regions where topography limits recharge to a greater extent.

2.7.2 Bay/Aquifer Boundaries

The dividing line that demarcates areas that drain to streams and areas that drain to the estuary is important as it determines how SGD and baseflow are classified. Flux from boundaries in the Base model was divided into: (1.) fluxes through stream boundaries as baseflow; and fluxes through constant head boundaries as SGD into (2.) the upper bay; (3.) the bays proper; (4.) the Assawoman Bay and Canal; and (5.) the Ocean (Figure 2.12). Delineations separating these regions are somewhat arbitrary in tidal systems, but illustrate that the definition of ‘bay’ vs. ‘stream’ (and thus SGD vs. baseflow) greatly affects calculated fluxes. In the Base model more flux leaves the model as SGD than through stream boundaries; the majority of SGD is to the upper, streamlike arms of the bay. A slight shift in the representation of the boundary between the bays and contributing streams could significantly alter the ratio of SGD to baseflow. Sanford [2011] previously showed the importance of how aquifer-bay boundaries were by defined by showing that baseflow to streambeds between 0 and 1 m above sea level accounts for approximately 20% of total discharge from the Delmarva Peninsula; with tidal ranges of 1m throughout much of the Delmarva, a portion of this baseflow is likely SGD. Figure 2.12 also makes clear that the inclusion of Assawoman Bay and Canal within the model domain results in increased modeled SGD over what flows only to Indian and Rehoboth Bays; but, because of low discharge rates to Assawoman Bay, inclusion does not greatly affect model interpretations. The bays intercept groundwater that might otherwise discharge to the ocean because they span almost the entire shore-parallel width of the watershed; SGD to the ocean is accordingly low.

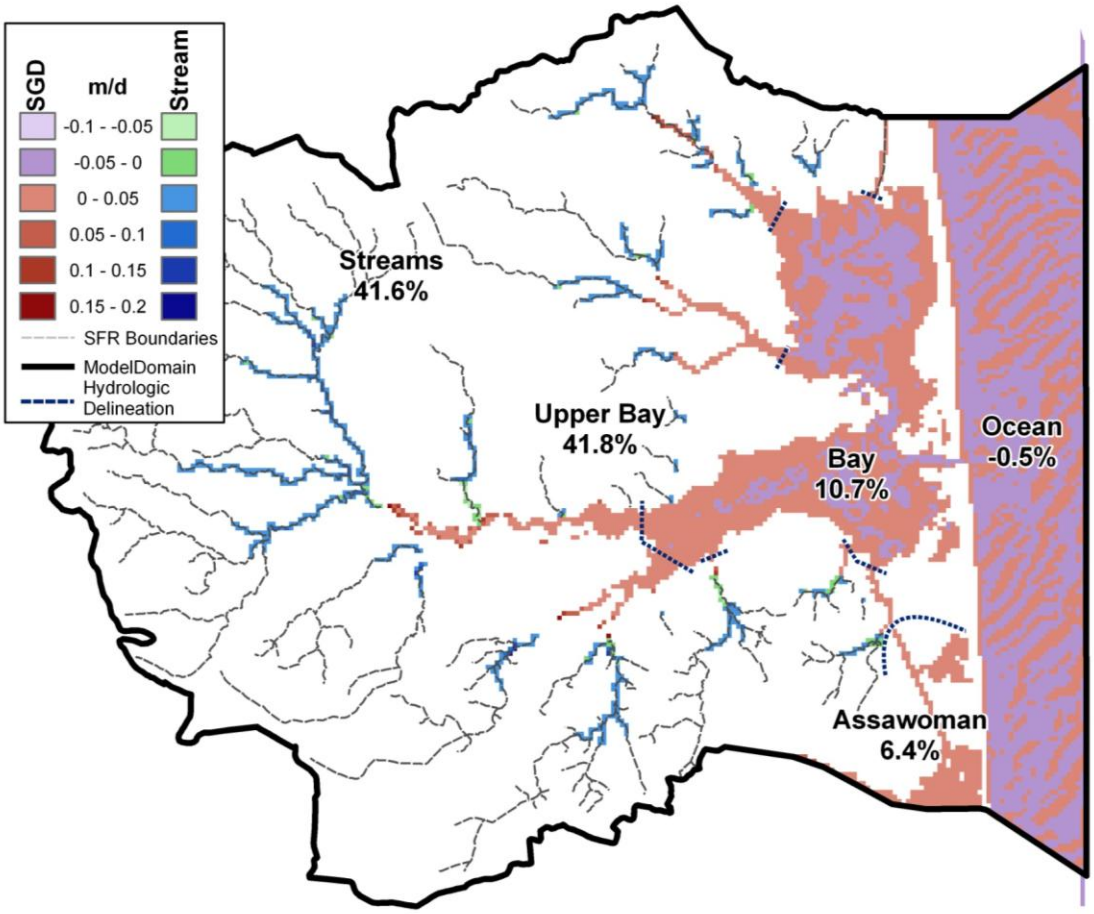

Figure 2.12: Discharges through bay vs. stream boundaries. Time-averaged fluxes to different parts of the system are plotted by color (SGD flux in red and purple, baseflow flux in blue and green). "Upper bay" refers to all channelized portions of the bays landward of the dashed "hydrologic delineation" line, which is arbitrarily drawn at the bayward end of linear bay arms.

2.7.3 Comparison to Previous Studies

2.7.3.1 Submarine Groundwater Discharge Rates

The simulations suggest that greater than half of the groundwater recharge in the model domain leaves the aquifer as SGD, which is significantly higher than expected for the Delmarva Peninsula as a whole and the global average. A model of the entire Delmarva Peninsula predicts that fresh SGD accounts for about 5% (up to 25% of flux to rivers and bays cells of elevation < 1m) of all freshwater leaving coastal aquifers [Sanford, 2011]; estimates of global values vary widely but generally range from 1-10% of river discharge [Zektser and Loaiciga, 1993; Taniguchi et al., 2002]. Sensitivity analyses show that K is a primary factor affecting the proportion of SGD compared to baseflow: higher K values resulted in elevated SGD. Thus, the high permeability of sandy sediments in this and other sandy watersheds results in a large direct freshwater discharge and groundwater-associated nutrient load into these estuaries.

2.7.3.2 Spatial Distribution of SGD

The spatial pattern of modeled SGD (Figure 2.12) is similar to patterns inferred from satellite thermal imagery [Wang et al., 2008]. The thermal imagery was collected during cooler winter months, so warmer surface water values were presumably indicative of high SGD. Thermal values were highest along shorelines with the neighboring landscape is characterized by high topographic gradients and convergent flowpaths such as the Indian River and other creeks reaching westward from the two bays, while lower-lying coastal shorelines and especially bay centers are marked by cooler values. Along the north shore of Rehoboth Bay, warm thermal values indicate relatively high groundwater discharge rates that are not simulated by the model. A small fraction of exchange (0.5%) occurs across the ocean bed as an artifact from the equivalent freshwater head simplification of the boundary condition, but this does not affect overall conclusions

2.7.3.3 Groundwater Ages

MODFLOW particle ages are consistent with field measurements of groundwater age. Bratton et al. [2004] analyzed groundwater ages of water collected from wells offshore of Holt's Landing, with a variety of natural tracers. Estimations of freshwater age were based on 4 analyses for each sample location. Predicted ages from ^3H-^3He, SF_6, and CFC-12 analyses ranged from 22 to 37 years while tritium concentrations suggested ages between 4.4 and 9.3 years. MODPATH simulations predict water discharging along the Holt's Landing shoreline ranges in age from 2 days to 5.3 years in age. This result falls within the range of field measured values.

The absence of geological complexity and non-conservative transport from the current model may partially explain why the non-tritium ages are older than modeled ages. Samples collected for age analysis were collected from below a bayfloor aquitard that forces terrestrial freshwater offshore beneath the confining layer, which lengthens the flowpath and presumably increases residence time [Bratton et al., 2004]. MODPATH-predicted ages ignore dispersion, so whereas field samples of water are a mixed sample of waters with different ages tracked particles give a single age value. These mixed samples may contain older water extracted from confining layers and younger water from permeable layers; this may explain the inconsistency between different dating methods [Böhlke and Krantz, 2003].

2.7.4 Response to Seasonal Forces

Comparison between steady state and transient models shows that SGD and baseflow flux rates respond to seasonal recharge variations but fluxes through each boundary are similar to the steady state model. Recharge changes are quickly reflected in SGD rates, but baseflow response lags (Figure 2.9). This lag yields an SGD 5% greater than baseflow during March but 73% greater during August.

Because algal blooms and other biological effects of eutrophication are less likely in winter due to lower temperatures and limited sunlight, this seasonal nutrient loading may decrease the loads of nutrients available to harmful organisms during their most productive seasons versus that expected from the average annual load. Estimated residence times of surface water are 90-100 days for Indian River Bay and 80 days for Rehoboth Bay [DNREC 1995]. Thus, nutrient loads delivered in autumn and early winter have the potential to flush from the system prior to spring and summer growing seasons. Conversely, SGD rates are highest between January and March, so a 3 month baywater residence time suggests these elevated winter nutrient loads will remain in the bay at the beginning of the growing season.

2.8 Conclusions

Submarine Groundwater Discharge to estuaries is controlled by a complex relationship between heterogeneous geologic properties and temporally-varying forces on a range of time scales. Because fresh discharge to estuaries is the primary pathway for new chemicals to enter, and the chemical composition and along-path chemical evolution of surface and ground waters are distinct, it is important to understand the factors controlling the balance between SGD and stream baseflow. Simulation results with best-estimate parameter values suggest 52% of recharge discharges as SGD, which is greater than generally expected for Mid-Atlantic coastal watersheds.

The controls on the proportion SGD to baseflow were complex. The water table elevation relative to boundary elevations directly controls the balance between baseflow and SGD locally. Water only exits the system as baseflow if the water table elevation is higher than the stream boundary. So, lower water table elevations preferentially favor SGD over baseflow whereas baseflow preferentially increases when the water table is raised in relation to stream beds. Topography is well defined compared to other parameters, so the elevation of the water table (controlled by K and recharge) is the most important variable. That bay arms reach to higher elevation inland is a less direct control on the balance. Groundwater discharged directly to these bay arms instead of upland streams as would be expected in a watershed where estuaries did not reach far inland.

Determination of the effect of different parameters on the magnitude and proportions of fresh SGD and baseflow to the estuary was determined sensitivity analysis across reasonable ranges of parameter values. Of tested parameters, the system is most sensitive to K because it controls the elevation of the water table for a given recharge rate and thus how much water exits as baseflow. For the same reason it is also sensitive to recharge for a given K distribution.

Understanding controls on the balance between SGD and baseflow and net fresh SGD rates is important from an ecological standpoint because groundwater is known to carry elevated loads of nutrients and other chemicals and different amounts of chemical cycling/transformation occur along fast pathways in streams than in slow SGD pathways. Elevated groundwater discharge rates could have implications for estuarine nutrient loading. From a management standpoint, this work suggests that when the water table is elevated, additional nutrient-rich SGD may be expected, but that even at low water table elevations, SGD is a continuous source of nutrients to coastal waters.

Solutes in SGD encounter different chemical pathways than those carried by streamflow, which has implications for the quantity and form of nutrients and other contaminant as they enter estuaries. This may result in elevated nutrient loads from SGD as compared to baseflow. Thus, the implication of elevated SGD flux is that nutrient loads to the bay are greater than otherwise expected. These higher discharge rates could result in increased risk of eutrophication or other nutrient-related ecological issues.

Simulations suggest that greater than 40% of groundwater is greater than a year old and 10% is greater than 10 years. Compared to surface water, these long residence times show that much of the groundwater–borne nutrient load will be delivered to the bay years after recharge. Thus, it will take years before efforts to reduce nutrient loading to land surface will be seen in reduced nutrient loading through SGD. It is important for managers to consider implications of these complexities in estimates of SGD and related nutrient loads.

Chapter 3

GEOLOGIC CONTROLS ON GROUNDWATER SALINITY AND DISCHARGE INTO AN ESTUARY

3.1 Introduction

Submarine groundwater discharge (SGD), the flow of water across the sediment/water interface from the seabed to the coastal ocean [Burnett et al., 2006]. SGD is an important source of nutrients to coastal waters, often with harmful effects to ecosystems [Johannes, 1980; Slomp and Van Cappellen, 2004; Bowen et al., 2007]. The fresh component of SGD contributes new nutrients to coastal systems, thus quantification of the fresh and saline components is important for estimation of nutrient loads. The distribution of SGD is also important because processes that affect the evolution of nutrients and oxidative precipitation of metals [e.g. Charette and Sholkovitz, 2002; Kroeger and Charette, 2008; Santoro, 2010] can occur along groundwater flowpaths prior to discharging as SGD. Geologic features have been shown to act as hydrogeologic controls on SGD [e.g. Krantz et al, 2004; Mulligan et al, 2007; Bokuniewicz et al. 2008; Weinstein et al., 2011]. In the mid-Atlantic region, large features such as low-permeability paleovalley fill sequences complicate coastal groundwater flowpaths already convoluted by bedding-scale heterogeneity and variable-density flow. However, SGD is often estimated with methods that provide spatially averaged predictions of SGD on the scale of kilometers, but cannot be used to characterize the spatial distribution of SGD on small scales. These include tracers such as radionuclides [e.g., Moore, 1996; Abraham et al., 2003] and salinity [Lee and Kim, 2007; Ganju, 2011], water budgets [e.g. Cambareri and Eichner, 1998], and numerical models [e.g. Langevin, 2003]. Direct measurements of SGD with seepage meters are better suited to investigate some types of geologic effects of spatial discharge patterns, though a large number of measurements must be combined to overcome often extreme small-scale heterogeneity [Michael et al., 2003; Cable et al., 2006; Rosenberry and LaBaugh, 2008]. Direct measurements also enable separation of fresh and saline components of SGD.

Numerous processes drive saline exchange flux across the sediment/water interface and are responsible for the saline SGD component. The angled density fresh/saline interface drives saltwater circulation [Cooper et al., 1964]. Waves [Shum, 1992; King et al, 2009], currents [Precht and Huettel, 2003; Cardenas and Wilson, 2006], tides [Lee 1977, Taniguchi, 2002], and bioirrigation [Martin et al., 2006] are also known drivers of shallow saline exchange at the seafloor, among other mechanisms. These smaller-scale processes are expected to produce zero net discharge on the temporal (tide, wave) and spatial (wavelength or bedform width) scales of exchange; inflow should balance outflow. Seasons [Michael et al., 2005] and interannual climate oscillations [Anderson and Emanuel, 2010] can drive measurable movement of freshwater-saltwater interfaces, resulting in longer-timescale saltwater exchange.

Geophysical techniques have been widely used in coastal systems to characterize subsurface geology and pore fluids both on land and offshore. Seismic techniques are employed to image contacts between fine- and coarse-grained sediments [Bratton et al., 2004; Cross et al, 2010]. In conjunction with independent observations of sediment types, resistivity can be used to map the distribution of relative porewater salinity [Swarzenski and Izbicki, 2009; Cross et al., 2010]. These measurements may enable identification of small-scale geologic features without drilling boreholes [e.g. Evans et al., 2000] or mapping the porewater beneath large swaths of the seafloor on a scale that would be impossible without remote sensing techniques [e.g. Cohen et al., 2010]. Recently, hydrogeologists have used resistivity profiles to identify zones where fresh groundwater is present beneath bodies of saline surface water [Manheim et al., 2004; Swarzenski et al., 2008; Stieglitz et al, 2008; Viso et al., 2009], which can help guide flux measurements to spatially characterize SGD.

In this chapter the effects of geologic heterogeneity in controlling groundwater flowpaths, salinity distributions, and spatial patterns of fresh and saline groundwater discharging into an estuary are examined. Previously collected data from an array of geophysical tools (CHIRP seismic and resistivity) and resulting characterization of the geometry of a paleovalley fill feature guided direct measurements (porewater salinity and SGD flux and salinity with seepage meters) intended to characterize distributions of salinity and flux in Indian River Bay, Delaware. These measurements are interpreted in the context of the hydrogeologic system.

3.2 Study Site

Indian River Bay, Delaware is a shallow estuary (Figure 3.1) that is representative of numerous estuaries on the Atlantic Coastal Plain. The aquifer system draining to this bay consists of a stack of sedimentary units capped either by Early Pleistocene alluvium of the surficial Beaverdam Fm. or Late Pleistocene estuarine and coastal deposits [Andres, 1986; Ramsey, 2010]. Holocene sea level rise drowned the paleo-Indian River and deposited reworked fine-grained tidal channel and tidal flat deposits in the incised river valleys, creating today's shallow Indian River Bay [Chrzastowski, 1986]. These infilled paleovalley fill features were ultimately capped by low-permeability peat and estuarine mud left by marshes fringing the retreating bayshore prior to submergence by rising water of the estuary.

Numerous studies have aimed to characterize the geology, nutrient cycling, and water fluxes of the watershed in an attempt to understand and manage stresses caused by agricultural and residential development that have negatively impacted the ecosystem [e.g. Andres, 1991; Miller et al., 2003; Bratton et al., 2004; Ullman et al., 2007].

At Holts Landing State Park (HLSP), located on the south-central shore of Indian River Bay (Figure 3.1), three shore-perpendicular paleovalley fill features extend approximately one kilometer offshore [Krantz et al., 2004]. These paleovalley features are believed to control flowpaths of discharging terrestrial water into the bay [Bratton et al., 2004] so it is an appropriate location to study how geologic heterogeneity affects SGD. These paleovalley features are filled with low permeability peat and mud and are up to several meters thick. The paleovalley caps are generally overlain by a thin (perhaps 10-50 cm) layer of more permeable, sandy sediment deposited in the modern bay. The shallowest regionally continuous formation at the site is the Beaverdam Fm., which is sandy and relatively permeable. At this site, the Beaverdam has a basal contact at about 30 m depth and subcrops beneath paleovalley fill features or shallow reworked bayfloor sediments in the interfluves [Krantz et al., 2004; Andres and Klingbeil, 2006]. The lack of a more continuous bayfloor aquitard suggests a hydraulic connection between the bay and groundwater where the low-permeability paleovalley cap is absent.

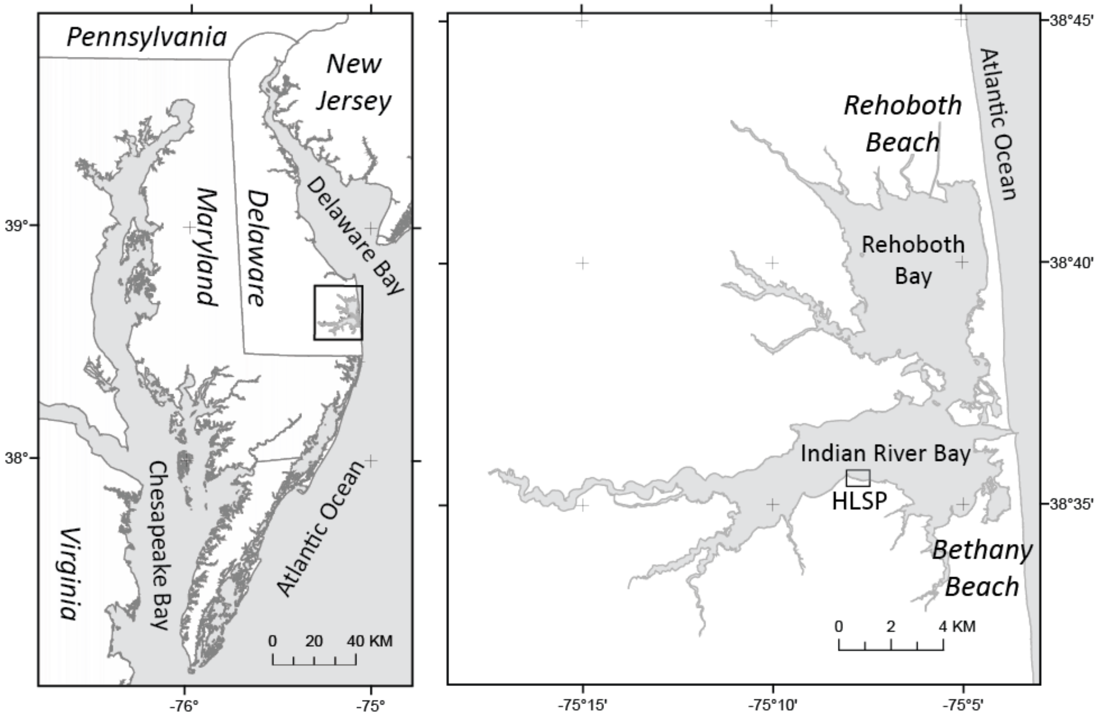

Figure 3.1: Indian River Bay and Holts Landing State Park (HLSP) study site.

3.3 Hydrogeologic Measurement Methods

Hydrogeologic investigations at this site include 1.) direct measurement of SGD with seepage meters, 2.) calculation of the proportion of fresh and saline SGD through measurement of SGD, and 3.) sampling of shallow porewater conductivity. Measurement locations were guided by interpretation of geophysical data (marine chirp seismic and continuous resistivity profiling interpretation from collaborative fieldwork shown in Figure 3.2) and borehole data. Measurement locations were determined with WAAS-enabled GPS (nominal horizontal error < 2m). Specific-conductivity of ground and surface water samples was measured with a YSI EC300 handheld conductivity instrument (expected error less than 1% of the reading) and converted to salinity [Wagner et al., 2006]. In calculations of percent freshwater and saltwater in SGD, a salinity of 0 and baywater salinity (as measured on the day of the experiment) were used to represent fresh and saline endmembers, respectively.

3.3.1 Seepage Meters

Thirty Lee-type seepage meters [Lee, 1977] were constructed to collect SGD (see Appendix A1 for figure and details). Meters were pushed into the bayfloor so that a constant 5 cm headspace below the chamber lid was maintained. SGD was collected in thin-walled plastic bags prefilled with 2 kg of baywater, which allowed measurement of bayfloor recharge (flow from the bay into the aquifer) as well as discharge (flow from the aquifer into the bay) [e.g. Rosenberry and LaBaugh, 2008] from the difference between the initial (pre-filled) and final water mass. Mass was measured to an accuracy of 0.05 kg with a digital postal scale. Given deployment times of approximately 2 hours, the accuracy of total flux measurements was +/- 0.20 cm/d. Assuming that baywater used to prefill the bag did not mix with water in the headspace, the salinity of discharging groundwater (S_{SGD}) may be calculated

$$S_{SGD} = \frac{S_f * M_f - S_i * M_i}{M_f - M_i}$$

where S_i and S_f are measured salinities of water in the bag before and after deployment, respectively, and M_i and M_f are initial and final bag mass, respectively.

Five-hundred-and-fifty-two seepage meter measurements were collected on 11 days between July 2010 and June 2011 (Figure 3.2). Two to 6 2-hour measurements were collected during each deployment in order to measure temporal changes in SGD on a tidal time scale and to provide an indication of measurement reproducibility. SGD was measured over a complete 12-hour tidal cycle on July 15 and 16, and again on August 12, 2010. Seepage meters were deployed on August 12, 2010, as well as

March 28, May 25, June 1 and June 22, 2011 at duplicate locations to detect seasonal changes. Two clusters of 5 tightly-spaced meters (less than 2 m apart) were deployed on July 7 and 8, 2010 to analyze small scale spatial heterogeneity of SGD. Five 2-hour measurements were recorded over the 2-day period from each meter.

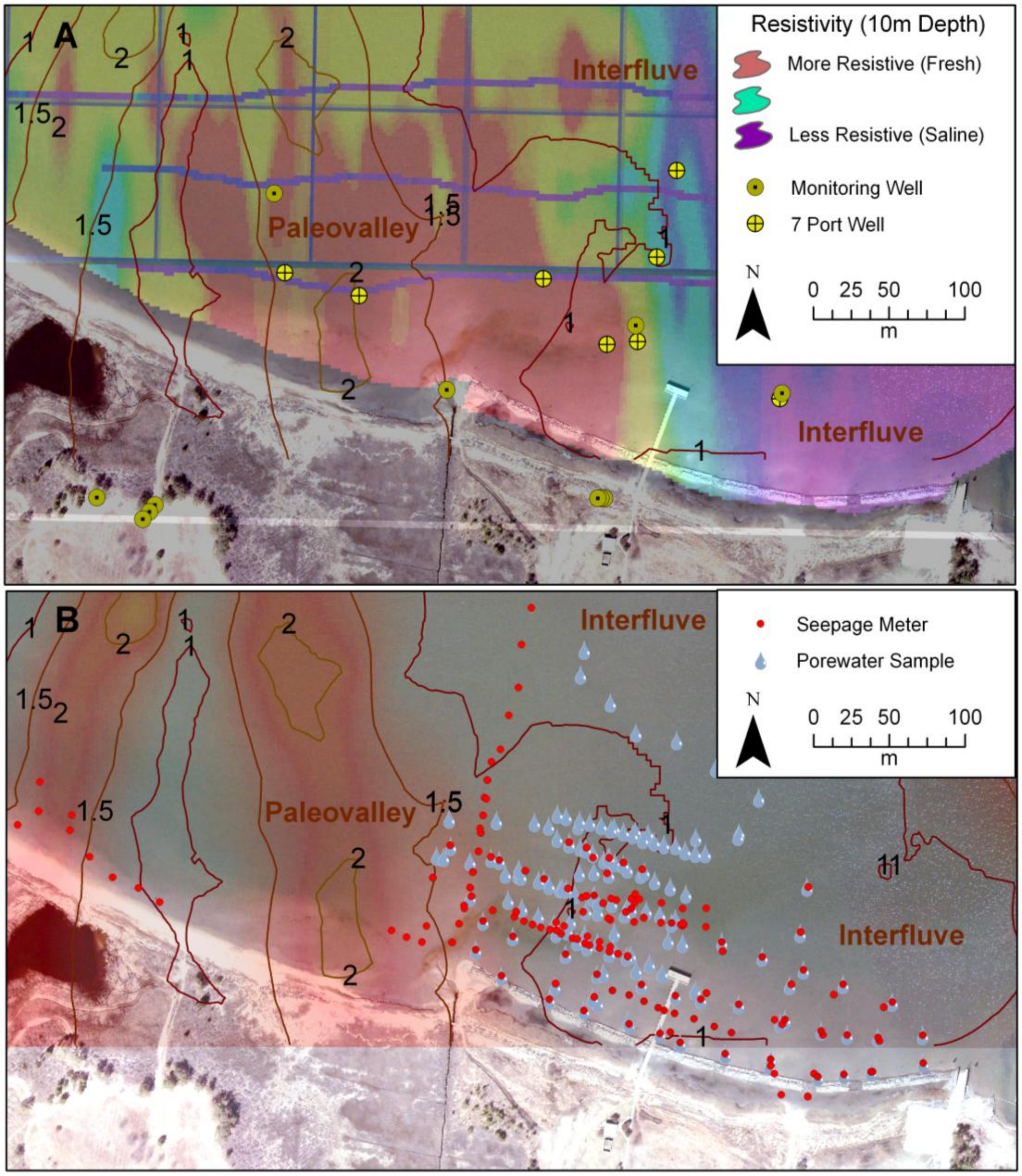

Figure 3.2: Overview of hydrogeologic and geophysical field work conducted at the field site during and concurrent with this study. Panel A.) shows monitoring wells and contours of paleovalley thickness (0.5 m contour interval) overlain on resistivity survey data. Panel B shows seepage meter and porewater sample locations and contours of paleovalley thickness (0.5 m contour interval) overlain on paleochannel thickness shading.

The time required to completely flush baywater trapped in a seepage meter during installation such that salinity of water entering the seepage meter bag was equal to S_{SGD} (equilibration) is dependent on the magnitude and salinity of SGD. The number of chamber volumes required for equilibration can be determined by multiplying the seepage rate by the equilibration period and dividing by the chamber volume Data loggers recording conductivity (CTDs) were deployed inside seepage meters on three occasions to determine the equilibration period.

3.3.2 Porewater Sampling

Ninety-two pore water samples were collected by inserting a 0.64 cm diameter stainless-steel pipe screened over 5 cm manually to a depth of 20 cm below the bay bottom (Figure 3.2) and withdrawing water with an attached syringe. Care was taken to avoid applying excess suction, which could induce leakage of baywater along the sampler and into the screen. Eight pairs of porewater measurements located 2 m apart were collected in close proximity (within 1 m) to seepage meters for comparison with SGD salinity. Salinity was measured immediately in all samples. These pairs also allowed evaluation of small-scale spatial variability in shallow porewater salinity.

3.4 Results

3.4.1 Submarine Groundwater Discharge Rates

3.4.1.1 Seepage Meter Equilibration Periods

Equilibration required a flux equal to 5.0 and 6.4 times the headspace volume for the two meters capturing SGD with salinity different than that of the baywater (Table 3.1). SGD salinity was the same as baywater in the third meter, so essentially equilibration was immediate. In this study, we report only salinity values measured in meters installed more than 2 days (average 4.6 days) prior to measurement, these are considered be equilibrated. This occurred for 299 of the 551 seepage meter measurements. The number of headspace volumes passing through each meter prior to first measurement was calculated; 87% of meters used to measure S_{SGD} flushed once fully and 39% flushed 5 times. We expect meters that did not flush fully were mostly saline as they showed little freshening over time. When deployed 1 week prior to an initial sampling and left deployed for another two weeks before a second sampling meters showed little sign of freshening. Thus, these low-flow meters should not affect our results significantly.

Table 3.1: Data from seepage meters with internal conductivity loggers:

	Meter 11	**Meter 21**	**Meter 32**
Deployment Salinity (mS/cm)	26.2	28.6	26.4
Equilibration Salinity (ms/cm)	0.4	28.6	17.6
Time to Equilibrate (hrs)	37	0	107
Average Measured SGD (cm/d)	16.3	1.2	7.21

3.4.1.2 Measured SGD Flux

Seepage meter measurements show substantial heterogeneity in SGD flux. The 552 measurements of total (fresh and saline) SGD (Figure 3.3a) are log-normally distributed as determined by a Shapiro-Wilk test ($p = 0.97$) [Analyse-it, 2009] with values spread over 3.5 orders of magnitude (Figure 3.4). The average measured flux (reported as specific discharge) out of the bayfloor was 12.4 ± 23.3 cm/d. Only 9 measurements recorded recharge of water into bayfloor sediments (Figures 3.3a and 3.4). 90% of measured SGD was saline (approximately 90% of SGD) (Table 3.2), which indicates high variability in total SGD was due primarily to variability in the magnitude of saline SGD.

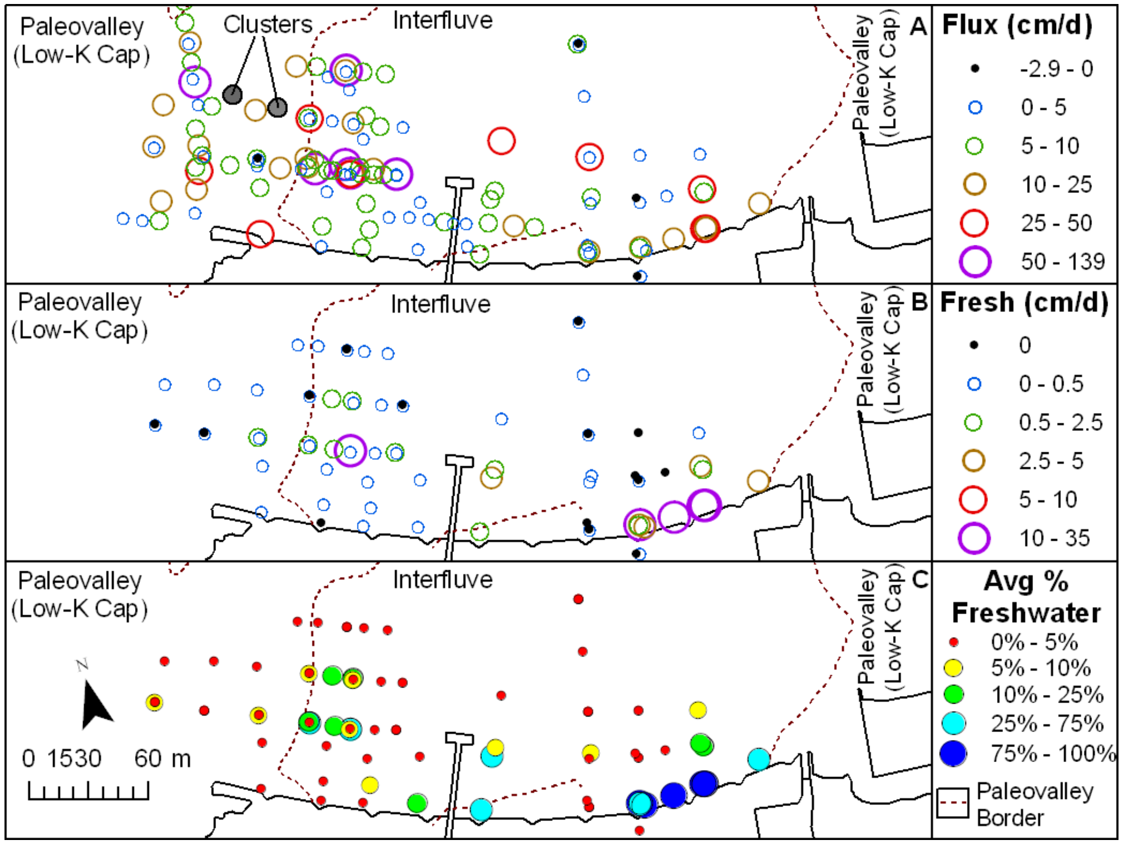

Figure 3.3: Results from direct measurement of SGD. Plots show spatial distribution of A.) total (fresh and saline) SGD flux B.) fresh SGD flux C.) SGD percent fresh as determined with seepage meters.

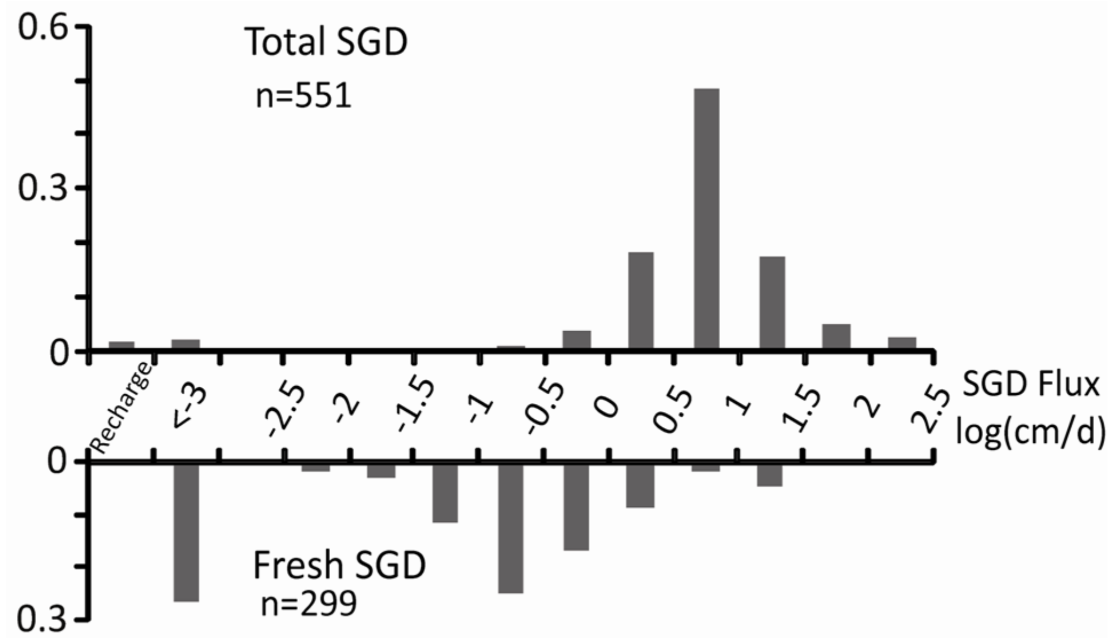

Figure 3.4: Probability mass function of log total and fresh SGD magnitudes.

Table 3.2: SGD Flux and percent fresh for seepage meter measurements. Zones are delineated in Figure 3.6. Mean, standard deviation (sigma), and range of fluxes are reported.

		Zone 1 (n=112/*88**)	Zone 2 (n=122/*72**)	Zone 3 (n=209/*61**)	Zone 4 (n=108/*78**)	All Zones (n=552/*299**)
Avg. by Meter Percent Fresh*‡		*18.9%*	*7.2%*	*2.0%*	*2.0%*	*6.6%*
Flux-Weighted Percent Fresh*†		*43.5%*	*5.2%*	*1.6%*	*1.1%*	*11.3%*
Total Flux (cm/d)	Mean	7.7	19.4	11.8	10.5	12.4
	Σ	7.9	32.0	24.6	17.3	23.25
	Range	-1.0 - 36.8	-2.4 - 149.0	-2.8 - 197.4	-2.9 - 105.7	-2.9 - 197.4
Saline Flux (cm/d)*	Mean	*4.7*	*19.7*	*8.7*	*11.1*	*10.8*
	σ	*4.5*	*33.8*	*8.3*	*19.6*	*20.57*
	Range	*-1.0 - 30.5*	*0.0 - 148.1*	*-2.8 - 35.2*	*-2.9 - 105.7*	*-2.9 - 148.1*
Fresh Flux (cm/d)*	Mean	*3.6*	*1.1*	*0.1*	*0.1*	*1.4*
	σ	*7.4*	*2.8*	*0.2*	*0.2*	*4.47*
	Range	*0.0 - 32.2*	*0.0 - 15.1*	*0.0 - 0.9*	*0.0 - 1.4*	*0.0 - 32.2*

*Italicized numbers include only measurements from 299 well-equilibrated meters used to calculate fresh and saline components of flux.‡ Avg. by Meter Percent Fresh was calculated as the average percentage freshwater of all measurements in the zone.
† Flux-Weighted Percent Fresh was determined as the sum of all fresh SGD divided by the sum of total SGD in each zone.

Freshwater accounted for only 11% of all measured SGD (standard deviation of 19.7%) in 299 well-equilibrated measurements (Table 3.2). Mean fresh SGD flux was 1.4 cm/d. Values above the detectability limit were log-normally distributed as determined by a Shapiro-Wilk test (p = 0.96) [Analyse-it, 2009] (Figure 3.4), and varied over 4 orders of magnitude. Fresh SGD flux was below detectable limits in 26% of equilibrated measurements (Figures 3.3b and c). Highest freshwater fluxes were measured nearshore and along the paleovalley edge.

Measurements from the two cluster experiments indicate that variability of SGD over a tidal timescale is less than meter-scale spatial variability. The average total SGD from cluster experiments was in agreement with other data. Large data ranges demonstrate the high variability of SGD over the spatial scale of the cluster (2 m). In both clusters, small data ranges (Table 3.3) and overlapping error bars (Figure 3.5) between measurements in different time periods shows similarity of measurements in the same meter at different times. Larger data ranges and lack of error bar overlap between measurements from nearby meters shows dissimilarity of SGD on small spatial scales. The data indicate that temporal variability of SGD on tidal cycle-scale is less than spatial variability small scale (several meters).

Table 3.3: Results of 2 cluster experiments.

	Cluster 1		**Cluster 2**	
	Average	Range	Average	Range
All Measurements in Cluster	15.3	1.0 - 72.5	20.8	3.0 - 51.0
Averaged by Meter	15.8	1.8 - 40.0	19.4	4.1 - 42.1
Averaged by Time	15.5	6.1 - 28.5	21.7	15.8 - 29.8

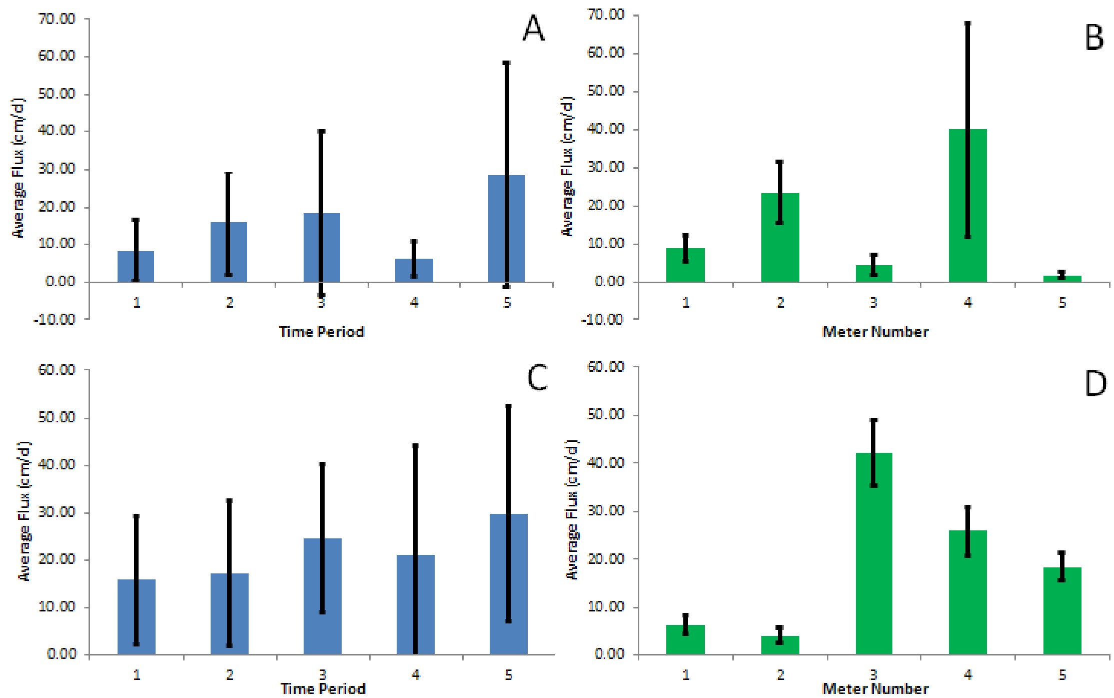

Figure 3.5: Column plots of 2 cluster experiments. Plots above (A&B) show data for cluster 1; plots below (C&D) show data for cluster 2. Plots display (A&C) average value of 5 meters in each time period in blue and (B&D) average value of measurements of all time periods for each meter in green. Error bars show 1 standard deviation.

3.4.2 Tidal/Seasonal Variation of Submarine Groundwater Discharge

No strong correlation between SGD flux and tidal stage was found in measurements made over a 12.5 hour tidal cycle in twenty meters on July 15-16, 2010 and in thirty meters on August 12, 2011. Correlation coefficients (R^2 = 0.12 and -0.72, respectively) indicate a weak negative relationship between tidal stage and average flux on one day, but correlation between individual meters and tidal stage (mean = -0.08 and 0.24 respectively) was poor on both days. Repeat measurements during different seasons were intended to test seasonality of SGD. A seasonal signal was not observable among other sources of variability.

3.4.3 Porewater Salinity Measurements

The average porewater salinity at 20 cm depth was 15% fresh with a standard deviation of 21% fresh. A standard deviation that is greater than the mean may be partially explained by geology-controlled patterns of porewater salinity distribution (Figure 3.6). A grouping of fresher porewater salinity measurements was observed nearshore in the interfluve and along the low-permeability cap edge (locations marked X in Figure 3.6). Outside of these two areas porewater was consistently less than 10% fresh. The percentage freshwater in 8 pairs of contemporaneous, porewater measurements (samples drawn at a distance of 2 m marked p in Figure 3.6) differs by 12% on average with a maximum difference of 25% (Locations). This illustrates the heterogeneous distribution of fresh porewater in these sediments. The salinity relationship between porewater and neighboring seepage meters is discussed in section 3.5.1.3

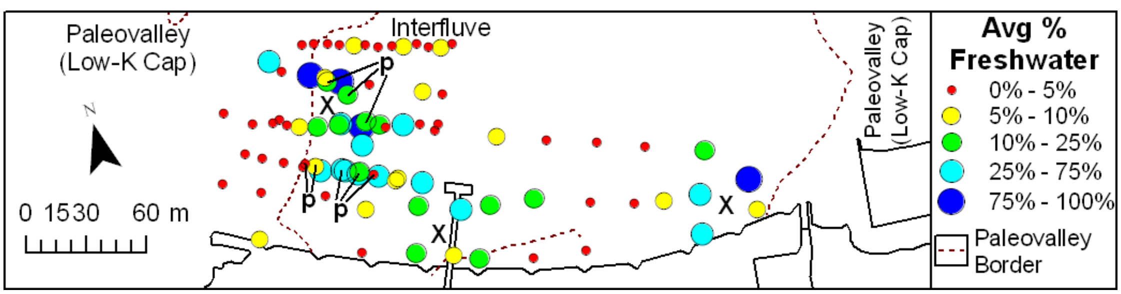

Figure 3.6. Spatial distribution of percentage freshwater in water extracted with porewater sampler. Areas near ‘X’ are freshened; ‘p’ marks locations of 8 pairs of nearby measurements.

3.4.4 Submarine Groundwater Discharge Zones

Measurements of SGD were divided into four zones based on their spatial relation to the paleovalley feature, proximity to shore, and trends observed amongst measurements in that area. This zonation allowed characterization of the effect of the low-permeability paleovalley cap on SGD; zones are labeled from freshest to most saline (Figure 3.7, Table 3.2). Zone 1 (Z1) encompasses the nearshore (<45 m from shore) in the interfluve. Zone 2 (Z2) includes a shore-perpendicular swath along the paleovalley/interfluve border. Zone 3 (Z3) encompasses the zone above the low-permeability cap of the paleovalley. Zone 4 (Z4) includes the area more than 40 m offshore in the interfluve.

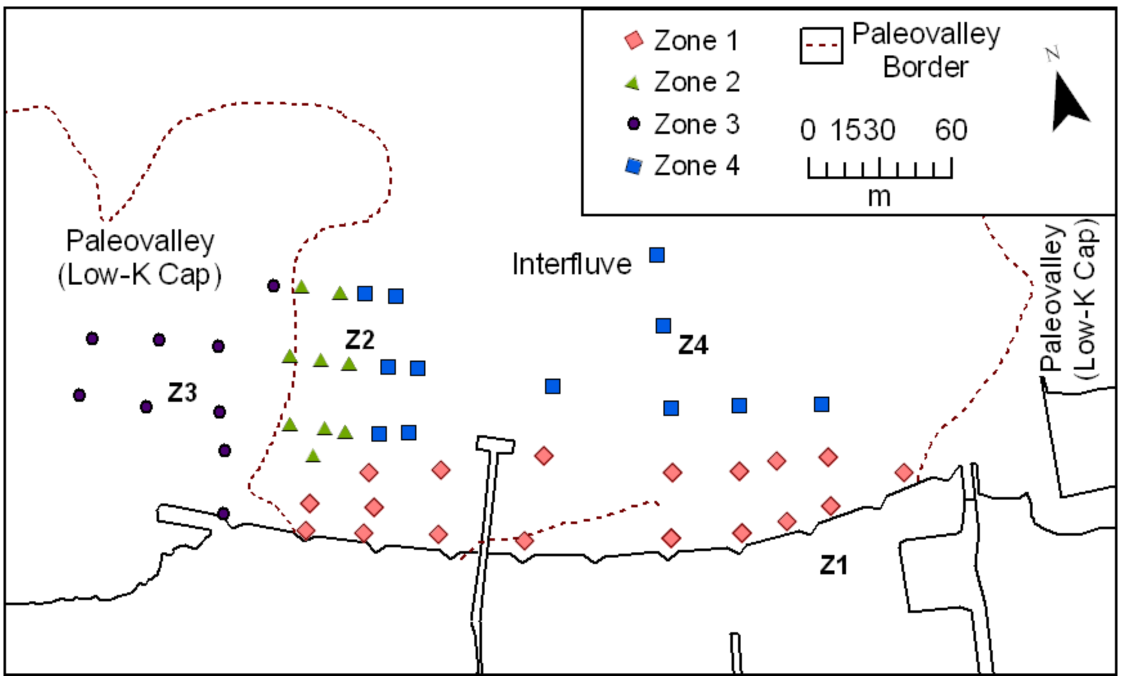

Figure 3.7: Zoning scheme based on hydrogeologic framework.

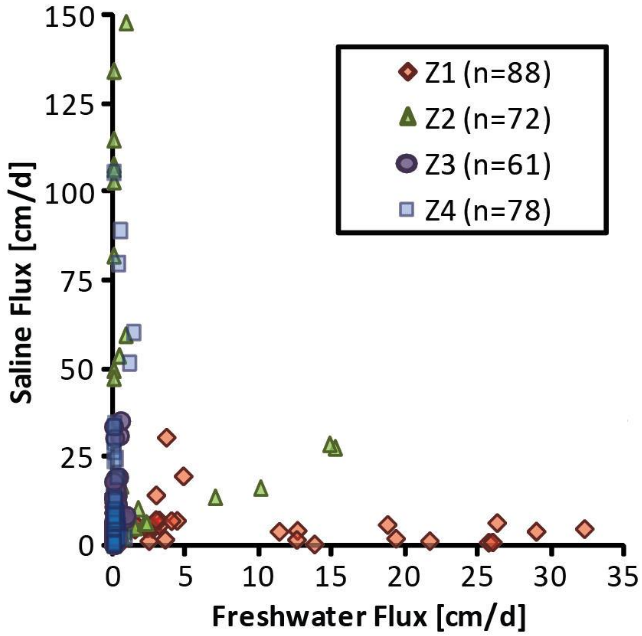

Figure 3.8: Plot of fresh vs. saline SGD by the zones displayed in Figure 3.7.

Saline SGD flux is greater than fresh SGD flux in all four zones and measurements with appreciable fluxes (> 5 cm/d) and high percent freshwater were only recorded in Z1 and Z2 (Table 3.2, Figures 3.3 and 3.8). Fresh groundwater accounted for 44% of volumetric SGD in Z1 (Table 3.2). In Z2, fresh SGD accounted for 5.2% of volumetric SGD; much less than in Z1, but measurable. Freshwater discharge was almost completely absent in Z3 and Z4 and accounted for only 1% of volumetric SGD in those zones. No measurement in either Z3 or Z4 with appreciable fluxes (> 5 cm/d) was greater than 10% fresh. Saline flux magnitudes were also different among zones (Table 3.2 and Figure 3.8). Average saline SGD flux in Z1 was 2 to 4 times lower in comparison to the other zones. Average saline SGD flux in Z3 and Z4 were similar, and on average nearly twice that of Z1. Average saline SGD into Z2 was high: double that of Z3 and Z4 and fourfold that of Z1.

3.5 Discussion

3.5.1 Conceptual Model

A conceptual model of regions where certain types of SGD are expected may be built from the geophysical framework. Fresh SGD in the interfluve should be expected to be confined to discharge near the shoreline (Figure 3.9, Z1). In the interfluve the low-K paleovalley fill sequence is expected to act as a barrier to fresh SGD such that the fresh plume is pushed offshore and fresh groundwater discharges alongside the edges of the paleovalley (Figure 3.9, Z2) but not through it. This fresh groundwater travels along longer flowpaths than water discharging to the interfluve shoreline. As such, water in the flowpaths is expected to mix with saltwater prior to discharge and the SGD measured along the paleovalley border is expected to be more saline than along the interfluve shoreline. Saline SGD is expected from two density-driven circulation cells, the first perpendicular to the interfluve shoreline (Figure 3.9, Z1) and the second perpendicular to the paleovalley/interfluve border (Figure 3.9, Z2). Temporally short-scale processes such as tides, waves and currents are expected to drive shallow saline circulation through both interfluve and paleovalley sediments (Figure 3.9, all zones).

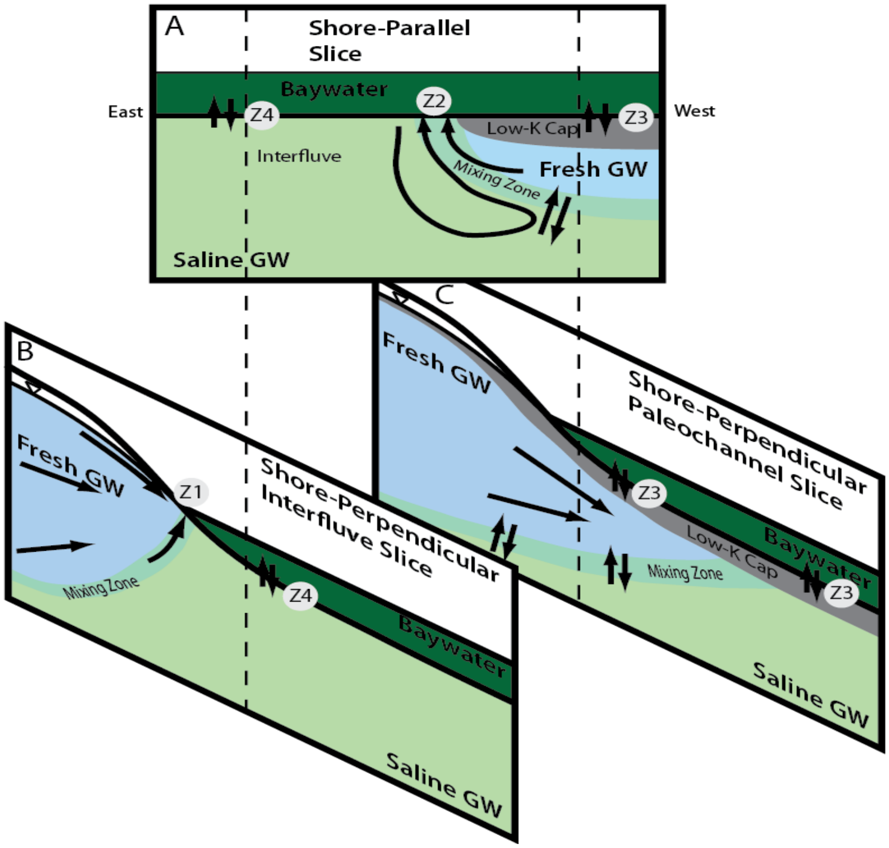

Figure 3.9: Schematic of the geophysical framework at the Holts Landing field site. Schematic depicts the low-permeability (low-K) paleovalley cap and groundwater (GW) flowpaths for A.) a shore-parallel slice across both the interfluve and paleovalley along with shore-perpendicular slices through B.) the interfluve and C.) the paleovalley.

3.5.2 Fresh SGD

In the interfluve, fresh SGD is high nearshore and absent offshore. Despite high variability in SGD flux and salinity, along the interfluve shoreline (Z1) fresh SGD averaged 3.6 cm/d and was focused (SGD > 50% fresh), while offshore (Z4) it was not different than zero (Table 3.2) and is dominated by saline recirculation (Z4) (Figure 3.3b and c, Table 3.2). These trends are consistent with the conceptual model.

Measurements of SGD across the paleovalley (Figure 3.3b, Table 3.2) support the conceptual model. Fresh SGD rates were not different from zero above the paleovalley (Z3), whereas along the paleovalley edge (Z2) fresh SGD was 7.2% of total discharge. Groundwater salinity measurements from offshore wells (Fernandez, 2012) and resistivity data (Figure 3.2) also show the existence of a fresh plume beneath the paleovalley cap in agreement with the conceptual model. This plume is absent in the interfluve sediments.

Freshwater flowing offshore beneath the low-permeability cap mixes with saline water prior to discharge to a greater extent than it does in areas not affected by this geologic feature. Resistivity and offshore well data [Fernandez, 2012] indicate that the center of the plume is fresh, with significant freshwater-saltwater mixing zones along the bottom, lateral and distal boundaries. The mixing is evident in the lower salinity of discharging water at the paleovalley/interfluve boundary (Z2) compared to salinity offshore in the interfluve and paleovalley (Z3 and Z4) (Table 3.2). Nearshore discharge from the interfluve (Z1) is 2.5 times as fresh (Table 3.2) and has 3 times the fresh flux rates (Table 3.2) as water discharging at the edge of the paleovalley (Z2). Appreciable fluxes (> 5 cm/d) of focused fresh SGD between 75% and 99% fresh were measured 11 times along the interfluve shoreline (Z1) (Figure 3.3c, Figure 3.8) while SGD along the paleovalley edge (Z2) never exceeded 38% fresh. Measurements with measurable freshwater recorded along the edges of the plume (Z2) are more diffuse than the fresher, more focused discharge along the more typical interface in the interfluve (Z1). This may be due to the lower fresh discharge velocities, which provide less resistance to mechanisms driving saltwater into the subsurface (i.e., tides, waves, diffusion; see section 3.5.3), or to longer flowpaths along the freshwater-saltwater interface extending offshore, resulting in more dispersion and interface spreading.

3.5.3 Saline SGD

The recirculated saline component of SGD is of greater magnitude in all zones than the fresh component. This is consistent with other studies in sandy aquifers that measure discharge salinity [e.g. Michael et al., 2005; Martin et al., 2007; Santos et al., 2009]. Nearshore (Z1) fresh and saline discharge components are nearly equal, but offshore (Z4) the saline component is ten times higher than the fresh component (Table 3.2 and Figure 3.3c). Saline waters exceed 50% in every measurement with appreciable fluxes (93.4% saline average), except for 11 focused fresh measurements in Z1 (Figure 3.8) (discussed in section 3.5.2).

Numerous processes may drive the large observed saline exchange flux including waves, tides currents and bioirrigation. The sum of these smaller-scale processes may produce enough net saline SGD to explain our measurements, but are expected to produce zero net discharge on the temporal (tide, wave) and spatial (wavelength or bedform width) scales of exchange; inflow should balance outflow. Because migration of offshore interfaces was not observed at Holts Landing [Fernandez, 2012] seasons [Michael et al., 2005] and interannual climate oscillations [Anderson and Emanuel, 2010] are not expected as major drivers of saline SGD. It is possible that seepage meters are preferentially measuring outflow or that the meters themselves create discharge artifacts (discussed in section 3.5.7).

Observed patterns of saline SGD are also consistent with density-driven circulation cell that runs parallel to the paleovalley axis similar to the density-driven cell. Bratton et al. [2004] and Bohlke and Krantz, [2003] determined that the plume of freshened groundwater beneath the paleovalley sediments is older (22 years) than the younger (12 years) saline pore water beside and below the plume (20 m deep) the paleovalley. They conclude that discharging freshwater must be driving a complex, rapid and relatively deep seawater circulation system beneath the paleovalley cap. Near the paleovalley edge (Z2), the average measured saline SGD flux was twice that in the neighboring paleovalley (Z3) or interfluve (Z4) (Table 3.2). High saline flux rates (50-150 cm/d) were recorded in 15 seepage meters along the border (Z2 & Z4) (Figures 3.3b and 3.8) and exceeded 36 cm/d outside of that area in only one measurement. Although saline exchange is limited in areas where fresh discharge is measureable, in Z2 there is an approximately linear correlation between fresh and saline flux in measurements with high fresh SGD (> 5 cm/d) (Figure 3.8). This linear mixing is expected where deep density-driven circulation exists [Smith, 2004], because density gradients are created by dispersion along the interface between parallel fresh and saline flowpaths. Thus, our observations are consistent with the conceptual model of a shore-perpendicular density-driven circulation cell (Figure 3.9, Z2).

3.5.4 Shallow Saline Exchange

Evidence of shallow, small-scale saline exchange processes likely driven by waves, tides, currents and bioirrigation can be inferred from porewater salinity measurements. Porewater that is less saline at 20 cm depth (2.8 % fresher) than the discharging groundwater suggests that shallow (less than tens of cm deep) exchange processes are responsible for fresh/saline mixing prior to groundwater discharge. The variability of porewater from 28% fresher to 14% more saline shows these processes are spatially heterogeneous. Porewater measurements that are more saline than neighboring SGD measurements may indicate sampling error; baywater may have been pulled down along the edge of the porewater sampler as some samples were being drawn by suction from the formation. This suggests porewater samples are skewed more saline and strengthens the case for shallow mixing.

Similar rates of saline discharge both where bay is hydraulically connected to the deeper aquifer and where the low-K paleovalley cap inhibits hydraulic connection are indicate that much of the saline SGD is driven by shallow circulation. The cap confines a freshwater plume a few meters beneath the bayfloor and fresh SGD is absent from this zone. The lack of a fresh SGD component indicates the majority (if not the entirety) of saltwater exchange occurs in the re-worked bayfloor sands in the uppermost tens of centimeters of the subsurface (Figure 3.9, Z3). SGD rates in the interfluve (Z4) where the cap is absent are only 27% larger than SGD rates in the paleovalley (Z3) (Table 3.2) suggesting shallow circulation is responsible for the majority of saline SGD.

3.5.5 Influence of Ambient Fresh Discharge on Saline Circulation

SGD measurements may be divided into two populations; one with elevated saline and low fresh flux and a less prevalent population with elevated fresh and low saline flux. Where fresh flux exceeded 1.5 cm/d, the maximum saline flux was consistently <30 cm/d, compared to values reaching 148 cm/d saline flux where fresh flux was <1.5 cm/d (Figure 3.8). Measurements where fresh flux exceeded 1.5 cm/d and 5 cm/d averaged 52% and 75% fresh, respectively, versus an average of 6.6% fresh for the entire dataset. These findings suggest that fresh discharge is impeding exchange of saltwater; the gradient driving upward fresh SGD reduces the effect of tide, wave, and current driven forces. Similar results have been observed in another estuary [Stieglitz et al., 2008; Rapaglia and Bokuniewicz, 2009], and rivers [Cardenas and Wilson, 2007].

3.5.6 Variability in Submarine Groundwater Discharge

Results of cluster experiments show that meter-scale spatial variability of SGD is much greater than the temporal variability observed at a single location on a tidal timescale. For example the ratio of standard deviation to the mean for five measurements from any single meter averaged 0.49 and 0.25 for the two clusters, compared to 0.96 and 0.85 for contemporaneous measurements within each cluster, respectively. The largest flux measured in a single meter averaged 3.8 times the value of the smallest from that same meter; the largest flux within a cluster averaged 16 times the smallest contemporaneous flux. Because seepage meters were constructed identically and deployed less than 2 m from one another, it is likely that permeability of the underlying sediments is the primary control on the spatial variability in discharge.

Variability shown by these data is consistent with other studies [e.g. Belanger and Montgomery, 1992; Michael et al., 2003], and highlight the importance of deploying a large number of seepage meters to resolve effects of geologic heterogeneity or other controls on SGD variability. Because of this small-scale variability, care must be taken comparing data from meters removed and redeployed with commonly used WAAS-GPS, which has a 2 m nominal accuracy.

3.5.7 Confidence in Seepage Meter Measurements

During the deployments in this study, seepage meters measured high rates of saline discharge from the bayfloor, but did not measure the high rates of saline recharge necessary to balance outflow. Of 552 total SGD measurements, saline discharge averaged 10.8 cm/d. Only 9 deployments recorded recharge, averaging 1.5 cm/d. Density-driven circulation is likely the mechanism with the greatest spatial separation between recharge and discharge, and seasonal or interannual exchange would produce net recharge or discharge on longer timescales. However, seepage meters were deployed at different times of year and across an area believed large enough to capture the density driven circulation, with no observable recharge trend. Thus, it is unlikely, that these mechanisms explain all of the observed saline discharge. The use of pre-filled bags minimizes potential for bags to induce flow [Shaw and Prepas, 1989] and the occurrence of low current and wave energy at this site indicate that pressure fields induced by the presence of seepage meters were not responsible [Shinn et al., 2002; Cable et al., 2006; Smith et al., 2009].

At other sites, similarly-constructed seepage meters have been shown to measure inflow [e.g. Israelson and Reeve 1944, Rosenberry and Pitlick, 2009], though most estuarine studies have measured outflow-dominated exchange [e.g. Shaw and Prepas 1989; Michael et al., 2003; Cable et al., 2006]. It is possible that seepage meters preferentially measure outflow rather than inflow, despite pre-filling bags with water, due to greater resistance to flow in the inward than outward direction [Lee, 1977; King et al., 2009]. If that is the case, then the saline outflow measured, or some portion of it, is only the outflow component of net-zero exchange processes. This would suggest that discharge measurements are likely a lower bound on the total amount of saline exchange occurring.

The repeatability of measurements from a single meter is demonstrated by the greater consistency among multiple measurements at the same location than among adjacent contemporaneous measurements (see section 3.5.6). Much of the observed temporal variation is likely caused by changes in the tide, wave, or current driven component of SGD as conditions changed throughout a day [e.g. Cable et al., 2006].

3.5.8 Implications for Chemical Fluxes

The results of this study highlight the role of geologic heterogeneity in control of fresh groundwater flowpaths toward and discharge to coastal waters. Reactions occurring along flowpaths, such as denitrification [e.g. Kroeger and Charette, 2008; Santoro, 2010] may have greater opportunity to occur in highly heterogeneous settings, resulting in reduction of freshwater-bourne nutrient load to the estuary. Mixing with oxygenated saltwater along density-driven circulation cells or in the top few centimeters of the bayfloor may similarly result in reactions; an example is the 'iron curtain' [Charette and Sholkovitz, 2002] where a change in redox potential along flowpaths induces precipitation of iron oxides that immobilize terrestrially-derived phosphorous and other solutes in fresh discharge zones. Conclusions

Geologic heterogeneity is a primary control on groundwater flowpaths, salinity distributions, and patterns, rates and salinity of SGD. At Holts Landing State Park we observe a shore-perpendicular paleovalley feature filled with low-permeability estuarine peat and clay and underlain by relatively permeably sediments of the Beaverdam Fm. This feature corresponds with a subsurface plume of terrestrial freshwater. Observations indicate that the low-permeability cap prevents nearshore fresh discharge, resulting in offshore flowpaths and discharge around cap edges. Freshwater flow in the interfluve is unimpeded by pervasive low-permeability material and the subsurface salinity distribution and discharge patterns are consistent with those associated with a density-driven circulation cell. Smaller-scale heterogeneity is also demonstrated to greatly affect SGD: neighboring flux measurements varied more than an order of magnitude.

Results of this work indicate that freshwater discharge rates and patterns differ between settings within and away from the paleovalley feature. Longer flowpaths beneath the paleovalley feature result in more extensive mixing between fresh and saline porewater prior to discharge along the shore-perpendicular paleovalley edge than that affecting freshwater discharging to the interfluve.

Saline SGD accounts for the majority of measured flux in all zones at our site and occurs in both presence and absence of fresh SGD. Saline SGD rates are lowest where fresh discharge is focused along the interfluve shoreline, moderate above the paleovalley cap and offshore in the interfluve and highest along the paleovalley edge. Low saline discharge rates in the zone of focused freshwater discharge may be due to advective fresh SGD impeding exchange of saline waters between the bay and aquifer. High rates of saline SGD along the interfluve/paleovalley border and the presence of young saltwater underlying the older freshwater plume beneath the paleovalley cap are consistent with shore-perpendicular density-driven circulation.

The impact of both large-scale and small-scale geological heterogeneity on SGD illustrates the importance of considering SGD variability when studying fluxes of water and chemicals to estuaries. Complex flowpaths with different residence times and mixing may affect chemical reactions and in turn the loads of nutrients and other chemicals contributed by SGD.

Chapter 4

CONCLUSIONS

Submarine Groundwater Discharge (SGD) is a known chemical vector to estuaries and an important source of nutrients. These nutrient loads directly impact estuarine ecology, so understanding sources and loading rates is important for managers hoping to increase the ecological health of these fragile systems.

The flux of fresh SGD to a watershed is controlled by a complex relationship between heterogeneous spatial properties and temporally-varying forces on a range of time scales. Simulation results from a Mid-Atlantic watershed suggest that 52% of recharge exits the system as SGD, which is greater than generally expected for other coastal systems. This high rate is attributed to system geometry (large estuarine area and bay arms that reach far inland) and the relation between topography, recharge and hydrogeologic properties.

Topography and water table elevation are the primary controls on the balance between stream baseflow and SGD. With a raised water table, the hydraulic gradient from aquifers to streams is increased and baseflow increases disproportionately; when the water table drops below a streambed, baseflow is shut off. SGD is not dependent on water table elevation but rather only to the hydraulic gradient. Even when the water table drops below streambed elevation, SGD occurs so long as there is any gradient toward the coast.

The water table is controlled by hydraulic conductivity and recharge. Sensitivity analyses show that horizontal conductivity (Kx) is the most important parameter controlling the SGD/baseflow; with a system flux prescribed by recharge rate, the water table elevation is primarily controlled by the velocity at which water can flow through the system. Similarly, the water table elevation is directly linked to recharge rates.

Natural heterogeneity is invariably present on many scales, but it is difficult to numerically model different scales of heterogeneity simultaneously. Data from a coastal site show geologic heterogeneity is a primary control on groundwater flowpaths and salinity distributions, which in turn affect patterns, rates and salinity of SGD. Geophysical investigation identified 3 shore-perpendicular low-K paleovalley fill sequences that controlled fresh SGD. The low-K cap prevents discharge of terrestrial groundwater nearshore and directs a fresh plume offshore to discharge around the cap edges, whereas in the interfluve fresh SGD is limited to nearshore reflecting the narrow focused outflow gap predicted by classical theory. High saline SGD rates along the paleovalley/interfluve border combined with offshore fresh SGD are consistent with a shore-parallel, density-driven circulation cell along the paleovalley edge. Neighboring flux measurements varied over more than an order of magnitude even where the underlying geology was not obviously distinct and showed spatial variability of SGD was larger than temporal variability on a tidal scale. Spatial variability was greater than temporal variability of SGD over tidal scales and could explain why tidal variations were not measured.

The impact of both large-scale and small-scale heterogeneity of coastal sediments illustrates the importance of considering SGD variability when studying fluxes of water and chemicals to estuaries. Geological heterogeneity affects flowpaths and SGD distributions, which in turn affects chemistry, so studies that neglect the variability of SGD in coastal areas will fail to accurately capture rates and effects of coastal SGD and will be limited in relevance.

REFERENCES

Abraham, D. M., M. A. Charette, M. C. Allen, A. Rago and K. D. Kroeger (2003), Radiochemical Estimates of Submarine Groundwater Discharge to Waquoit Bay, Massachusetts. Biol. Bull., 205(2), 246-7.

Analyse-it for Microsoft Excel (version 2.20) (2009), Analyse-it Software, Ltd.). [Available online at http://www.analyse-it.com/]

Anderson, W. P., Jr., R. E. Emanuel (2010), Effect of interannual climate oscillations on rates of submarine groundwater discharge. Water Resour. Res., 46, W05503, doi:10.1029/2009WR008212.

Andres, A. S. (1986), Stratigraphy and depositional history of the post-Choptank Chesapeake Group Report of Investigations - Delaware Geological Survey, 42, 39.

Andres, A. S. (1987), Estimate of direct discharge of fresh ground water to Rehoboth and Indian River bays, Report of Investigations - Delaware Geological Survey, 43, 37.

Andres, A. S. (1991), Ground-water level and chemistry data from the coastal Sussex County, Delaware, ground-water quality survey, Open File Report - Delaware Geological Survey, 33, 31.

Andres, A. S. (2004), Ground-water recharge potential mapping in Kent and Sussex Counties, Delaware, Report of Investigations - Delaware Geological Survey, 66, 14.

Andres, A. S. (2010), Discussion of groundwater withdrawal in Delaware with Senior Scientist (Hydrogeologist) at the Delaware Geological Survey.

Andres, A. S., A. D. Klingbeil (2006), Thickness and transmissivity of the unconfined aquifer of eastern Sussex County, Delaware, Report of Investigations - Delaware Geological Survey, 70, 19.

Andres, A. S., C. S. Howard (2002), Results of hydrogeologic studies of the Cypress Swamp Formation, Delaware, Report of Investigations - Delaware Geological Survey, 16.

Andres, A. S., M. J. Martin (2005), Estimation of the water table for the Inland Bays watershed, Delaware, Report of Investigations - Delaware Geological Survey, 20.

Beck, A. J., Y. Tsukamoto, A. Tovar-Sanchez, M. Huerta-Diaz, H. J. Bokuniewicz, and S. A. Sanudo-Wilhelmy (2007), Importance of geochemical transformations in determining submarine groundwater discharge-derived trace metal and nutrient fluxes, Appl. Geochem., 22(2), 477-490, doi:10.1016/j.apgeochem.2006.10.005.

Belanger, T.V., and M. T. Montgomery (1992), Seepage Meter Errors. Limnol. Oceanogr., 37(8) 1787-1795

Benson, R. N., A. S. Andres, J. H. Roberts, and K. D. Woodruff (1986), Seismic stratigraphy along three multichannel seismic reflection profiles off Delaware's coast, Miscellaneous Map Series - Delaware Geological Survey, 4, 1 sheet.

Bohlke, J. K., D. E. Krantz (2003), Isotope geochemistry and chronology of offshore ground water beneath Indian River Bay, Delaware Water-Resources Investigations - U.S.Geological Survey, WRI 03-4192, 37.

Bokuniewicz, H., M. Taniguchi, T. Ishitoibi, M. Charette, M. Allen, and E. A. Kontar (2008), Direct measurements of submarine groundwater discharge (SGD) over a fractured rock aquifer in Flamengo Bay Brazil Estuarine Coastal and Shelf Science, 76(3), 466-472, doi:10.1016/j.ecss.2007.07.047.

Bowen, J. L., K. D. Kroeger, G. Tomasky, W. J. Pabich, M. L. Cole, R. H. Carmichael, and I. Valiela (2007), A review of land-sea coupling by groundwater discharge of nitrogen to New England estuaries: Mechanisms and effects Appl. Geochem., 22(1), 175-191, doi:10.1016/j.apgeochem.2006.09.002.

Bratton, J. F., J. K. Boehlke, F. T. Manheim, and D. E. Krantz (2004), Ground water beneath coastal bays of the Delmarva Peninsula; ages and nutrients; Ground water discharge to estuarine and coastal ocean environments Ground Water, 42(7), 1021-1034.

Burnett, W. C., P. K. Aggarwal, A. Aureli, H. Bokuniewicz, J. E. Cable, M. A. Charette, E. Kontar, S. Krupa, K. M. Kulkarni, A. Loveless, W. S. Moore, J. A. Oberdorfer, J. Oliveira, N. Ozyurt, P. Povinec, A. M. G. Privitera, R. Rajar, R. T. Ramassur, J. Scholten, T. Stieglitz, M. Taniguchi, and J. V. Turner (2006), Quantifying submarine groundwater discharge in the coastal zone via multiple methods Sci. Total Environ., 367(2-3), 498-543, doi:10.1016/j.scitotenv.2006.05.009.

Cable, J. E., J. B. Martin, and J. Jaeger (2006), Exonerating Bernoulli? On evaluating the physical and biological processes affecting marine seepage meter measurements Limnology and Oceanography-Methods, 4, 172-183.

Cambareri, T. C. and Eichner, E. M. (1998), Watershed Delineation and Ground Water Discharge to a Coastal Embayment. Ground Water, 36: 626–634. doi: 10.1111/j.1745-6584.1998.tb02837.x

Cardenas, M. B., J. L. Wilson (2006), The influence of ambient groundwater discharge on exchange zones induced by current-bedform interactions RID B-4940-2011 Journal of Hydrology, 331(1-2), 103-109, doi:10.1016/j.jhydrol.2006.05.012.

Cardenas, M. B., J. L. Wilson (2007), Exchange across a sediment-water interface with ambient groundwater discharge RID B-4940-2011 Journal of Hydrology, 346(3-4), 69-80, doi:10.1016/j.jhydrol.2007.08.019.

Charette, M.A., Buesseler, K.O., 2004. Submarine groundwater discharge of nutrients and copper to an urban subestuary of Chesapeake Bay (Elizabeth River). Limnology and Oceanography 49, 376–385.

Charette, M. A., E. R. Sholkovitz (2002), Oxidative precipitation of groundwater-derived ferrous iron in the subterranean estuary of a coastal bay Geophys. Res. Lett., 29(10), 1444, doi:10.1029/2001GL014512.

Chinkuyu, A., A. Guber, T.J. Gish, D.J. Timlin, J.L. Starr, T. Nicholson, R. Cady, A. Schwartzman, G.W. McCarty (2007), Field studies to confirm uncertainty estimates of Ground Water Discharge. Office of Nuclear Regulatory Commission. NUREG.CR-6946. p. 46. Chrzastowski, M. J. (1986), Stratigraphy and geologic history of a holocene lagoon Rehoboth Bay and Indian River Bay, Delaware. Masters Thesis, University of Delaware, Newark, DE

Cohen, D., M. Person, P. Wang, C. W. Gable, D. Hutchinson, A. Marksamer, B. Dugan, H. Kooi, K. Groen, D. Lizarralde, R. L. Evans, F. D. Day-Lewis, and J. W. Lane Jr. (2010), Origin and Extent of Fresh Paleowaters on the Atlantic Continental Shelf, USA RID B-4689-2011 RID A-2651-2011 Ground Water, 48(1), 143-158, doi:10.1111/j.1745-6584.2009.00627.x.

Cooper, H. H.,Jr, F. A. Kohout, H. R. Henry, and R. E. Glover (1964), Sea water in coastal aquifers U.S.Geological Survey Professional Paper, Report: P 0400-B, P 0400-B, C1-C84.

Cross, V. A., D. S. Foster, and J. F. Bratton (2010), Continuous resistivity profiling and seismic-reflection data collected in 2006 from the Potomac River estuary, Virginia and Maryland, OF 2009-1151.

Custodio, E. (1987), Prediction methods, in Hydrology: Groundwater Problems in Coastal Areas, edited by G.A. Bruggeman, and E. Custodio, United Nations Educational, Scientific and Cultural Organization, Paris.

Delaware Department of Natural Resources and Environmental Control (DNREC) (1995), A Comprehensive Conservation and Management Plan for Delaware's Inland Bays. Delaware Department of Natural Resources and Environmental Control (March 1995). Dover, DE.

Delaware Department of Natural Resources and Environmental Control (DNREC) (2007), Inland Bays pollution control strategy (April 2007), DNREC, Dover, DE.

Delaware Geological Survey (DGS) (2012), Unpublished DGS well records accessed through the DGS watsys database stored on the local server at the DGS headquarters, Newark, DE.

Delaware Population Consortium (2006), Delaware Population Projections, October 26, 2006, Version 2006.0: Office of State Planning Coordination,

Evans, R. L., L. K. Law, B. St Louis, and S. Cheesman (2000), Buried paleo-channels on the New Jersey continental margin; channel porosity structures from electromagnetic surveying Mar. Geol., 170(3-4), 381-394.

Evans, R., L. Law, B. St Louis, and S. Cheesman (2000), Buried paleo-channels on the New Jersey continental margin: channel porosity structures from electromagnetic surveying RID C-6887-2011 Mar. Geol., 170(3-4), 381-394, doi:10.1016/S0025-3227(00)00081-5.

Fernandez, C (2012), Relationship of the Spatial and Temporal Distribution of Salinity, Nutrients, and Water Quality Parameters to Hydrogeology at Indian River Bay, Delaware: Field Observations and Modeling Masters Thesis, University of Delaware, Newark, DE

Fetter, C. W. (2001), Applied hydrogeology, Prentice-Hall, Upper Saddle River, NJ, United States (USA), United States (USA).

Ganju, N. K. (2011), A novel approach for direct estimation of fresh groundwater discharge to an estuary, Geophys. Res. Lett., 38, L11402, doi:10.1029/2011GL047718.

Ganju, N. K., D. H. Schoellhamer (2006), Annual sediment flux estimates in a tidal strait using surrogate measurements, Estuar. Coast. Shelf Sci., 69(1-2), 165-178, doi:10.1016/j.ecss.2006.04.008.

Google Inc. (2009), Google Earth, Version 5.1.3533.1731.

Guo, W., C. D. Langevin (2002), User's guide to SEAWAT; a computer program for simulation of three-dimensional variable-density ground-water flow, Open-File Report - U.S.Geological Survey, 77.

Harbaugh, A. W. (2000), MODFLOW-2000, an updated version of the U. S. Geological Survey modular ground-water model, EOS Trans. Am. Geophys. Union, 81(48, Suppl.), 426.

Hill, M. C., E. R. Banta, A. W. Harbaugh, and E. R. Anderman (2000), MODFLOW-2000, the U.S. Geological Survey modular ground-water model; user guide to the observation, sensitivity, and parameter-estimation processes and three post-processing programs, Open-File Report - U.S.Geological Survey, 209.

Hill, M.C. (2006), The Practical Use of Simplicity in Developing Ground Water Models, Ground Water 4(6), 775-81, doi: 10.1111/j.1745-6584.2006.00227.x

Hubbert, M. K. (1940), The theory of ground-water motion J. Geol., 48(8), 785-944.

Israelsen, O. W., R. C. Reeve (1944), Canal lining experiments in the Delta area, Utah, Utah Agricultural Experiment Station, Logan.

Johannes, R. (1980), The Ecological Significance of the Submarine Discharge of Groundwater, Marine Ecology-Progress Series, 3(4), 365-373, doi:10.3354/meps003365.

Johnston, R. H. (1973), Hydrology of the Columbia (Pleistocene) deposits of Delaware; an appraisal of a regional water-table aquifer, Bulletin - Delaware Geological Survey(14), 67.

Kaleris, V., G. Lagas, S. Marczinek, and J.A. Piotrowski, (2002), Modelling submarine groundwater discharge: an example from the Western Baltic Sea. Journal of Hydrology 265, 76–99.

King, J. N., A. J. Mehta, and R. G. Dean (2009), Generalized analytical model for benthic water flux forced by surface gravity waves Journal of Geophysical Research-Oceans, 114, C04004, doi:10.1029/2008JC005116.

Knee, K.L., and A. Paytan (2011), Submarine Groundwater Discharge: A Source of Nutrients, Metals, and Pollutants to the Coastal Ocean. In: Wolanski E and McLusky DS (eds.) Treat. Est.Coast. Sci., 4, 205–233. Waltham: Academic Press.

Konikow, L. F., G. Z. Hornberger, K. J. Halford, R. T. Hanson, and A. W. Harbaugh (2009), Revised Multi-Node Well (MNW2) package for MODFLOW ground-water flow model, U.S.Geological Survey Techniques and Methods, 67.

Krantz, D. E., F. T. Manheim, J. F. Bratton, and D. J. Phelan (2004), Hydrogeologic setting and ground water flow beneath a section of Indian River Bay, Delaware; Ground water discharge to estuarine and coastal ocean environments Ground Water, 42(7), 1035-1051.

Kroeger, K. D., M. A. Charette (2008), Nitrogen biogeochemistry of submarine groundwater discharge Limnol. Oceanogr., 53(3), 1025-1039, doi:10.4319/lo.2008.53.3.1025.

Kroeger, K. D., P. W. Swarzenski, W. J. Greenwood, and C. Reich (2007), Submarine groundwater discharge to Tampa Bay: Nutrient fluxes and biogeochemistry of the coastal aquifer, *Mar. Chem.*, 104(1-2), 85-97, doi:10.1016/j.marchem.2006.10.012.

Langevin, C. (2003), Simulation of submarine ground water discharge to a marine estuary: Biscayne Bay, Florida, Ground Water, 41(6), 758-771, doi:10.1111/j.1745-6584.2003.tb02417.x.

Langevin, C. (2003), Simulation of submarine ground water discharge to a marine estuary: Biscayne Bay, Florida Ground Water, 41(6), 758-771, doi:10.1111/j.1745-6584.2003.tb02417.x.

Lee, D. R. (1977), A Device for Measuring Seepage Flux in Lakes and Estuaries Limnol. Oceanogr., 22(1), 140-147.

Lee, J., G. Kim (2007), Estimating submarine discharge of fresh groundwater from a volcanic island using a freshwater budget of the coastal water column Geophys. Res. Lett., 34(11), L11611, doi:10.1029/2007GL029818.

Li, X., B. X. Hu*, W. C. Burnett, I. R. Santos, and J. P. Chanton (2009), Submarine Ground Water Discharge Driven by Tidal Pumping in a Heterogeneous Aquifer, Ground Water, 47(4), 558-568, doi:10.1111/j.1745-6584.2009.00563.x.

Manheim, F. T., D. E. Krantz, and J. F. Bratton (2004), Studying Ground Water Under Delmarva Coastal Bays Using Electrical Resistivity Ground Water, 42(7), 1052-1068, doi:10.1111/j.1745-6584.2004.tb02643.x.

Martin, J. B., J. E. Cable, C. Smith, M. Roy, and J. Cherrier (2007), Magnitudes of submarine groundwater discharge from marine and terrestrial sources: Indian River Lagoon, Florida Water Resour. Res., 43(5), W05440, doi:10.1029/2006WR005266.

Masterson, J. P., P. M. Barlow (1997), Effects of simulated ground-water pumping and recharge on ground-water flow in Cape Cod, Martha's Vineyard, and Nantucket Island basins, Massachusetts, U.S.Geological Survey Water-Supply Paper, 79, 1 sheet.

McCabe, G. J., S. L. Markstrom (2007), A monthly water-balance model driven by a graphical user interface, Open-File Report - U.S.Geological Survey, 6.

McLaughlin, P. P., K. G. Miller, J. V. Browning, K. W. Ramsey, R. N. Benson, J. L. Tomlinson, and P. J. Sugarman (2008), Stratigraphy and correlation of the Oligocene to Pleistocene section at Bethany Beach, Delaware, Report of Investigations - Delaware Geological Survey, 41.

Michael, H. A., L. A. Byron, and C. J. Russoniello (in review), Global assessment of vulnerability to sea-level rise in topography-limited and8 recharge-limited coastal groundwater systems, doi:2012WR012548.

Michael, H. A., M. A. Charette, and C. F. Harvey (2011), Patterns and variability of groundwater flow and radium activity at the coast: A case study from Waquoit Bay, Massachusetts, Mar. Chem., 127(1–4), 100-114, doi:10.1016/j.marchem.2011.08.001.

Michael, H., A. Mulligan, and C. Harvey (2005), Seasonal oscillations in water exchange between aquifers and the coastal ocean RID F-8447-2010, Nature, 436(7054), 1145-1148, doi:10.1038/nature03935.

Michael, H., J. Lubetsky, and C. Harvey (2003), Characterizing submarine groundwater discharge: a seepage meter study in Waquoit Bay, Massachusetts RID F-8447-2010, Geophys. Res. Lett., 30(6), 1297, doi:10.1029/2002GL016000.

Moore, W. S. (2010b), A reevaluation of submarine groundwater discharge along the southeastern coast of North America Global Biogeochem. Cycles, 24, GB4005, doi:10.1029/2009GB003747.

Moore, W. S. (2010a), The Effect of Submarine Groundwater Discharge on the Ocean. An. Rev. Mar. Sci., 2, 59-88, doi: 10.1146/annurev-marine-120308-081019.

Moore, W. S., T. M. Church (1996), Submarine groundwater discharge, Nature, 382(6587), 122-122.

Motz, L. H., A. Sedighi (2009), Representing the Coastal Boundary Condition in Regional Groundwater Flow Models, J. Hydrol. Eng., 14(8), 821-831, doi:10.1061/(ASCE)HE.1943-5584.0000049.

Mulligan, A. E., M. A. Charette (2006), Intercomparison of submarine groundwater discharge estimates from a sandy unconfined aquifer Journal of Hydrology, 327(3-4), 411-425, doi:10.1016/j.jhydrol.2005.11.056.

Mulligan, A. E., R. L. Evans, and D. Lizarralde (2007), The role of paleochannels in groundwater/seawater exchange Journal of Hydrology, 335(3-4), 313-329, doi:10.1016/j.jhydrol.2006.11.025.

National Oceanic and Atmospheric Administration (NOAA)/National Geophysical Data Center (NGDC), 2012: Bathymetry Data Viewer. [Available online at http://maps.ngdc.noaa.gov/viewers/bathymetry/].

National Oceanographic and Atmospheric Administration (NOAA)/National Climactic Data Center (NCDC), 2012: Time bias corrected divisional temperature-precipitation-drought index (TD-9640). [Available online at http://www1.ncdc.noaa.gov/pub/data/cirs/drd964x.pcpst.txt].

National Oceanographic and Atmospheric Administration (NOAA)/National Ocean Service (NOS), 2012: INDIAN RIVER INLET (COAST GUARD STATION). [Available online at http://tidesandcurrents.noaa.gov/noaatidepredictions/NOAATidesFacade.jsp?Stationid=8558690].

New Jersey Geological Survey (NJGS) (2005), DGS02-3: Ground-Water Recharge for New Jersey Map Series, 1:24,000(New Jersey).

Niswonger, R. G., D. E. Prudic (2006), Documentation of the streamflow-routing (SFR2) package to include unsaturated flow beneath streams; a modification to SFRI techniques, U.S.Geological Survey Techniques and Methods, 57.

Oertel, G.F., and J. C. Kraft (1994), New Jersey and Delmarva barrier islands; in Geology of Barrier Island edited by Davis, R.A., Springer-Verlag, Heidelberg, Germany pp. 207-226.

Oki, D., (1999), Geohydrology and numerical simulation of the ground-water flow system of Kona, Island of Hawaii. United States Geological Survey Water Resources. Investigations Report 99-4073.

Precht, E., M. Huettel (2003), Advective pore-water exchange driven by surface gravity waves and its ecological implications Limnol. Oceanogr., 48(4), 1674-1684.

Ramsey, K. W. (2010), Stratigraphy, correlation, and depositional environments of the middle to late Pleistocene interglacial deposits of southern Delaware, Report of Investigations - Delaware Geological Survey 76, 43.

Ramsey, K. W. (2011), Geologic map of the Fairmount and Rehoboth Beach Quadrangle, Delaware, Geologic Map Series - Delaware Geological Survey, 1 sheet.

Rapaglia, J. P., H. J. Bokuniewicz (2009), The effect of groundwater advection on salinity in pore waters of permeable sediments Limnol. Oceanogr., 54(2), 630-643, doi:10.4319/lo.2009.54.2.0630.

Rosenberry, D. O., J. Pitlick (2009), Local-scale variability of seepage and hydraulic conductivity in a shallow gravel-bed river Hydrol. Process., 23(23), 3306-3318, doi:10.1002/hyp.7433.

Rosenberry, D. O., J. W. LaBaugh, and R. J. Hunt (2008), Use of monitoring wells, portable piezometers, and seepage meters to quantify flow between surface water and ground water; Field techniques for estimating water fluxes between surface water and ground water, TM 04-D2, 39-70.

Sanford, W. E. (2010), Delmarva Peninsula groundwater model input files and modeling results of a United States Geological Survey modeling project to understand nutrient flux on the Delmarva Peninsula.

Santoro, A. E. (2010), Microbial nitrogen cycling at the saltwater-freshwater interface Hydrogeol. J., 18(1), 187-202, doi:10.1007/s10040-009-0526-z.

Santos, I. R., W. C. Burnett, T. Dittmar, I. G. N. A. Suryaputra, and J. Chanton (2009), Tidal pumping drives nutrient and dissolved organic matter dynamics in a Gulf of Mexico subterranean estuary, Geochim. Cosmochim. Acta, 73(5), 1325-1339, doi:10.1016/j.gca.2008.11.029.

Selman, M., S. Greenhalgh (2007) Eutrophication: An Overview of Status, Trends, Policies, and Strategies. World Resources Institute. Washington, DC. [Available online at http://pdf.wri.org/eutrophication_policies_actions_and_strategies.pdf].

Shaw, R. D., and E. E. Prepas (1989), Anomalous, short-term influx of water into seepage meters, Limnol. Oceanogr., 34(7), 1343-1351.

Sheridan, R. E., C. E. Dill, JR. and J. C. Kraft (1974), Holocene Sedimentary Environment of the Atlantic Inner Shelf off Delaware, Geol. Soc. Am. Bul. 85(8) 1319-1328, doi: 10.1130/0016-7606(1974)85<1319:HSEOTA> 2.0.CO;2.

Shinn, E. A., C. D. Reich, and T. D. Hickey (2002), Seepage meters and Bernoulli's revenge Estuaries, 25(1), 126-132, doi:10.1007/BF02696056.

Shum, K. (1992), Wave-Induced Advective Transport Below a Rippled Water-Sediment Interface J. Geophys. Res. Oceans, 97(C1), 789-808, doi:10.1029/91JC02101.

Slomp, C. P., P. van Cappellen (2004), Nutrient inputs to the coastal ocean through submarine groundwater discharge; controls and potential impact Journal of Hydrology, 295(1-4), 64-86, doi:10.1016/j.jhydrol.2004.02.018.

Smith, A., D. Herne, and J. Turner (2009), Wave effects on submarine groundwater seepage measurement Adv. Water Resour., 32(6), 820-833, doi:10.1016/j.advwatres.2009.02.003.

Sophocleous, M. A., Groundwater Recharge; in, Groundwater, in Encyclopedia of Life Support Systems (EOLSS), edited by L. Silveira et al, Oxford, UK, Eolss Publishers.

Spiteri, C., C. P. Slomp, M. A. Charette, K. Tuncay, and C. Meile (2008), Flow and nutrient dynamics in a subterranean estuary (Waquoit Bay, MA, USA); field data and reactive transport modeling, Geochim. Cosmochim. Acta, 72(14), 3398-3412, doi:10.1016/j.gca.2008.04.027.

Stieglitz, T., J. Rapaglia, and H. Bokuniewicz (2008), Estimation of submarine groundwater discharge from bulk ground electrical conductivity measurements, J. Geophys. Res. Oceans, 113 (C08007), doi:10.1029/2007JC004499.

Swarzenski, P, C, Reich, and D. Rudnick (2009), Examining submarine ground-water discharge into Florida Bay by using 222Rn and continuous resistivity profiling: Open-File Report - U.S. Geological Survey 2008-1342, 66 [Available online at http://pubs.usgs.gov/of/2008/1342/]

Swarzenski, P. W., J. A. Izbicki (2009), Coastal groundwater dynamics off Santa Barbara, California: Combining geochemical tracers, electromagnetic seepmeters, and electrical resistivity Estuarine Coastal and Shelf Science, 83(1), 77-89, doi:10.1016/j.ecss.2009.03.027.

Taniguchi, M. (2002), Tidal effects on submarine groundwater discharge into the ocean Geophys. Res. Lett., 29(12), 1561, doi:10.1029/2002GL014987.

Taniguchi, M., W. Burnett, J. Cable, and J. Turner (2002), Investigation of submarine groundwater discharge, Hydrol. Process., 16(11), 2115-2129, doi:10.1002/hyp.1145.

U.S. Environmental Protection Agency (U.S. EPA) (2002), Environmental conditions in the mid-Atlantic estuaries, summary report for the mid-Atlantic integrated assessment (MAIA) estuaries 1997-98, vol. EPA/620/R-02/003, , EPA, Philadelphia.

Ullman, W. J., A. S. Andres, J. R. Scudlark, and K. B. Savidge (2002), Storm-water and base-flow sampling and analysis in the Delaware inland bays; preliminary report of findings 1998-2000, Open File Report - Delaware Geological Survey, 40.

US Department of Agriculture (USDA) (2009), 2007 Census of Agriculture: Delaware State and Country Data. Volume 1. Geographic Area Series. Part 8., USDA, Washington, DC.

Viso, R., C. McCoy, P. Gayes, and D. Quafisi (2010), Geological controls on submarine groundwater discharge in Long Bay, South Carolina (USA) Cont. Shelf Res., 30(3-4), 335-341, doi:10.1016/j.csr.2009.11.014.

Voss, C. I. (1984), A finite-element simulation model for saturated-unsaturated, fluid-density-dependent ground-water flow with energy transport or chemically-reactive single-species solute transport, Water-Resources Investigations - U.S.Geological Survey, 409.

Wagner, R. J., Geological Survey (U.S.), 2006: Guidelines and standard procedures for continuous water-quality monitors station operation, record computation, and data reporting.

Wang, L. T., T. E. McKenna (2008), Locating groundwater discharge areas using Landsat 7 imagery, First State Geology, 26(1), 2.

Waska, H., G. Kim (2011), Submarine groundwater discharge (SGD) as a main nutrient source for benthic and water-column primary production in a large intertidal environment of the Yellow Sea, J. Sea Res., 65(1), 103-113, doi:10.1016/j.seares.2010.08.001.

Weinstein, Y., Y. Yechieli, Y. Shalem, W. C. Burnett, P. W. Swarzenski, and B. Herut (2011), What Is the Role of Fresh Groundwater and Recirculated Seawater in Conveying Nutrients to the Coastal Ocean? Environ. Sci. Technol., 45(12), 5195-5200, doi:10.1021/es104394r.

Wheeler, J. C. (1999), Freshwater use in Delaware, 1995, Fact Sheet. U.S.Geological Survey, 2.

Winston, R. B. (2000), Graphical user interface for MODFLOW, version 4, Open-File Report. U.S.Geological Survey, 27.

Zekster, I., H. Loaiciga (1993), Groundwater Fluxes in the Global Hydrologic-Cycle - Past, Present and Future, Journal of Hydrology, 144(1-4), 405-427, doi:10.1016/0022-1694(93)90182-9.

Appendix A

SEEPAGE METER CONSTRUCTION

A.1 Benthic Chamber parts and construction

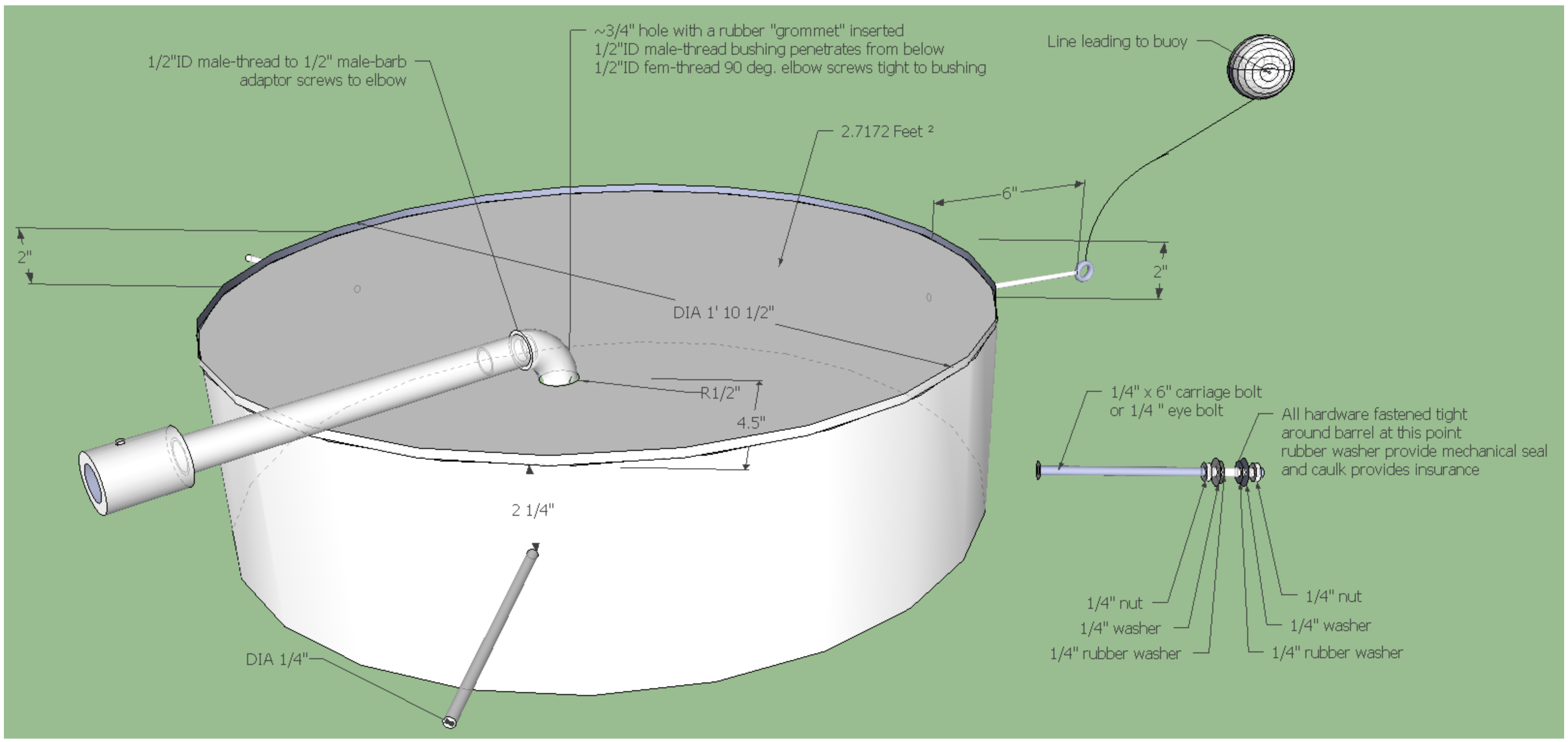

Figure A1: Drawing of seepage meter and components.

Table A1: Components required for construction of a seepage meter. Most parts were acquired from the hardware or plumbing sections of a large hardware store, or from a lab supply store accessed via the internet. ‘Number/Meter’ column described how many of each item were required for construction of a single meter.

Part	Comment	Distributer/ Manufacturer	Number/ Meter
55 Gal Drum End (6”x22.5”)	Cut with metal blade in handheld circular saw with guide set to 6”	First State Steel Drum, Newcastle, DE	1
90° Elbow (½”fem fem-½”fem threading)	Galvanized plumbing hardware	Home Depot	1
Bushing (½” male x $^3/_8$” fem threading)	Galvanized plumbing hardware	Home Depot	1
Neoprene Grommet (¾”)	In hardware drawers	Home Depot	1
Hose Barb Adaptor (½” barb x ½” MIP)	Brass plumbing fixture (A-385)	Home Depot	1
PVC Tubing (1’ x ½” id)		Amazon.com	1
1/2 Hose Barb Non-Valved In-Line Coupling Body (fem)	Large body, easy to find underwater	Colder Products Company	1
Plastic Hose Clamp (0.702" x 0.801")	2 each where hose attaches to barbed adaptors	Cole Parmer	4
6” x ¼” SS Carriage Bolts		Home Depot	2
6” x ¼” SS Eye Bolt		Home Depot	1
¼” SS Nuts		Home Depot	6
¼” SS Washers		Home Depot	6
¼” Rubber Washers	In hardware drawers	Home Depot	6

Materials were stainless, or brass if possible, but galvanized if difficult to obtain or prohibitively expensive.

All through-fittings were caulked with outdoor caulk both on the threads and around the hardware after tightened to ensure watertight seal.

Non-coated parts of barrel and rusty fittings were sprayed with “Rust-Oleum” brand enamel paint after initial deployments to reduce corrosion. Future construction would benefit from application prior to initial deployment.

Figure A2: A.) Assembled elbow fixture attached to seepage meter, B.) ½" Female quick connect, C.) Elbow joint, D.) Bushing, E.) Female-female barbed adaptor, and F.) Neoprene grommet

A.2 Collection bag parts and construction

Autoclave bags provided a cost effective, durable, yet flexible means of collecting seepage. These were connected to a plastic ball-valve, which attached to one end of a 7cm-long ½” PVC tube, the other end of which was attached to a male quick connect. The bags used in this study measured 61.0x76.2cm (24x30 inches) and were capable of holding up to 54 liters. Twice as many bags were constructed as seepage meters so that prefilled replacement bag could be ready for deployment at the end of the previous run without delay. Each bag was labeled with the seepage meter number and either “A” or “B” for repeatability. Bags were reexamined prior to every deployment for leaks and were repaired/replaced as necessary.

Table A2: Components required for construction of seepage collecting bags. Parts were ordered from a lab supply store, or an irrigation supply store accessed via the internet. 'Number/Bag' column described how many of each item were required for construction of a single bag.

Part	Comment	Distributer/Manufacturer	Number/Bag
Autoclave Bag(24" x 30")		VWR.com	1
PVC Tubing (1" x ½" id)	Between barbed valve and bag	Amazon.com	1
PVC Tubing (4" x ½" id)	Between quick-connect and barbed valve	Amazon.com	1
Plastic Hose Clamp (0.702" x 0.801")	2 each where hose attaches to barbed quick connect	Cole Parmer	2
Plastic Hose Clamp (0.859" x 0.989")	2 each where bag attaches to barbed valve	Cole Parmer	2
Barbed Ball Valve (½" od)	BVA	dripworksusa.com	1
1/2 Hose Barb Non-Valved In-Line Coupling Body (male)	Large body	Colder Products Company	1

Ball valves fit tightly enough into tubing to not require hose clamps
On the bag end of the valve, a short piece of tubing was attached, onto which the bag was hose-clamped. Bags were attached to this short tubing section with pleated folds to ensure tight seal and minimize head loss.
Area between valve and quick connect is taped with colored electrical tape and labeled with bag number and letter, such that every meter has an assigned "A" and "B" bag, so that the proper bag could be quickly identified and minimize confusion that might result in compromised data.

Figure A3: Bag assembly prior to autoclave bag attachment.

Appendix B

MEASURED DISCHARGE VALUES

Table B1: Seepage data from measurements made between July 2010 and June 2011

Date	Run	Meter	Easting	Northing	Time On	Time Off	Mass On	Mass Off	Cond On	Cond Off
7/15/2010	1	1	488798.33	4271546.56	9:55	11:55	1.00	2.30	43.65	46.35
7/15/2010	1	2	488786.00	4271550.30	9:55	11:55	1.00	3.00	43.65	46.43
7/15/2010	1	3	488776.41	4271553.14	9:55	11:55	1.00	1.60	43.65	45.18
7/15/2010	1	4	488768.15	4271556.67	9:55	11:55	1.00	2.25	43.65	44.67
7/15/2010	1	5	488760.49	4271559.60	9:55	11:55	1.00	6.20	43.65	45.03
7/15/2010	1	6	488753.23	4271562.22	9:55	11:55	1.00	1.75	43.65	45.40
7/15/2010	1	7	488741.73	4271565.50	9:55	11:55	1.00	3.75	43.65	39.15
7/15/2010	1	8	488729.61	4271570.44	9:55	11:55	1.00	2.15	43.65	43.18
7/15/2010	1	9	488715.25	4271574.62	9:55	11:55	1.00	3.00	43.65	42.65
7/15/2010	1	10	488696.33	4271577.86	9:55	11:55	1.00	4.70	43.65	46.32
7/15/2010	1	11	488693.05	4271566.05	9:55	11:55	1.00	5.25	43.65	45.37
7/15/2010	1	12	488688.47	4271553.91	9:55	11:55	1.00	2.00	43.65	45.56
7/15/2010	1	13	488700.24	4271589.49	9:55	11:55	1.00	1.25	43.65	45.28
7/15/2010	1	14	488705.96	4271613.01	9:55	11:55	1.00	2.25	43.65	45.85
7/15/2010	1	15	488702.15	4271599.55	9:55	11:55	1.00	2.75	43.65	46.20
7/15/2010	1	16	488707.38	4271625.12	9:55	11:55	1.00	47.00	43.65	45.33
7/15/2010	1	17	488709.00	4271636.44	9:55	11:55	1.00	2.70	43.65	45.76
7/15/2010	1	18	488709.95	4271647.89	9:55	11:55	1.00	2.25	43.65	45.90
7/15/2010	1	19	488711.63	4271659.25	9:55	11:55	1.00	4.00	43.65	45.87
7/15/2010	1	20	488714.43	4271671.19	9:55	11:55	1.00	2.45	43.65	45.66
7/15/2010	2	1	488798.33	4271546.56	11:55	14:06	1.00	2.25	44.67	47.16
7/15/2010	2	2	488786.00	4271550.30	11:55	14:06	1.00	3.00	44.67	46.03
7/15/2010	2	3	488776.41	4271553.14	11:55	14:05	1.00	1.65	44.67	44.87
7/15/2010	2	4	488768.15	4271556.67	11:55	14:05	1.00	2.40	44.67	44.28
7/15/2010	2	5	488760.49	4271559.60	11:55	14:06	1.00	39.00	44.67	45.59
7/15/2010	2	6	488753.23	4271562.22	11:55	14:08	1.00	1.75	44.67	45.00
7/15/2010	2	7	488741.73	4271565.50	11:55	14:22	1.00	5.20	44.67	38.55

7/15/2010	2	8	488729.61	4271570.44	11:55	14:24	1.00	2.50	44.67	43.89
7/15/2010	2	9	488715.25	4271574.62	12:05	14:12	1.00	2.60	44.67	43.13
7/15/2010	2	10	488696.33	4271577.86	12:05	14:13	1.00	2.25	44.67	46.76
7/15/2010	2	11	488693.05	4271566.05	12:05	14:06	1.00	5.20	44.67	46.83
7/15/2010	2	12	488688.47	4271553.91	12:05	14:07	1.00	2.20	44.67	46.80
7/15/2010	2	13	488700.24	4271589.49	12:05	14:08	1.00	8.50	44.67	46.96
7/15/2010	2	14	488705.96	4271613.01	12:05	14:09	1.00	2.25	44.67	47.25
7/15/2010	2	15	488702.15	4271599.55	12:05	14:13	1.00	2.70	44.67	47.44
7/15/2010	2	16	488707.38	4271625.12	12:30	14:16	1.00	15.60	44.67	46.35
7/15/2010	2	17	488709.00	4271636.44	12:20	14:09	1.00	2.20	44.67	45.80
7/15/2010	2	18	488709.95	4271647.89	12:20	14:09	1.00	1.80	44.67	45.74
7/15/2010	2	19	488711.63	4271659.25	12:20	14:10	1.00	2.50	44.67	45.87
7/15/2010	2	20	488714.43	4271671.19	11:55	N/A	1.00	N/A	N/A	N/A
7/15/2010	3	1	488798.33	4271546.56	14:06	16:06	1.00	2.45	45.34	45.97
7/15/2010	3	2	488786.00	4271550.30	14:06	16:06	1.00	3.25	45.34	46.13
7/15/2010	3	3	488776.41	4271553.14	14:05	16:07	1.00	2.00	45.34	45.88
7/15/2010	3	4	488768.15	4271556.67	14:05	16:15	1.00	2.50	45.34	44.92
7/15/2010	3	5	488760.49	4271559.60	14:00	16:17	1.00	20.55	45.34	47.15
7/15/2010	3	6	488753.23	4271562.22	14:18	16:20	1.00	2.25	45.34	45.10
7/15/2010	3	7	488741.73	4271565.50	14:22	16:20	1.00	4.20	45.34	40.55
7/15/2010	3	8	488729.61	4271570.44	14:21	16:15	1.00	2.80	45.34	43.40
7/15/2010	3	9	488715.25	4271574.62	14:12	16:10	1.00	2.75	45.34	43.16
7/15/2010	3	10	488696.33	4271577.86	14:13	16:09	1.00	2.50	45.34	46.45
7/15/2010	3	11	488693.05	4271566.05	14:06	16:08	1.00	5.90	45.34	46.50
7/15/2010	3	12	488688.47	4271553.91	14:07	16:05	1.00	2.00	45.34	45.89
7/15/2010	3	13	488700.24	4271589.49	14:08	16:07	1.00	4.10	45.34	46.96
7/15/2010	3	14	488705.96	4271613.01	14:09	16:09	1.00	2.20	45.34	46.72
7/15/2010	3	15	488702.15	4271599.55	14:13	16:11	1.00	3.20	45.34	47.28
7/15/2010	3	16	488707.38	4271625.12	14:16	16:13	1.00	42.00	45.34	46.70
7/15/2010	3	17	488709.00	4271636.44	14:09	16:07	1.00	1.80	45.34	47.72
7/15/2010	3	18	488709.95	4271647.89	14:09	16:08	1.00	2.20	45.34	47.40
7/15/2010	3	19	488711.63	4271659.25	14:10	16:09	1.00	2.60	45.34	47.46
7/15/2010	3	20	488714.43	4271671.19	14:11	16:10	1.00	2.20	45.34	47.03
7/15/2010	4	4	488768.15	4271556.67	16:15	18:09	1.00	2.50	46.11	43.94
7/15/2010	4	5	488760.49	4271559.60	16:17	18:10	1.00	13.75	46.11	45.94
7/15/2010	4	6	488753.23	4271562.22	16:20	18:11	1.00	2.00	46.11	44.11
7/15/2010	4	7	488741.73	4271565.50	16:20	18:12	1.00	6.25	46.11	39.09
7/15/2010	4	8	488729.61	4271570.44	16:15	18:13	1.00	2.50	46.11	41.96
7/15/2010	4	9	488715.25	4271574.62	16:15	18:12	1.00	2.75	46.11	41.90
7/15/2010	4	10	488696.33	4271577.86	16:09	18:11	1.00	2.25	46.11	45.28
7/15/2010	4	11	488693.05	4271566.05	16:08	18:09	1.00	4.25	46.11	45.74

7/15/2010	4	12	488688.47	4271553.91	16:05	18:09	1.00	1.75	46.11	45.23
7/15/2010	4	13	488700.24	4271589.49	16:07	18:10	1.00	2.25	46.11	45.65
7/15/2010	4	14	488705.96	4271613.01	16:09	18:12	1.00	1.90	46.11	45.40
7/15/2010	4	15	488702.15	4271599.55	16:11	18:11	1.00	2.75	46.11	45.80
7/15/2010	4	16	488707.38	4271625.12	16:13	18:13	1.00	50.00	46.11	46.42
7/15/2010	4	17	488709.00	4271636.44	16:13	18:11	1.00	2.40	46.11	45.35
7/15/2010	4	19	488711.63	4271659.25	16:09	18:11	1.00	2.50	46.11	45.70
7/16/2010	5	4	488768.15	4271556.67	7:25	9:15	1.00	2.85	45.88	41.53
7/16/2010	5	5	488760.49	4271559.60	7:25	9:18	1.00	18.00	45.88	52.10
7/16/2010	5	6	488753.23	4271562.22	7:20	9:21	1.00	2.30	45.88	41.03
7/16/2010	5	7	488741.73	4271565.50	7:20	9:25	1.00	6.50	45.88	37.05
7/16/2010	5	8	488729.61	4271570.44	7:20	9:29	1.00	2.75	45.88	39.59
7/16/2010	5	9	488715.25	4271574.62	7:20	9:21	1.00	3.25	45.88	40.40
7/16/2010	5	10	488696.33	4271577.86	7:20	9:19	1.00	3.25	45.88	43.90
7/16/2010	5	11	488693.05	4271566.05	7:20	9:17	1.00	3.90	45.88	44.80
7/16/2010	5	12	488688.47	4271553.91	7:20	9:15	1.00	2.60	45.88	44.30
7/16/2010	5	13	488700.24	4271589.49	7:20	9:25	1.00	3.00	45.88	44.40
7/16/2010	5	14	488705.96	4271613.01	7:20	9:30	1.00	2.50	45.88	44.60
7/16/2010	5	15	488702.15	4271599.55	7:20	9:28	1.00	3.00	45.88	44.40
7/16/2010	5	16	488707.38	4271625.12	7:20	9:28	1.00	30.00	45.88	44.40
7/16/2010	5	17	488709.00	4271636.44	7:20	9:22	1.00	2.45	45.88	44.60
7/16/2010	5	19	488711.63	4271659.25	7:20	9:20	1.00	2.20	45.88	44.80
7/16/2010	5	21	488901.95	4271503.48	7:20	9:28	1.00	1.85	45.88	53.90
7/16/2010	5	22	488901.90	4271468.64	7:20	9:23	1.00	2.20	45.88	54.10
7/16/2010	5	23	488906.35	4271454.90	7:20	9:18	1.00	1.13	45.88	52.40
7/16/2010	5	24	488736.08	4271567.66	7:20	9:27	1.00	1.75	45.88	44.10
7/16/2010	5	25	488747.00	4271563.66	7:20	9:23	1.00	3.75	45.88	41.40
7/16/2010	6	4	488768.15	4271556.67	9:15	11:30	1.00	2.55	44.90	41.75
7/16/2010	6	5	488760.49	4271559.60	9:18	11:30	1.00	17.00	44.90	44.06
7/16/2010	6	6	488753.23	4271562.22	9:21	11:30	1.00	2.65	44.90	41.71
7/16/2010	6	7	488741.73	4271565.50	9:25	11:30	1.00	6.00	44.90	37.59
7/16/2010	6	8	488729.61	4271570.44	9:29	11:30	1.00	0.90	44.90	39.64
7/16/2010	6	9	488715.25	4271574.62	9:21	11:30	1.00	3.15	44.90	39.84
7/16/2010	6	10	488696.33	4271577.86	9:19	11:30	1.00	5.00	44.90	43.69
7/16/2010	6	11	488693.05	4271566.05	9:17	11:30	1.00	5.00	44.90	44.50
7/16/2010	6	12	488688.47	4271553.91	9:15	11:30	1.00	1.75	44.90	44.06
7/16/2010	6	13	488700.24	4271589.49	9:25	11:30	1.00	3.30	44.90	44.28
7/16/2010	6	14	488705.96	4271613.01	9:30	11:30	1.00	2.50	44.90	44.20
7/16/2010	6	15	488702.15	4271599.55	9:28	11:30	1.00	3.00	44.90	44.27
7/16/2010	6	16	488707.38	4271625.12	9:26	11:30	1.00	27.50	44.90	44.45
7/16/2010	6	17	488709.00	4271636.44	9:22	11:30	1.00	2.50	44.90	44.45

7/16/2010	6	19	488711.63	4271659.25	9:20	11:30	1.00	2.25	44.90	44.44
7/16/2010	6	21	488901.95	4271503.48	9:28	11:30	1.00	2.25	51.90	43.30
7/16/2010	6	22	488901.90	4271468.64	9:23	11:30	1.00	1.55	51.90	43.42
7/16/2010	6	23	488906.35	4271454.90	9:18	11:30	1.00	1.50	44.90	43.15
7/16/2010	6	24	488736.08	4271567.66	9:27	11:30	1.00	1.75	44.90	44.03
7/16/2010	6	25	488747.00	4271563.66	9:23	11:30	1.00	3.75	44.90	40.52
7/21/2010	1	1	488253.77	4271686.39	9:02	10:54	1.05	3.55	43.53	43.12
7/21/2010	1	2	488300.19	4271690.21	9:00	10:50	1.15	2.70	43.53	43.48
7/21/2010	1	3	488328.56	4271678.96	8:58	10:52	1.10	2.00	43.53	43.62
7/21/2010	1	4	488357.29	4271669.59	8:56	10:50	1.15	2.20	43.53	43.99
7/21/2010	1	5	488383.83	4271657.13	8:52	10:56	1.15	1.60	43.53	43.82
7/21/2010	1	6	488414.72	4271639.11	8:54	10:41	1.00	1.50	43.53	44.02
7/21/2010	1	7	488435.43	4271626.76	8:55	10:55	1.15	1.50	43.53	43.70
7/21/2010	1	8	488448.47	4271609.54	9:13	10:54	1.15	4.55	44.53	44.44
7/21/2010	1	9	488463.69	4271596.09	8:53	10:52	1.20	1.55	43.53	43.79
7/21/2010	1	10	488480.75	4271589.19	8:51	10:50	1.20	2.25	43.53	43.95
7/21/2010	1	11	488494.84	4271579.96	8:49	10:49	1.15	2.45	43.53	44.14
7/21/2010	1	12	488353.44	4271655.51	9:04	10:56	1.15	4.15	43.53	44.16
7/21/2010	1	13	488400.69	4271630.25	9:04	10:58	1.15	3.30	43.53	44.29
7/21/2010	1	14	488270.44	4271713.77	8:55	10:51	1.10	2.50	43.53	43.09
7/21/2010	1	15	488300.48	4271711.07	8:57	10:53	1.10	3.25	43.53	43.62
7/21/2010	1	16	488333.91	4271704.47	8:51	N/A	N/A	N/A	N/A	N/A
7/21/2010	1	17	488362.37	4271687.79	9:01	10:57	1.05	2.15	43.53	44.26
7/21/2010	1	18	488384.73	4271676.32	8:54	10:59	1.05	1.70	43.53	43.99
7/21/2010	1	19	488415.44	4271658.08	8:52	10:57	1.05	2.10	43.53	44.03
7/21/2010	1	20	488436.57	4271636.63	8:51	10:51	1.05	12.10	43.53	44.50
7/21/2010	2	1	488253.77	4271686.39	10:54	12:51	1.10	2.40	44.13	43.53
7/21/2010	2	2	488300.19	4271690.21	10:50	12:53	1.05	2.45	44.13	43.69
7/21/2010	2	3	488328.56	4271678.96	10:52	12:52	1.10	2.30	44.13	43.92
7/21/2010	2	4	488357.29	4271669.59	10:50	12:50	1.10	2.15	44.13	44.26
7/21/2010	2	5	488383.83	4271657.13	10:41	12:44	1.15	1.45	44.13	44.19
7/21/2010	2	6	488414.72	4271639.11	10:56	12:56	1.00	1.40	44.13	44.12
7/21/2010	2	7	488435.43	4271626.76	10:55	12:54	1.15	1.65	44.13	44.07
7/21/2010	2	8	488448.47	4271609.54	10:54	12:53	1.05	4.70	44.13	44.36
7/21/2010	2	9	488463.69	4271596.09	10:52	12:52	1.10	1.70	44.13	43.98
7/21/2010	2	10	488480.75	4271589.19	10:50	12:51	1.15	2.45	44.13	44.09
7/21/2010	2	11	488494.84	4271579.96	10:49	12:50	1.15	2.55	44.13	44.31
7/21/2010	2	12	488353.44	4271655.51	10:56	12:52	1.05	1.40	44.13	44.30
7/21/2010	2	13	488400.69	4271630.25	10:58	12:56	1.05	2.65	44.13	44.49
7/21/2010	2	14	488270.44	4271713.77	10:51	12:53	1.15	2.65	44.13	43.32
7/21/2010	2	15	488300.48	4271711.07	10:53	12:55	1.15	3.05	44.13	43.52

7/21/2010	2	16	488333.91	4271704.47	10:55	12:56	1.20	6.75	44.13	44.34
7/21/2010	2	17	488362.37	4271687.79	10:57	12:57	1.15	2.70	44.13	44.22
7/21/2010	2	18	488384.73	4271676.32	10:59	12:56	1.15	1.50	44.13	44.23
7/21/2010	2	19	488415.44	4271658.08	10:57	12:53	1.15	2.30	44.13	44.20
7/21/2010	2	20	488436.57	4271636.63	10:51	12:50	1.10	13.10	44.13	44.48
7/21/2010	3	1	488253.77	4271686.39	12:51	14:20	1.25	3.40	44.50	44.05
7/21/2010	3	2	488300.19	4271690.21	12:53	14:23	1.10	2.10	44.50	43.77
7/21/2010	3	3	488328.56	4271678.96	12:52	14:22	1.10	2.45	44.50	43.77
7/21/2010	3	4	488357.29	4271669.59	12:50	14:21	1.20	2.35	44.50	44.36
7/21/2010	3	5	488383.83	4271657.13	12:44	14:20	1.15	1.40	44.50	44.42
7/21/2010	3	6	488414.72	4271639.11	12:56	14:26	1.25	1.55	44.50	44.48
7/21/2010	3	7	488435.43	4271626.76	12:54	14:25	1.25	1.80	44.50	44.33
7/21/2010	3	8	488448.47	4271609.54	12:53	14:24	1.15	3.00	44.50	44.21
7/21/2010	3	9	488463.69	4271596.09	12:52	14:23	1.20	1.70	44.50	44.32
7/21/2010	3	10	488480.75	4271589.19	12:51	14:21	1.15	2.20	44.50	44.32
7/21/2010	3	11	488494.84	4271579.96	12:50	14:20	1.15	2.50	44.50	44.40
7/21/2010	3	12	488353.44	4271655.51	12:57	14:30	1.20	5.35	44.50	44.17
7/21/2010	3	13	488400.69	4271630.25	12:56	14:28	1.20	3.15	44.50	44.58
7/21/2010	3	14	488270.44	4271713.77	12:53	14:22	1.10	2.50	44.50	43.30
7/21/2010	3	15	488300.48	4271711.07	12:55	14:24	1.25	3.85	44.50	43.42
7/21/2010	3	16	488333.91	4271704.47	12:56	14:26	1.15	8.30	44.50	44.12
7/21/2010	3	17	488362.37	4271687.79	12:57	14:28	1.20	2.20	44.50	44.41
7/21/2010	3	18	488384.73	4271676.32	12:56	14:26	1.20	1.50	44.50	44.43
7/21/2010	3	19	488415.44	4271658.08	12:53	14:24	1.20	1.95	44.50	44.46
7/21/2010	3	20	488436.57	4271636.63	12:50	14:20	1.15	4.95	44.50	44.31
7/22/2010	1	1	488794.60	4271522.61	10:13	12:08	1.20	2.15	44.12	44.12
7/22/2010	1	2	488805.57	4271519.71	10:12	12:07	1.15	1.25	44.12	44.23
7/22/2010	1	3	488815.49	4271515.59	10:11	12:06	1.20	1.25	44.12	44.30
7/22/2010	1	4	488824.80	4271511.47	10:10	12:05	1.15	2.75	44.12	43.90
7/22/2010	1	5	488835.77	4271507.79	10:11	12:04	1.15	1.65	44.12	43.80
7/22/2010	1	6	488848.57	4271504.22	10:12	12:05	1.20	2.75	44.12	44.21
7/22/2010	1	7	488862.06	4271499.21	10:13	12:07	1.20	4.60	44.12	44.03
7/22/2010	1	8	488873.37	4271495.20	10:15	12:09	1.15	3.00	44.12	44.10
7/22/2010	1	9	488828.89	4271509.58	10:14	12:04	1.10	2.20	44.12	44.25
7/22/2010	1	10	488832.88	4271495.48	10:17	12:11	1.15	1.90	44.12	44.05
7/22/2010	2	1	488794.60	4271522.61	12:08	13:56	1.20	2.40	43.65	43.67
7/22/2010	2	2	488805.57	4271519.71	12:07	13:56	1.10	2.15	43.65	44.13
7/22/2010	2	3	488815.49	4271515.59	12:06	13:55	1.10	2.15	43.65	44.07
7/22/2010	2	4	488824.80	4271511.47	12:05	13:55	1.15	3.20	43.65	43.06
7/22/2010	2	5	488835.77	4271507.79	12:04	13:54	1.20	1.95	43.65	43.10
7/22/2010	2	6	488848.57	4271504.22	12:05	13:56	1.15	2.45	43.65	43.79

7/22/2010	2	7	488862.06	4271499.21	12:07	13:57	1.20	7.55	43.65	43.30
7/22/2010	2	8	488873.37	4271495.20	12:09	13:57	1.20	2.70	43.65	44.00
7/22/2010	2	9	488828.89	4271509.58	12:04	13:54	1.20	1.30	43.65	44.18
7/22/2010	2	10	488832.88	4271495.48	12:11	13:55	1.20	1.85	43.65	43.80
7/27/2010	1	1	488696.61	4271575.90	12:11	14:11	1.15	7.00	44.82	44.96
7/27/2010	1	3	488706.88	4271627.81	12:12	14:15	1.15	1.75	44.82	45.04
7/27/2010	1	4	488711.08	4271647.12	12:14	14:16	1.10	3.45	44.82	45.20
7/27/2010	1	5	488720.45	4271679.28	12:16	14:19	1.30	1.95	44.82	45.34
7/27/2010	1	6	488725.96	4271701.30	12:19	14:20	1.35	1.80	44.82	45.02
7/27/2010	1	7	488732.43	4271719.32	12:20	14:22	1.30	1.85	44.82	45.00
7/27/2010	1	8	488734.30	4271747.28	12:22	14:25	1.25	3.40	44.82	45.52
7/27/2010	1	9	488740.87	4271771.24	12:24	14:30	1.15	1.85	44.82	45.40
7/27/2010	2	1	488696.61	4271575.90	14:11	16:11	1.25	12.50	45.01	45.06
7/27/2010	2	3	488706.88	4271627.81	14:15	16:13	1.25	1.80	45.01	45.32
7/27/2010	2	4	488711.08	4271647.12	14:16	16:14	1.15	7.40	45.01	45.07
7/27/2010	2	5	488720.45	4271679.28	14:19	16:15	1.25	2.35	45.01	45.85
7/27/2010	2	6	488725.96	4271701.30	14:20	16:16	1.15	1.60	45.01	45.35
7/27/2010	2	7	488732.43	4271719.32	14:22	16:17	1.30	1.75	45.01	44.89
7/27/2010	2	8	488734.30	4271747.28	14:25	16:18	1.25	4.50	45.01	45.29
7/27/2010	2	9	488740.87	4271771.24	14:30	16:19	1.15	2.05	45.01	45.44
7/28/2010	1	11	488658.18	4271557.22	7:30	9:28	1.15	1.15	44.71	44.85
7/28/2010	1	12	488658.18	4271557.22	7:30	9:29	1.25	1.75	44.71	45.25
7/28/2010	1	13	488648.43	4271561.54	7:30	9:26	1.20	1.50	44.71	45.20
7/28/2010	1	14	488648.43	4271561.54	7:30	9:30	1.15	2.25	44.71	44.98
7/28/2010	1	15	488668.37	4271554.08	7:26	9:28	1.20	3.55	44.71	44.89
7/28/2010	1	16	488668.37	4271554.08	7:27	9:29	1.15	4.55	44.71	45.38
7/28/2010	1	17	488671.39	4271564.39	7:29	9:31	1.15	4.70	44.71	45.05
7/28/2010	1	18	488671.39	4271564.39	7:30	9:31	1.15	1.85	44.71	45.57
7/28/2010	2	11	488658.18	4271557.22	9:28	11:27	1.35	1.95	45.45	44.97
7/28/2010	2	12	488658.18	4271557.22	9:29	11:28	1.30	1.80	45.45	45.31
7/28/2010	2	13	488648.43	4271561.54	9:26	11:29	1.10	1.50	45.45	45.23
7/28/2010	2	14	488648.43	4271561.54	9:30	11:31	1.35	2.45	45.45	45.63
7/28/2010	2	15	488668.37	4271554.08	9:28	11:28	1.30	2.80	45.45	45.45
7/28/2010	2	16	488668.37	4271554.08	9:29	11:29	1.15	4.45	45.45	45.60
7/28/2010	2	17	488671.39	4271564.39	9:31	11:31	1.15	4.75	45.45	45.23
7/28/2010	2	18	488671.39	4271564.39	9:31	11:32	1.10	1.90	45.45	45.70
7/28/2010	3	11	488658.18	4271557.22	11:27	13:26	1.15	1.90	45.52	44.86
7/28/2010	3	12	488658.18	4271557.22	11:28	13:27	1.35	1.75	45.52	45.36
7/28/2010	3	13	488648.43	4271561.54	11:29	13:28	1.25	1.80	45.52	45.30
7/28/2010	3	14	488648.43	4271561.54	11:31	13:29	1.25	2.25	45.52	45.55
7/28/2010	3	15	488668.37	4271554.08	11:28	13:27	1.10	3.05	45.52	45.22

7/28/2010	3	16	488668.37	4271554.08	11:29	13:28	1.30	4.50	45.52	45.32
7/28/2010	3	17	488671.39	4271564.39	11:31	13:29	1.25	4.60	45.52	45.33
7/28/2010	3	18	488671.39	4271564.39	11:32	13:30	1.20	1.90	45.52	45.45
8/5/2010	1	11	488804.82	4271544.68	7:25	9:27	1.15	1.35	45.68	45.50
8/5/2010	1	12	488793.24	4271551.02	7:25	9:27	1.10	4.20	45.68	45.70
8/5/2010	1	13	488786.11	4271554.25	7:25	9:27	1.10	2.15	45.68	44.56
8/5/2010	1	14	488778.01	4271557.70	7:25	9:27	1.05	33.20	45.68	45.90
8/5/2010	1	15	488762.70	4271564.49	7:25	9:27	1.05	2.25	45.68	45.66
8/5/2010	1	16	488757.21	4271566.82	7:25	9:27	1.15	5.26	45.68	45.87
8/5/2010	1	17	488791.70	4271569.44	7:25	9:27	1.20	0.60	45.68	45.48
8/5/2010	1	18	488797.12	4271581.31	7:25	9:27	1.15	2.50	45.68	43.07
8/5/2010	1	19	488791.13	4271598.73	7:25	9:27	1.05	1.25	45.68	45.82
8/5/2010	1	20	488781.66	4271608.96	7:25	9:27	1.00	1.15	45.68	45.97
8/5/2010	2	11	488804.82	4271544.68	9:27	11:27	1.05	1.80	45.70	45.14
8/5/2010	2	12	488793.24	4271551.02	9:27	11:27	1.00	7.70	45.70	45.48
8/5/2010	2	13	488786.11	4271554.25	9:27	11:27	1.00	2.60	45.70	43.55
8/5/2010	2	14	488778.01	4271557.70	9:27	11:27	1.05	7.30	45.70	45.22
8/5/2010	2	15	488762.70	4271564.49	9:27	11:27	1.05	2.70	45.70	45.35
8/5/2010	2	16	488757.21	4271566.82	9:27	11:27	1.00	5.45	45.70	45.20
8/5/2010	2	17	488791.70	4271569.44	9:27	11:27	1.00	2.60	45.70	44.69
8/5/2010	2	18	488797.12	4271581.31	9:27	11:27	1.05	3.50	45.70	42.07
8/5/2010	2	19	488791.13	4271598.73	9:27	11:27	1.05	1.75	45.70	45.75
8/5/2010	2	20	488781.66	4271608.96	9:27	11:27	1.05	1.80	45.70	45.35
8/12/2010	1	1	488899.25	4271473.85	7:05	9:02	1.20	1.75	46.00	45.63
8/12/2010	1	2	488906.94	4271500.66	7:07	9:10	1.20	2.30	46.00	45.40
8/12/2010	1	3	488913.11	4271526.61	7:10	9:13	1.10	14.50	46.00	45.14
8/12/2010	1	4	488919.25	4271560.66	7:14	9:16	1.10	1.40	46.00	45.80
8/12/2010	1	5	488924.19	4271589.89	7:17	9:19	1.10	2.90	46.00	45.38
8/12/2010	1	6	488782.49	4271518.52	7:22	9:09	1.15	2.35	46.00	44.36
8/12/2010	1	7	488756.90	4271527.21	7:24	9:13	1.10	2.45	46.00	44.84
8/12/2010	1	8	488856.86	4271520.97	7:19	9:24	0.95	2.35	46.00	43.54
8/12/2010	1	9	488804.56	4271545.01	7:38	9:11	1.25	2.20	46.00	44.91
8/12/2010	1	10	488792.63	4271547.91	7:28	9:13	1.10	2.40	46.00	44.72
8/12/2010	1	11	488779.39	4271552.15	7:29	9:16	1.10	14.45	46.00	45.42
8/12/2010	1	12	488771.22	4271556.06	7:29	9:17	1.05	2.35	46.00	43.57
8/12/2010	1	13	488757.66	4271561.75	7:30	9:19	1.10	3.80	46.00	41.47
8/12/2010	1	14	488730.84	4271573.85	7:30	9:21	1.10	0.85	46.00	45.84
8/12/2010	1	15	488701.27	4271583.93	7:23	9:29	1.00	2.75	46.00	45.01
8/12/2010	1	16	488675.57	4271595.90	7:22	9:26	1.15	2.55	46.00	45.07
8/12/2010	1	17	488867.61	4271548.25	7:13	9:23	1.10	6.40	46.00	45.60
8/12/2010	1	18	488815.30	4271569.96	7:14	9:11	1.10	1.50	46.00	45.14

8/12/2010	1	19	488803.48	4271573.64	7:15	9:12	1.10	2.55	46.00	45.64
8/12/2010	1	20	488788.41	4271579.36	7:16	9:14	1.20	4.00	46.00	44.99
8/12/2010	1	21	488777.37	4271583.99	7:17	9:15	1.15	2.45	46.00	43.51
8/12/2010	1	22	488765.19	4271588.83	7:18	9:16	1.05	2.55	46.00	43.53
8/12/2010	1	23	488736.91	4271600.47	7:19	9:18	1.15	4.65	46.00	45.42
8/12/2010	1	24	488714.17	4271609.50	7:20	9:19	1.10	2.95	46.00	44.88
8/12/2010	1	25	488687.23	4271617.07	7:22	9:21	1.10	5.90	46.00	45.35
8/12/2010	1	26	488814.33	4271601.47	7:15	9:28	1.10	3.80	46.00	45.24
8/12/2010	1	27	488801.99	4271605.76	7:17	9:33	1.05	3.70	46.00	45.18
8/12/2010	1	28	488792.40	4271608.88	7:19	9:30	1.20	2.50	46.00	45.25
8/12/2010	1	29	488777.43	4271615.50	7:20	9:23	1.15	3.30	46.00	44.83
8/12/2010	1	30	488765.79	4271619.02	7:21	9:35	1.10	4.30	46.00	45.23
8/12/2010	2	1	488899.25	4271473.85	9:02	12:23	1.20	0.90	45.58	45.46
8/12/2010	2	2	488906.94	4271500.66	9:10	12:21	1.05	2.05	45.58	45.46
8/12/2010	2	3	488913.11	4271526.61	9:13	12:28	1.15	10.80	45.58	45.77
8/12/2010	2	4	488919.25	4271560.66	9:16	13:55	1.20	3.10	45.58	45.62
8/12/2010	2	5	488924.19	4271589.89	9:19	13:05	1.20	4.45	45.58	45.37
8/12/2010	2	6	488782.49	4271518.52	9:09	12:50	1.10	3.40	45.58	45.94
8/12/2010	2	7	488756.90	4271527.21	9:13	13:02	1.10	4.65	45.58	44.79
8/12/2010	2	8	488856.86	4271520.97	9:24	13:01	1.05	3.35	45.58	43.41
8/12/2010	2	9	488804.56	4271545.01	9:11	12:20	1.20	2.90	45.58	44.90
8/12/2010	2	10	488792.63	4271547.91	9:13	12:27	1.10	3.50	45.58	44.54
8/12/2010	2	11	488779.39	4271552.15	9:16	12:32	1.10	23.00	45.58	45.28
8/12/2010	2	12	488771.22	4271556.06	9:17	12:43	1.10	4.15	45.58	42.30
8/12/2010	2	13	488757.66	4271561.75	9:19	12:44	1.15	3.55	45.58	41.14
8/12/2010	2	14	488730.84	4271573.85	9:21	12:49	1.10	1.15	45.58	45.44
8/12/2010	2	15	488701.27	4271583.93	9:29	12:52	1.15	3.95	45.58	44.82
8/12/2010	2	16	488675.57	4271595.90	9:26	12:52	1.10	3.70	45.58	44.73
8/12/2010	2	17	488867.61	4271548.25	9:23	12:39	1.05	15.05	45.58	45.52
8/12/2010	2	18	488815.30	4271569.96	9:11	12:18	1.15	2.25	45.58	45.07
8/12/2010	2	19	488803.48	4271573.64	9:12	12:20	1.10	3.40	45.58	45.59
8/12/2010	2	20	488788.41	4271579.36	9:14	12:22	1.00	5.70	45.58	44.46
8/12/2010	2	21	488777.37	4271583.99	9:15	12:24	1.10	2.55	45.58	42.94
8/12/2010	2	22	488765.19	4271588.83	9:16	12:27	1.10	3.00	45.58	43.17
8/12/2010	2	23	488736.91	4271600.47	9:18	12:30	1.10	4.65	45.58	45.48
8/12/2010	2	24	488714.17	4271609.50	9:19	12:32	1.15	4.45	45.58	45.01
8/12/2010	2	25	488687.23	4271617.07	9:21	12:34	1.00	6.45	45.58	45.44
8/12/2010	2	26	488814.33	4271601.47	9:28	12:32	1.15	4.40	45.58	45.20
8/12/2010	2	27	488801.99	4271605.76	9:33	12:31	1.10	3.65	45.58	45.26
8/12/2010	2	28	488792.40	4271608.88	9:30	12:37	1.10	N/A	45.58	-99.00
8/12/2010	2	29	488777.43	4271615.50	9:23	12:39	1.10	3.45	45.58	44.78

8/12/2010	2	30	488765.79	4271619.02	9:35	12:40	1.10	6.70	45.58	45.19
8/12/2010	3	1	488899.25	4271473.85	12:23	15:12	1.20	1.35	45.40	44.60
8/12/2010	3	2	488906.94	4271500.66	12:21	15:13	1.15	1.45	45.40	44.48
8/12/2010	3	3	488913.11	4271526.61	12:28	15:15	1.15	5.90	45.40	45.25
8/12/2010	3	4	488919.25	4271560.66	13:55	15:18	1.15	1.40	45.40	45.05
8/12/2010	3	5	488924.19	4271589.89	13:05	15:20	1.25	2.30	45.40	N/A
8/12/2010	3	6	488782.49	4271518.52	12:50	15:30	1.25	3.05	45.40	43.62
8/12/2010	3	7	488756.90	4271527.21	13:02	15:32	1.20	3.70	45.40	44.63
8/12/2010	3	8	488856.86	4271520.97	13:01	15:21	1.10	1.90	45.40	43.05
8/12/2010	3	9	488804.56	4271545.01	12:20	15:12	1.25	3.80	45.40	44.22
8/12/2010	3	10	488792.63	4271547.91	12:27	15:14	1.15	2.85	45.40	44.18
8/12/2010	3	11	488779.39	4271552.15	12:32	15:15	1.25	28.90	45.40	45.50
8/12/2010	3	12	488771.22	4271556.06	12:43	15:17	1.15	3.30	45.40	42.12
8/12/2010	3	13	488757.66	4271561.75	12:44	15:19	1.10	3.20	45.40	40.40
8/12/2010	3	14	488730.84	4271573.85	12:49	15:23	1.20	1.25	45.40	44.51
8/12/2010	3	15	488701.27	4271583.93	12:52	15:25	1.10	2.55	45.40	44.63
8/12/2010	3	16	488675.57	4271595.90	12:52	15:27	1.20	2.65	45.40	44.37
8/12/2010	3	17	488867.61	4271548.25	12:39	15:14	1.15	10.55	45.40	45.44
8/12/2010	3	18	488815.30	4271569.96	12:18	15:25	1.10	2.00	45.40	44.44
8/12/2010	3	19	488803.48	4271573.64	12:20	15:15	1.20	2.65	45.40	45.06
8/12/2010	3	20	488788.41	4271579.36	12:22	15:17	1.25	4.50	45.40	44.37
8/12/2010	3	21	488777.37	4271583.99	12:24	15:18	1.15	2.45	45.40	42.50
8/12/2010	3	22	488765.19	4271588.83	12:27	15:19	1.20	3.00	45.40	42.73
8/12/2010	3	23	488736.91	4271600.47	12:30	15:21	1.25	4.90	45.40	45.27
8/12/2010	3	24	488714.17	4271609.50	12:32	15:23	1.25	3.60	45.40	44.60
8/12/2010	3	25	488687.23	4271617.07	12:34	15:25	1.25	6.85	45.40	45.12
8/12/2010	3	26	488814.33	4271601.47	12:32	15:12	1.20	4.00	45.40	44.91
8/12/2010	3	27	488801.99	4271605.76	12:31	15:16	1.20	2.95	45.40	44.78
8/12/2010	3	28	488792.40	4271608.88	12:37	15:17	1.15	2.55	45.40	44.86
8/12/2010	3	29	488777.43	4271615.50	12:39	15:19	1.15	3.20	45.40	44.35
8/12/2010	3	30	488765.79	4271619.02	12:40	15:21	1.20	6.75	45.40	44.98
8/12/2010	4	1	488899.25	4271473.85	15:12	17:13	1.15	1.70	45.57	45.55
8/12/2010	4	2	488906.94	4271500.66	15:13	17:16	1.15	1.85	45.57	45.40
8/12/2010	4	3	488913.11	4271526.61	15:15	17:17	1.15	9.60	45.57	45.69
8/12/2010	4	4	488919.25	4271560.66	15:18	17:19	1.35	1.45	45.57	45.57
8/12/2010	4	5	488924.19	4271589.89	15:20	17:22	1.10	N/A	45.57	N/A
8/12/2010	4	6	488782.49	4271518.52	15:30	17:40	1.20	3.10	45.57	43.83
8/12/2010	4	7	488756.90	4271527.21	15:32	17:42	1.20	3.35	45.57	44.75
8/12/2010	4	8	488856.86	4271520.97	15:21	17:30	1.20	3.40	45.57	43.01
8/12/2010	4	9	488804.56	4271545.01	15:12	17:18	1.20	2.00	45.57	44.77
8/12/2010	4	10	488792.63	4271547.91	15:14	17:19	1.20	2.60	45.57	44.65

8/12/2010	4	11	488779.39	4271552.15	15:15	17:20	1.15	29.00	45.57	45.62
8/12/2010	4	12	488771.22	4271556.06	15:17	17:24	1.15	2.85	45.57	42.73
8/12/2010	4	13	488757.66	4271561.75	15:19	17:25	1.10	3.00	45.57	41.52
8/12/2010	4	14	488730.84	4271573.85	15:23	17:26	1.20	0.50	45.57	45.44
8/12/2010	4	15	488701.27	4271583.93	15:25	17:28	1.20	2.75	45.57	44.95
8/12/2010	4	16	488675.57	4271595.90	15:27	17:31	1.20	2.00	45.57	44.80
8/12/2010	4	17	488867.61	4271548.25	15:14	17:26	1.25	8.50	45.57	45.68
8/12/2010	4	18	488815.30	4271569.96	15:25	17:18	1.20	1.80	45.57	44.46
8/12/2010	4	19	488803.48	4271573.64	15:15	17:24	1.15	1.70	45.57	45.53
8/12/2010	4	20	488788.41	4271579.36	15:17	17:20	1.15	3.65	45.57	44.70
8/12/2010	4	21	488777.37	4271583.99	15:18	17:22	1.20	2.85	45.57	42.70
8/12/2010	4	22	488765.19	4271588.83	15:19	17:25	1.20	2.45	45.57	43.59
8/12/2010	4	23	488736.91	4271600.47	15:21	17:27	1.10	N/A	45.57	N/A
8/12/2010	4	24	488714.17	4271609.50	15:23	17:28	1.20	2.90	45.57	45.02
8/12/2010	4	25	488687.23	4271617.07	15:25	17:31	1.20	6.15	45.57	45.35
8/12/2010	4	26	488814.33	4271601.47	15:12	17:38	1.20	3.80	45.57	45.13
8/12/2010	4	27	488801.99	4271605.76	15:16	17:40	1.15	3.25	45.57	45.12
8/12/2010	4	28	488792.40	4271608.88	15:17	17:41	1.20	2.35	45.57	45.26
8/12/2010	4	29	488777.43	4271615.50	15:19	17:42	1.00	2.70	45.57	44.88
8/12/2010	4	30	488765.79	4271619.02	15:21	17:43	1.15	6.70	45.57	45.13
8/12/2010	5	1	488899.25	4271473.85	17:13	19:27	1.15	2.25	45.58	45.40
8/12/2010	5	2	488906.94	4271500.66	17:16	19:29	1.30	2.50	45.58	45.25
8/12/2010	5	3	488913.11	4271526.61	17:17	19:30	1.15	25.80	45.58	45.36
8/12/2010	5	4	488919.25	4271560.66	17:19	19:32	1.10	4.70	45.58	45.40
8/12/2010	5	5	488924.19	4271589.89	17:22	19:34	1.10	2.95	45.58	45.30
8/12/2010	5	6	488782.49	4271518.52	17:40	19:39	1.15	3.00	45.58	43.59
8/12/2010	5	7	488756.90	4271527.21	17:42	19:38	1.10	N/A	45.58	N/A
8/12/2010	5	8	488856.86	4271520.97	17:30	19:27	1.15	3.05	45.58	43.21
8/12/2010	5	9	488804.56	4271545.01	17:18	19:20	1.20	1.90	45.58	44.46
8/12/2010	5	10	488792.63	4271547.91	17:19	19:39	1.30	2.65	45.58	44.35
8/12/2010	5	11	488779.39	4271552.15	17:20	19:38	1.20	43.70	45.58	45.33
8/12/2010	5	12	488771.22	4271556.06	17:24	19:38	1.15	2.90	45.58	41.99
8/12/2010	5	13	488757.66	4271561.75	17:25	19:39	1.15	3.00	45.58	41.31
8/12/2010	5	14	488730.84	4271573.85	17:26	19:40	1.15	1.15	45.58	45.32
8/12/2010	5	15	488701.27	4271583.93	17:28	19:41	1.20	2.25	45.58	44.46
8/12/2010	5	16	488675.57	4271595.90	17:31	19:42	1.10	2.30	45.58	44.08
8/12/2010	5	17	488867.61	4271548.25	17:26	19:36	1.10	7.75	45.58	45.33
8/12/2010	5	18	488815.30	4271569.96	17:18	19:28	1.15	2.00	45.58	44.88
8/12/2010	5	19	488803.48	4271573.64	17:24	19:28	1.20	4.40	45.58	45.35
8/12/2010	5	20	488788.41	4271579.36	17:20	19:29	1.20	3.90	45.58	44.65
8/12/2010	5	21	488777.37	4271583.99	17:22	19:30	1.25	2.65	45.58	42.70

8/12/2010	5	22	488765.19	4271588.83	17:25	19:30	1.10	2.65	45.58	43.36
8/12/2010	5	23	488736.91	4271600.47	17:27	19:31	1.05	5.05	45.58	45.24
8/12/2010	5	24	488714.17	4271609.50	17:28	19:32	1.15	2.95	45.58	45.00
8/12/2010	5	25	488687.23	4271617.07	17:31	19:33	1.15	9.05	45.58	45.09
8/12/2010	5	26	488814.33	4271601.47	17:38	19:31	1.05	3.15	45.58	45.01
8/12/2010	5	27	488801.99	4271605.76	17:40	19:31	1.25	2.95	45.58	45.06
8/12/2010	5	28	488792.40	4271608.88	17:41	19:32	1.20	2.15	45.58	45.22
8/12/2010	5	29	488777.43	4271615.50	17:42	19:35	1.20	2.50	45.58	44.80
8/12/2010	5	30	488765.79	4271619.02	17:43	19:35	1.20	9.45	45.58	45.05
3/28/2011	1	1	488899.25	4271473.86	11:33	13:31	2.05	2.15	33.78	33.99
3/28/2011	1	3	488913.11	4271526.61	11:29	13:47	1.95	2.25	33.78	34.23
3/28/2011	1	5	488924.19	4271589.90	11:30	13:38	2.05	2.65	33.78	34.30
3/28/2011	1	9	488804.56	4271545.01	11:24	13:28	2.05	2.65	33.78	33.69
3/28/2011	1	11	488779.38	4271552.16	11:25	13:30	2.00	2.25	33.78	33.56
3/28/2011	1	13	488757.66	4271561.76	11:27	13:31	2.00	3.65	33.78	30.35
3/28/2011	1	14	488730.84	4271573.86	11:28	13:33	2.00	2.75	33.78	33.60
3/28/2011	1	15	488701.27	4271583.93	11:29	13:34	1.95	2.60	33.78	34.35
3/28/2011	1	16	488675.57	4271595.91	11:30	13:36	2.00	2.35	33.78	34.00
3/28/2011	1	18	488815.30	4271569.97	11:38	13:41	1.95	2.00	33.78	33.94
3/28/2011	1	20	488788.41	4271579.38	11:36	13:43	2.05	2.85	33.78	31.92
3/28/2011	1	22	488765.19	4271588.84	11:36	13:45	2.05	2.45	33.78	33.66
3/28/2011	1	28	488792.40	4271608.89	11:35	13:43	2.05	5.45	33.78	34.73
3/28/2011	1	31	488923.90	4271453.63	11:34	13:25	1.95	2.05	33.78	33.83
3/28/2011	1	32	488928.15	4271468.61	11:35	13:30	2.05	5.60	33.78	17.75
3/28/2011	2	1	488899.25	4271473.86	13:31	15:35	2.10	2.30	33.40	34.20
3/28/2011	2	3	488913.11	4271526.61	13:47	15:45	2.05	2.40	33.40	33.24
3/28/2011	2	5	488924.19	4271589.90	13:38	15:35	2.10	2.45	33.40	33.37
3/28/2011	2	9	488804.56	4271545.01	13:28	15:33	2.10	2.60	33.40	32.94
3/28/2011	2	11	488779.38	4271552.16	13:30	15:34	2.10	2.45	33.40	32.92
3/28/2011	2	13	488757.66	4271561.76	13:31	15:35	2.10	4.20	33.40	29.20
3/28/2011	2	14	488730.84	4271573.86	13:33	15:36	2.15	2.80	33.40	32.93
3/28/2011	2	15	488701.27	4271583.93	13:34	15:37	1.95	2.65	33.40	33.56
3/28/2011	2	16	488675.57	4271595.91	13:36	15:39	2.05	2.60	33.40	32.52
3/28/2011	2	18	488815.30	4271569.97	13:41	15:41	1.95	2.15	33.40	33.62
3/28/2011	2	20	488788.41	4271579.38	13:43	15:42	2.05	3.20	33.40	31.51
3/28/2011	2	22	488765.19	4271588.84	13:45	15:41	2.45	2.45	33.40	33.14
3/28/2011	2	28	488792.40	4271608.89	13:43	15:40	2.05	6.35	33.40	34.45
3/28/2011	2	31	488923.90	4271453.63	13:25	15:34	2.10	2.40	33.40	33.05
3/28/2011	2	32	488928.15	4271468.61	13:30	15:34	2.00	6.20	33.40	16.28
3/28/2011	2	33	488922.27	4271453.42	15:12	16:08	2.10	2.10	33.40	32.44
5/25/2011	1	1	488899.25	4271473.85	10:27	12:32	2.00	4.40	41.08	42.38

5/25/2011	1	3	488913.11	4271526.61	10:32	12:35	1.95	3.80	41.08	42.30
5/25/2011	1	5	488924.19	4271589.89	10:34	12:38	1.95	N/A	41.08	41.53
5/25/2011	1	9	488804.56	4271545.01	10:26	12:36	2.10	23.60	41.08	40.93
5/25/2011	1	11	488779.39	4271552.15	10:27	12:35	2.10	9.00	41.08	29.04
5/25/2011	1	13	488757.66	4271561.75	10:55	12:37	1.95	3.70	40.75	41.16
5/25/2011	1	14	488730.84	4271573.85	10:30	12:39	2.05	4.50	41.08	39.94
5/25/2011	1	15	488701.27	4271583.93	10:32	12:48	2.00	3.85	41.08	42.05
5/25/2011	1	16	488675.57	4271595.90	10:33	12:45	2.05	3.05	41.08	42.08
5/25/2011	1	20	488788.41	4271579.36	10:38	12:53	2.00	2.75	40.75	40.03
5/25/2011	1	22	488765.19	4271588.83	10:36	12:50	2.00	2.95	40.75	41.58
5/25/2011	1	28	488792.40	4271608.88	10:39	12:56	2.00	40.00	40.75	41.65
5/25/2011	1	32	488928.15	4271468.61	10:30	12:35	2.05	3.85	41.08	34.77
5/25/2011	1	33	488934.03	4271493.92	10:36	12:34	2.00	2.55	41.08	41.66
5/25/2011	1	34	488941.12	4271519.91	10:38	13:33	2.05	3.10	41.08	42.17
5/25/2011	1	37	488966.77	4271469.96	10:33	12:38	2.05	8.75	41.08	10.47
5/25/2011	1	38	488971.49	4271489.87	10:42	12:41	1.95	3.35	41.08	38.22
5/25/2011	1	39	488974.19	4271511.81	10:40	13:00	2.05	2.75	41.08	40.08
5/25/2011	2	1	488899.25	4271473.85	12:32	14:36	2.00	4.30	40.53	42.30
5/25/2011	2	3	488913.11	4271526.61	12:38	14:51	2.05	2.40	40.53	41.10
5/25/2011	2	5	488924.19	4271589.89	12:35	14:40	2.05	1.30	40.53	41.71
5/25/2011	2	9	488804.56	4271545.01	12:34	14:31	2.00	27.50	40.53	40.59
5/25/2011	2	11	488779.39	4271552.15	12:35	14:33	2.00	12.35	40.53	28.50
5/25/2011	2	13	488757.66	4271561.75	12:37	14:34	2.00	6.20	40.53	39.68
5/25/2011	2	14	488730.84	4271573.85	12:39	14:35	2.00	4.20	40.53	39.70
5/25/2011	2	15	488701.27	4271583.93	12:48	14:37	2.05	3.30	40.53	41.47
5/25/2011	2	16	488675.57	4271595.90	12:45	14:39	2.10	3.55	40.37	41.28
5/25/2011	2	20	488788.41	4271579.36	12:53	14:42	1.95	2.70	40.53	39.83
5/25/2011	2	22	488765.19	4271588.83	12:56	14:40	2.10	2.90	40.53	41.14
5/25/2011	2	28	488792.40	4271608.88	12:56	14:44	1.95	27.55	40.37	40.92
5/25/2011	2	32	488928.15	4271468.61	12:35	14:38	2.05	3.85	40.53	34.82
5/25/2011	2	33	488934.03	4271493.92	12:34	15:36	2.00	3.55	40.53	41.40
5/25/2011	2	34	488941.12	4271519.91	12:39	14:36	2.00	2.65	40.53	41.22
5/25/2011	2	37	488966.77	4271469.96	12:38	14:40	2.10	7.75	40.53	12.46
5/25/2011	2	38	488971.49	4271489.87	12:41	14:45	2.00	3.35	40.53	38.02
5/25/2011	2	39	488974.19	4271511.81	13:00	14:51	2.05	2.55	40.53	39.78
6/1/2011	1	1	488899.25	4271473.85	10:22	12:29	2.10	4.95	43.64	43.63
6/1/2011	1	3	488913.11	4271526.61	10:25	12:30	2.00	2.25	43.64	43.95
6/1/2011	1	5	488924.19	4271589.89	10:27	12:32	2.15	4.75	43.64	44.02
6/1/2011	1	9	488804.56	4271545.01	10:13	12:27	2.00	-99.00	43.64	-99.00
6/1/2011	1	11	488779.39	4271552.15	10:15	12:28	2.10	13.95	43.64	31.02
6/1/2011	1	13	488757.66	4271561.75	10:16	12:30	2.10	4.45	43.64	37.62

6/1/2011	1	14	488730.84	4271573.85	10:18	12:32	2.05	4.30	43.64	41.41
6/1/2011	1	15	488701.27	4271583.93	10:20	12:34	2.00	3.60	43.64	43.88
6/1/2011	1	16	488675.57	4271595.90	10:21	12:36	2.25	6.05	43.64	43.85
6/1/2011	1	20	488788.41	4271579.36	10:31	12:43	2.05	3.25	43.64	41.73
6/1/2011	1	22	488765.19	4271588.83	10:23	12:41	2.00	16.15	43.64	43.96
6/1/2011	1	28	488792.40	4271608.88	10:27	12:38	2.10	30.00	43.64	44.03
6/1/2011	1	32	488928.15	4271468.61	10:20	12:39	2.10	4.25	43.64	36.45
6/1/2011	1	33	488934.03	4271493.92	10:19	12:40	2.15	2.50	43.64	43.88
6/1/2011	1	34	488941.12	4271519.91	10:17	12:56	2.15	1.65	43.64	44.03
6/1/2011	1	37	488966.77	4271469.96	10:15	12:36	1.95	9.60	43.64	9.87
6/1/2011	1	38	488971.49	4271489.87	10:14	12:35	1.95	3.75	43.64	39.55
6/1/2011	1	39	488974.19	4271511.81	10:12	12:34	2.10	2.95	43.64	40.29
6/1/2011	2	1	488899.25	4271473.85	12:29	14:28	2.15	5.70	43.69	43.80
6/1/2011	2	3	488913.11	4271526.61	12:30	14:30	2.10	2.60	43.69	43.97
6/1/2011	2	5	488924.19	4271589.89	12:32	14:36	2.05	4.15	43.69	43.95
6/1/2011	2	9	488804.56	4271545.01	12:27	14:28	2.00	17.40	43.69	42.84
6/1/2011	2	11	488779.39	4271552.15	12:28	14:29	2.00	7.10	43.69	33.07
6/1/2011	2	13	488757.66	4271561.75	12:30	14:30	2.00	4.10	43.69	37.77
6/1/2011	2	14	488730.84	4271573.85	12:32	14:31	1.95	4.20	43.69	41.50
6/1/2011	2	15	488701.27	4271583.93	12:34	14:32	2.05	3.15	43.69	43.78
6/1/2011	2	16	488675.57	4271595.90	12:36	14:33	2.00	5.15	43.69	43.86
6/1/2011	2	20	488788.41	4271579.36	12:43	14:39	2.05	3.10	43.69	42.15
6/1/2011	2	22	488765.19	4271588.83	12:41	14:37	2.00	13.35	43.69	43.90
6/1/2011	2	28	488792.40	4271608.88	12:38	14:37	2.00	28.20	43.69	43.72
6/1/2011	2	32	488928.15	4271468.61	12:39	14:30	2.15	3.80	43.69	36.73
6/1/2011	2	33	488934.03	4271493.92	12:40	14:29	2.10	3.05	43.69	43.51
6/1/2011	2	34	488941.12	4271519.91	12:56	14:28	2.10	2.50	43.69	44.68
6/1/2011	2	37	488966.77	4271469.96	12:36	14:27	1.95	9.35	43.69	13.16
6/1/2011	2	38	488971.49	4271489.87	12:35	14:27	2.05	3.70	43.69	39.70
6/1/2011	2	39	488974.19	4271511.81	12:34	14:28	2.05	2.05	43.69	41.25
6/22/2011	1	11	488947.88	4271468.13	9:47	11:57	2.05	7.65	45.08	14.95
6/22/2011	1	12	488721.20	4271532.14	10:02	12:17	2.00	7.00	45.08	45.50
6/22/2011	1	13	488752.79	4271516.90	10:02	12:12	2.05	2.70	45.08	45.32
6/22/2011	1	14	488775.68	4271509.54	10:01	12:10	2.05	3.85	45.08	44.75
6/22/2011	1	15	488805.63	4271500.84	9:59	12:07	2.10	2.45	45.08	44.44
6/22/2011	1	16	488839.49	4271488.81	9:56	12:04	2.05	3.60	45.08	40.30
6/22/2011	1	17	488899.30	4271477.97	9:54	12:01	2.10	2.95	45.08	45.55
6/22/2011	1	18	488930.55	4271466.60	9:49	11:58	2.10	3.45	45.08	32.92
6/22/2011	1	19	488965.74	4271469.77	9:46	11:55	2.00	11.65	45.08	12.36
6/22/2011	1	20	489000.32	4271475.50	9:44	11:52	1.90	4.85	45.08	34.50
6/22/2011	1	21	488950.01	4271493.76	9:46	11:56	2.10	N/A	45.08	N/A

6/22/2011	1	22	488728.64	4271557.77	10:14	12:14	2.05	3.95	45.08	44.92
6/22/2011	1	23	488763.72	4271546.29	10:01	12:12	2.10	2.65	45.08	45.00
6/22/2011	1	24	488784.42	4271533.16	9:59	12:09	1.95	N/A	45.08	N/A
6/22/2011	1	25	488813.76	4271526.47	9:57	12:07	1.90	2.10	45.08	45.01
6/22/2011	1	26	488853.11	4271516.87	9:55	12:05	2.10	4.30	45.08	37.64
6/22/2011	1	27	488908.92	4271503.70	9:52	12:02	2.10	5.30	45.08	45.48
6/22/2011	1	28	488932.86	4271496.34	9:50	11:59	2.15	N/A	45.08	N/A
6/22/2011	1	29	488970.47	4271492.07	9:45	11:53	2.05	11.05	45.08	41.20
6/22/2011	2	11	488947.88	4271468.13	11:57	14:02	2.10	5.65	45.26	17.20
6/22/2011	2	12	488721.20	4271532.14	12:17	14:24	2.15	10.95	45.26	45.43
6/22/2011	2	13	488752.79	4271516.90	12:12	14:24	2.30	2.80	45.26	45.40
6/22/2011	2	14	488775.68	4271509.54	12:10	14:19	2.30	3.70	45.26	44.90
6/22/2011	2	15	488805.63	4271500.84	12:07	14:15	2.15	2.90	45.26	43.94
6/22/2011	2	16	488839.49	4271488.81	12:04	14:12	2.25	4.10	45.26	40.59
6/22/2011	2	17	488899.30	4271477.97	12:01	14:09	2.15	2.45	45.26	45.86
6/22/2011	2	18	488930.55	4271466.60	11:58	14:06	2.15	2.80	45.26	33.84
6/22/2011	2	19	488965.74	4271469.77	11:55	14:01	2.10	10.45	45.26	16.08
6/22/2011	2	20	489000.32	4271475.50	11:52	13:57	2.25	4.45	45.26	37.13
6/22/2011	2	21	488950.01	4271493.76	11:56	13:59	2.15	2.45	45.26	45.50
6/22/2011	2	22	488728.64	4271557.77	12:14	14:20	2.10	3.65	45.26	45.14
6/22/2011	2	23	488763.72	4271546.29	12:12	14:18	2.05	2.25	45.26	44.94
6/22/2011	2	24	488784.42	4271533.16	12:09	14:16	2.10	3.75	45.26	45.21
6/22/2011	2	25	488813.76	4271526.47	12:07	14:14	2.25	2.40	45.26	45.21
6/22/2011	2	26	488853.11	4271516.87	12:05	14:12	2.25	4.90	45.26	37.80
6/22/2011	2	27	488908.92	4271503.70	12:02	14:09	2.20	2.70	45.26	43.96
6/22/2011	2	28	488932.86	4271496.34	11:59	14:03	2.25	2.00	45.26	45.70
6/22/2011	2	29	488970.47	4271492.07	11:53	13:57	2.05	6.40	45.26	40.01
6/22/2011	3	11	488947.88	4271468.13	14:02	15:54	2.05	5.25	45.18	20.53
6/22/2011	3	12	488721.20	4271532.14	14:24	16:06	2.15	8.55	45.18	45.10
6/22/2011	3	13	488752.79	4271516.90	14:24	16:04	2.05	2.50	45.18	45.19
6/22/2011	3	14	488775.68	4271509.54	14:19	16:03	2.00	3.35	45.18	44.51
6/22/2011	3	15	488805.63	4271500.84	14:15	16:01	1.90	2.10	45.18	43.15
6/22/2011	3	16	488839.49	4271488.81	14:12	15:59	1.80	3.55	45.18	38.30
6/22/2011	3	17	488899.30	4271477.97	14:09	15:57	2.05	1.95	45.18	45.27
6/22/2011	3	18	488930.55	4271466.60	14:06	15:56	1.90	2.70	45.18	36.05
6/22/2011	3	19	488965.74	4271469.77	14:01	15:53	2.05	7.65	45.18	19.87
6/22/2011	3	20	489000.32	4271475.50	13:57	15:52	2.00	4.55	45.18	35.92
6/22/2011	3	21	488950.01	4271493.76	13:59	15:53	2.00	2.40	45.18	45.44
6/22/2011	3	22	488728.64	4271557.77	14:20	16:05	1.90	3.15	45.18	45.30
6/22/2011	3	23	488763.72	4271546.29	14:18	16:03	2.05	2.85	45.18	44.97
6/22/2011	3	24	488784.42	4271533.16	14:16	16:02	1.95	3.80	45.18	45.20

6/22/2011	3	25	488813.76	4271526.47	14:14	16:00	1.85	1.90	45.18	45.14
6/22/2011	3	26	488853.11	4271516.87	14:12	15:59	2.15	4.35	45.18	38.60
6/22/2011	3	27	488908.92	4271503.70	14:09	15:56	2.10	3.00	45.18	45.40
6/22/2011	3	28	488932.86	4271496.34	14:03	15:55	1.90	2.00	45.18	45.33
6/22/2011	3	29	488970.47	4271492.07	13:57	15:52	2.00	7.75	45.18	38.60

Masses measured in kg
Conductivities are specific in mS/cm corrected to 25 °c
Values of -99.00 represent No Data

Table B2: Seepage data from 2 cluster experiments conducted in July 2010

Date	Run	Cluster	Meter	Easting	Northing	Time On	Time Off	Start Volume	End Volume
7/6/2010	1	1	2	488840.70	4271565.55	9:50	11:50	1.00	3.70
7/6/2010	2	1	2	488840.70	4271565.55	11:50	13:50	1.00	3.25
7/6/2010	3	1	2	488840.70	4271565.55	13:50	15:50	1.00	2.00
7/7/2010	4	1	2	488840.70	4271565.55	9:45	11:45	1.00	3.00
7/7/2010	5	1	2	488840.70	4271565.55	11:45	13:45	1.00	4.25
7/6/2010	1	1	3	488839.70	4271565.55	9:50	11:50	1.00	6.25
7/6/2010	2	1	3	488839.70	4271565.55	11:50	13:50	1.00	8.50
7/6/2010	3	1	3	488839.70	4271565.55	13:50	15:50	1.00	9.00
7/7/2010	4	1	3	488839.70	4271565.55	9:45	11:45	1.00	3.90
7/7/2010	5	1	3	488839.70	4271565.55	11:45	13:45	1.00	6.50
7/6/2010	1	1	4	488840.70	4271564.55	9:50	11:50	1.00	1.25
7/6/2010	2	1	4	488840.70	4271564.55	11:50	13:50	1.00	2.75
7/6/2010	3	1	4	488840.70	4271564.55	13:50	15:50	1.00	2.25
7/7/2010	4	1	4	488840.70	4271564.55	9:45	11:45	1.00	1.75
7/7/2010	5	1	4	488840.70	4271564.55	11:45	13:45	1.00	2.60
7/6/2010	1	1	5	488840.70	4271566.55	9:50	11:50	1.00	2.45
7/6/2010	2	1	5	488840.70	4271566.55	11:50	13:50	1.00	8.80
7/6/2010	3	1	5	488840.70	4271566.55	13:50	15:50	1.00	13.50
7/7/2010	4	1	5	488840.70	4271566.55	9:45	11:45	1.00	N/A
7/7/2010	5	1	5	488840.70	4271566.55	11:45	13:45	1.00	19.00
7/6/2010	1	1	6	488841.70	4271565.55	9:50	11:50	1.00	1.70
7/6/2010	2	1	6	488841.70	4271565.55	11:50	13:50	1.00	1.45
7/6/2010	3	1	6	488841.70	4271565.55	13:50	15:50	1.00	1.20
7/7/2010	4	1	6	488841.70	4271565.55	9:45	11:45	1.00	1.45
7/7/2010	5	1	6	488841.70	4271565.55	11:45	13:45	1.00	20.00
7/6/2010	1	2	13	488809.70	42171581.85	9:50	11:50	1.00	2.00
7/6/2010	2	2	13	488809.70	42171581.85	11:50	13:50	1.00	2.75
7/6/2010	3	2	13	488809.70	42171581.85	13:50	15:50	1.00	3.25
7/7/2010	4	2	13	488809.70	42171581.85	9:45	11:45	1.00	2.25

7/7/2010	5	2	13	488809.70	42171581.85	11:45	13:45	1.00	2.50
7/6/2010	1	2	14	488809.70	42171580.85	9:50	11:50	1.00	1.80
7/6/2010	2	2	14	488809.70	42171580.85	11:50	13:50	1.00	2.50
7/6/2010	3	2	14	488809.70	42171580.85	13:50	15:50	1.00	N/A
7/7/2010	4	2	14	488809.70	42171580.85	9:45	11:45	1.00	1.75
7/6/2010	1	2	15	488808.70	42171581.85	9:50	11:50	1.00	9.50
7/6/2010	2	2	15	488808.70	42171581.85	11:50	13:50	1.00	10.00
7/6/2010	3	2	15	488808.70	42171581.85	13:50	15:50	1.00	11.50
7/7/2010	4	2	15	488808.70	42171581.85	9:45	11:45	1.00	12.50
7/7/2010	5	2	15	488808.70	42171581.85	11:45	13:45	1.00	13.60
7/6/2010	1	2	16	488809.70	42171582.85	9:50	11:50	1.00	6.25
7/6/2010	2	2	16	488809.70	42171582.85	11:50	13:50	1.00	6.00
7/6/2010	3	2	16	488809.70	42171582.85	13:50	15:50	1.00	7.74
7/7/2010	4	2	16	488809.70	42171582.85	9:45	11:45	1.00	8.00
7/7/2010	5	2	16	488809.70	42171582.85	11:45	13:45	1.00	9.00
7/6/2010	1	2	17	488810.70	42171581.85	9:50	11:50	1.00	5.00
7/6/2010	2	2	17	488810.70	42171581.85	11:50	13:50	1.00	5.00
7/6/2010	3	2	17	488810.70	42171581.85	13:50	15:50	1.00	5.75
7/7/2010	4	2	17	488810.70	42171581.85	9:45	11:45	1.00	6.50
7/7/2010	5	2	17	488810.70	42171581.85	11:45	13:45	1.00	N/A

Volumes measured in l
Values of N/A represent No Data